The European Master in Advanced Structural Analysis and Design using Composite Materials is a join initiative of:

Universidade do Minho

Universitat de Girona

Università degli Studi di Napoli Federico II

INSA Institut National des Sciences Appliquées Toulouse

Université de Toulouse

Life Cycle Assessment of Construction Materials Incorporating Wind Turbine Blade Powder Waste

Yasaman Jafari

FRP++ Advanced structural analysis and design using composite materials

UMinho | 2026

Universidade do Minho
Escola de Engenharia

Yasaman Jafari

Life Cycle Assessment of Construction Materials Incorporating Win Turbine Blade Powder Waste

FRP++
Advanced structural analysis and design using composite materials

Funded by the European Union

July 2026

Universidade do Minho
Escola de Engenharia

Yasaman Jafari

Life Cycle Assessment of Construction Materials Incorporating Wind Turbine Blade Powder Waste

FRP++
Advanced structural analysis and design using composite materials

Master Dissertation

European Master Advanced Structural Analysis and Design using Composite Materials

Work developed under the supervision of

Doctor Elisabete Rodrigues Teixeira

Funded by the European Union

July 2026

DIREITOS DE AUTOR E CONDIÇÕES DE UTILIZAÇÃO DO TRABALHO POR TERCEIROS

Este é um trabalho académico que pode ser utilizado por terceiros desde que respeitadas as regras e boas práticas internacionalmente aceites, no que concerne aos direitos de autor e direitos conexos.

Assim, o presente trabalho pode ser utilizado nos termos previstos na licença abaixo indicada.

Caso o utilizador necessite de permissão para poder fazer um uso do trabalho em condições não previstas no licenciamento indicado, deverá contactar o autor, através do RepositóriUM da Universidade do Minho.

Licença concedida aos utilizadores deste trabalho

[If the supervisor/author wishes to use one of the Creative Commons licences, they should choose and keep only one of the following icons and the corresponding lettering and URL, deleting the italicised text that follows. However, it is possible to choose another type of licence; in that case, the necessary information should be included by duly adapting this template.]



Atribuição CC BY

https://creativecommons.org/licenses/by/4.0/

[This licence allows others to distribute, remix, adapt, and build upon your work, even for commercial purposes, provided that they give you appropriate credit for the original creation. It is the most flexible of all available licences. It is recommended for maximising the dissemination and use of licensed materials.]

ACKNOWLEDGEMENTS

This dissertation was completed as part of the FRP++ Erasmus Mundus Joint Master's Programme, and I am grateful to the consortium and its partner institutions for the exceptional academic environment they provided, one that challenged me to grow not only as a researcher but as an engineer with an international perspective. The financial support provided through the FRP++ scholarship made this journey possible.

My sincere gratitude goes to my supervisor, Prof. Elisabete Teixeira, whose guidance and consistent encouragement shaped this work from its earliest stages. Her willingness to engage with both the technical and conceptual dimensions of this research made the process genuinely rewarding.

I also wish to thank Prof. Bruno Castanié, Prof. Jose Sena-Cruz, and Karine Giacomi for their support and collegiality throughout the programme.

I would like to express my deepest gratitude to my mother, father, and my beloved sister, Nazgol for their unconditional love and unwavering belief in me. Their sacrifices and constant support have been a source of strength and motivation for me all my life.

And to Babak, thanks for your love and always inspiring me to move forward with confidence.

Finally, to Mansoureh, Amir, Elham, Leo, Tina, Sarahi, and Diba, thank you for always listening.

The student would like to gratefully acknowledge the financial support provided by the European Union for participation in the Erasmus Mundus FRP++ European Master Course in Advanced Structural Analysis and Design using Composite Materials (Project no. 101048961). This work was also supported by FCT/MCTES under the R&D Unit Institute for Sustainability and Innovation in Structural Engineering (ISISE), under the references UID/4029/2025 (DOI: 10.54499/UID/04029/2025), UID/PRR/04029/2025 (DOI: 10.54499/UID/PRR/04029/2025) and UID/PRR2/04029/2025 (DOI: 10.54499/UID/PRR2/04029/2025), and under the Associate Laboratory Advanced Production and Intelligent Systems ARISE under reference LA/P/0112/2020 (DOI: 10.54499/LA/P/0112/2020).

STATEMENT OF INTEGRITY

I hereby declare having conducted this academic work with integrity. I confirm that I have not used plagiarism or any form of undue use of information or falsification of results along the process leading to its elaboration.

I further declare that I have fully acknowledged the Code of Ethics and Conduct of the University of Minho.

DECLARATION ON THE USE OF ARTIFICIAL INTELLIGENCE (AI) TOOLS

I hereby declare having acted this academic work with integrity and confirm that I have not resorted to any form of undue use of AI tools, nor to the falsification or omission of information, sources, data, results or processes in any of the stages leading to its elaboration.

I further declare that any use of AI tools was done in a transparent and responsible manner, being duly noted in the work, and that I critically verified the accuracy of the content produced with their support, assuming full responsibility for what I submit.

I further declare that I have fully acknowledged the Code of Ethics and Conduct of the University of Minho, as well as the applicable standards of academic integrity and data protection.

Avaliação do Ciclo de Vida de Materiais de Construção Com Incorporação de Resíduos de Pó de Pás de Turbinas Eólicas

RESUMO

A produção de pás de turbinas eólicas gera um resíduo sob a forma de pó durante a fase de acabamento, o qual é atualmente encaminhado, na sua maioria, para aterro ou incineração. No entanto, a sua caracterização revelou uma composição química compatível com aplicações cimentícias, evidenciando potencial para valorização como material de construção. Neste contexto, esta dissertação avalia a viabilidade ambiental da incorporação deste resíduo em argamassas de cimento como substituto parcial do cimento, do agregado fino, ou de ambos simultaneamente.

Foi realizada uma Avaliação do Ciclo de Vida (ACV) do berço ao portão para dezanove formulações de argamassa, com níveis de substituição entre 5% e 40%, considerando seis categorias de impacte. Para avaliar a influência das opções metodológicas na ACV, foram definidos três cenários para testar a sensibilidade dos resultados a diferentes tratamentos do pó: uma abordagem cut-off sem encargos atribuídos ao resíduo, uma abordagem cut-off incluindo o consumo energético resultante da moagem do pó, e uma alocação económica que incorpora parte dos impactos associados à produção do pó.

A substituição parcial do cimento pelo pó de pás reduziu consistentemente os impactes ambientais em todas as categorias analisadas e em todos os cenários considerados. As formulações com substituição combinada de cimento e agregado fino, em níveis moderados, apresentaram o melhor desempenho ambiental, enquanto a substituição exclusiva do agregado fino conduziu a benefícios mais limitados. Ainda assim, todas as misturas incorporando o resíduo evidenciaram um desempenho ambiental superior ao da argamassa de referência. A hierarquia ambiental das formulações manteve-se inalterada nos três cenários avaliados, demonstrando que as conclusões são independentes do método de alocação. Adicionalmente, a análise de sensibilidade não revelou correlação significativa entre desempenho ambiental e mecânico das argamassas.

Os resultados obtidos demonstram o potencial da valorização do pó proveniente do fabrico de pás de turbinas eólicas como matéria-prima para argamassas cimentícias, contribuindo simultaneamente para a redução da deposição de resíduos e para a diminuição dos impactes ambientais associados à produção destes materiais de construção.

PALAVRAS-CHAVE: Avaliação do ciclo de vida (ACV); Pó de pás de turbinas eólicas; Materiais de construção; Impacte ambiental; Economia circular.

Life Cycle Assessment of Construction Materials Incorporating Wind Turbine Blade Powder Waste

ABSTRACT

The production of wind turbine blades generates dust-like waste during the finishing phase, most of which is currently sent to landfills or incinerated. However, characterization of this waste revealed a chemical composition compatible with cementitious applications, indicating potential for its reuse as a construction material. In this context, this dissertation evaluates the environmental feasibility of incorporating this waste into cement mortars as a partial substitute for cement, fine aggregate, or both simultaneously.

A cradle-to-gate Life Cycle Assessment (LCA) was conducted for nineteen mortar formulations, with substitution levels ranging from 5% to 40% by volume, considering six impact categories. To assess the influence of methodological choices on the LCA, three scenarios were defined: a cut-off approach with no costs assigned to the waste, a cut-off approach including the energy consumption resulting from grinding the powder, and an economic allocation that incorporates part of the impacts associated with powder production.

The results demonstrated that the partial substitution of cement with shovel dust consistently reduces environmental impacts across all analysed categories and in all considered scenarios. Formulations with a combined substitution of cement and fine aggregate, at moderate levels, exhibited the best environmental performance, while the exclusive substitution of fine aggregate led to more limited benefits. Nevertheless, all mixtures incorporating the waste showed superior environmental performance compared to the reference mortar. The environmental ranking of the formulations remained unchanged across the three scenarios evaluated, demonstrating that the conclusions are independent of the allocation method. Additionally, the sensitivity analysis did not identify a significant correlation between the environmental performance and the mechanical performance of the mortars.

The results obtained demonstrate the potential for upcycling the dust generated during the manufacture of wind turbine blades as a raw material for cementitious mortars, thereby contributing both to reducing waste disposal and to mitigating the environmental impacts associated with the production of these construction materials.

KEYWORDS: Life Cycle Assessment (LCA); Fiber-polymer powder from wind turbine blades; Construction materials; Environmental impact; Circular economy

TABLE OF CONTENTS

Acknowledgements iii
Resumo v
Abstract vi
Table of Contents vii
List of Figures ix
List of Tables x
List of Abbreviations and Symbols xi
1. Introduction 1
1.1. Background and Motivation 1
1.2. Objectives 4
1.3. Structure of the Dissertation 5
2. Wind Turbine Blades and Composite Materials 7
2.1. Overview of Wind Turbine Blades 7
2.2. Materials Used in Blade Manufacturing 11
2.2.1. Fiber Reinforcement 11
2.2.2. Polymer Matrices 12
2.3. Manufacturing Processes and Waste Generation During Production 14
2.3.1. Blade Fabrication Methods 14
2.3.2. Waste Generation During Blade Manufacturing 15
3. Recycling and Reuse of Composite Waste 17
3.1. Discussion on Current Waste Management Practices in Europe 17
3.2. Recycling Methods for Composite Materials 18
3.3. Mechanical Recycling and Material Processing 21
3.4. Potential Applications in Construction Materials 23
3.4.1. Challenges and limitations of Recycling 25
3.5. WTB Powder Reuse in Cementitious Materials 29
3.5.1. Challenges and Limitations of Reusing Powder 31
4. Life Cycle Assessment (LCA) Framework 33
4.1. Fundamentals of LCA 33
4.2. Life Cycle Assessment of mortars with WTB powder waste incorporation 34
4.2.1. Studied Mortars Formulations 34
4.2.2. Life Cycle Assessment 36
4.2.3. System Boundaries 37
4.2.4. Life Cycle Inventory (LCI) 43
4.2.5. Life Cycle Inventory Assessment (LCIA) 45
4.2.6. Normalization, Aggregation and Global Assessment 46
4.2.7. Sensitivity Analysis 48
5. Results and Discussion 49
5.1. Results - Scenario 1 49
5.2. Results - Scenario 2 58
5.3. Results - Scenario 3 67

5.3.1. Allocation basis: production data, prices and the allocation coefficient 67
5.3.2. Sensitivity 76
5.3.3. Sensitivity analysis: strength–environment trade-off and weighting of criteria 80
5.3.4. Multi-criteria comparison with weight sensitivity 82
5.4. Comparison of Scenarios 84
6. Conclusions and Future Work 87
6.1. Conclusions 87
6.2. Limitations 88
6.3. Future Work 88
References 90

LIST OF FIGURES

Figure 1-1 Global Wind Power Installations and Cumulative Capacity (2013–2023) adapted from [4] ... 1
Figure 1-2 Waste hierarchy framework (adapted from [7]) ... 3
Figure 2-1 Wind Turbine Blade: a) general view- and b) root section with bolted metallic joint Adapted from [13] ... 8
Figure 2-2 Win Turbine Blade cross section Adapted from [14] ... 8
Figure 2-3 cross section of WTB, Explanation of numbers in picture: 1. Solid GFRP Laminated Panels; 2. Sandwich Panels adapted from[13] ... 9
Figure 2-4 Longitudinal section of WTB, Explanation of numbers in picture: 2. Sandwich Panels; 3. GFRP mesh adapted from [13] ... 9
Figure 2-5 Cross-section of a wind turbine blade identifying spar caps adapted from [15] ... 11
Figure 3-1 Recycling methods of WTB adapted from [16] ... 20
Figure 4-1 System boundary diagram for Scenario 1 ... 39
Figure 4-2 System boundary diagram for Scenario 2 ... 40
Figure 4-3 System boundary diagram for Scenario 3 ... 42
Figure 5-1 System Boundaries for all Scenarios ... 49
Figure 5-2 NDA sustainability score of the mixes, Scenario 3 (all prices) ... 74
Figure 5-4 Compressive strength and environmental score against the substitution level, per series ... 81
Figure 5-5 MCDM score of each mix under the three weighting schemes ... 83

LIST OF TABLES

Table 4-1 Mix design of the nineteen mortar formulations 35
Table 4-2 Mechanical and durability properties..... 36
Table 4-3 Source of Cement and Sand impacts..... 42
Table 4-4 Database name chosen in SimaPro 43
Table 4-5 EPD/Ecoinvent source table..... 43
Table 4-6 Inventory of material and transport inputs per 1 m^3 44
Table 4-7 Environmental impact factors (all per kg, transportation per tkm) 45
Table 4-8 Environmental impact categories assessed, with their reference units 46
Table 4-9 Weighting factors applied to each impact category adapted from [32]..... 48
Table 5-1 Contribution of life cycle stages to the environmental impact categories, Scenario 1. 50
Table 5-2 Total characterized environmental impact of mixes, Scenario 1..... 52
Table 5-3 Best (minimum) and worst (maximum) characterised values identified across the mixes, for each impact category, used as the normalisation reference points. 53
Table 5-4 Normalised Values, Scenario 1..... 53
Table 5-5 NDA sustainability score of the mixes, Scenario 1 54
Table 5-6 REF radar..... 55
Table 5-7 Radar charts, Scenario 1 55
Table 5-8 Additional grinding energy data, Scenario 2..... 59
Table 5-9 Contribution of life cycle stages to the environmental impact categories, Scenario 2. 60
Table 5-10 Total characterized environmental impact of mixes, Scenario 2..... 61
Table 5-11 Best (minimum) and worst (maximum) characterised values identified across the mixes, for each impact category, used as the normalisation reference points, Scenario 2. 62
Table 5-12 Normalised Values, Scenario 2..... 63
Table 5-13 NDA sustainability score of the mixes, Scenario 2..... 64
Table 5-14 Ref radar chart, Scenario 2..... 65
Table 5-15 Radar charts, Scenario 2 65
Table 5-16 Powder prices..... 68
Table 5-17 Economic allocation coefficient for all mixes, Scenario 3..... 69
Table 5-18 Contribution of life cycle stages to the environmental impact categories, Scenario 3 (50%) 69
Table 5-19 Total characterised environmental impact of mixes, Scenario 3 (50% price) 71
Table 5-20 Best (minimum) and worst (maximum) characterised values identified across the mixes, for each impact category, used as the normalisation reference points. 72
Table 5-21 Normalised Values, Scenario 3 (50% price) 73
Table 5-22 Reference radar chart, Scenario 3 74
Table 5-23 Radar charts Scenario 3 (50%) 75
Table 5-24 Sensitivity Data 77
Table 5-25 Sensitivity graphs (GWP) 78
Table 5-26 Sensitivity graphs (ADP-FF) 79
Table 5-27 Linear regression of environmental impact against engineering properties 79
Table 5-28 Compressive strength and environmental score by substitution level, Scenario 3, (50%), (best=1)..... 81
Table 5-29 MCDM scores and rankings under the three weighting schemes, Scenario 3 (50%) 82

List of Abbreviations and Symbols

Abbreviations

AFRP	Aramid Fibre Reinforced Polymer
ADP-FF	Abiotic Depletion Potential for Fossil Fuels
AP	Acidification Potential
ASR	Alkali–Silica Reaction
BFRP	Basalt Fibre Reinforced Polymer
C-(A)-S-H	Calcium (Aluminium) Silicate Hydrate
CF-EP	Carbon Fibre–Epoxy composite system
CML-IA	Centre of Environmental Science – Life Cycle Impact Assessment methodology
CO_2	Carbon Dioxide
EN	European Norm (standard)
EP	Eutrophication Potential
EPD	Environmental Product Declaration
EU	European Union
FRP	Fibre-Reinforced Polymer
GF-EP	Glass Fibre–Epoxy composite system
GF-UP	Glass Fibre–Unsaturated Polyester composite system
GFRP	Glass Fibre Reinforced Polymer
GFRPW	Glass Fibre Reinforced Polymer Waste
GW	Gigawatt
GWP	Global Warming Potential
HTP	High Temperature and Pressure (solvolysis)
ISO	International Organization for Standardization
LCA	Life Cycle Assessment
LCI	Life Cycle Inventory
LCIA	Life Cycle Impact Assessment
LTP	Low Temperature and Pressure (solvolysis)
MARS-SC	Methodology for the Relative Sustainability Assessment of Building Technologies
MJ	Megajoule
MW	Megawatt

NDA	Normalised Decision Aggregation
NREL	National Renewable Energy Laboratory
ODP	Ozone Depletion Potential
POCP	Photochemical Ozone Creation Potential
REF	Reference mortar formulation
SD	Standard Deviation
UK	United Kingdom
UP	Unsaturated Polyester
USD	United States Dollar
VARTM	Vacuum-Assisted Resin Transfer Moulding
wt%	Weight Percentage
WTB	Wind Turbine Blade
WTBW	Wind Turbine Blade Waste

1. INTRODUCTION

1.1. Background and Motivation

The cement and concrete industry, responsible for approximately 7% of global CO_2 emissions from human activities, is under increasing pressure to reduce its carbon footprint through the integration of waste-derived materials [1]. While wind energy, one of the principal pathways for decarbonising electricity generation, has simultaneously generated a growing volume of composite waste that current disposal routes cannot sustainably manage [2,3].

As illustrated in Figure 1-1 the expansion of wind power generation has been remarkable: global installed capacity grew from roughly 7,600 MW in 1998 to more than 364,000 MW by 2014, and so annual gross installations have continued to increase, surpassing 200 GW per year in recent projections [2]. In Europe alone, cumulative installed capacity reached 275 GW by 2023, and the trend has continued upward since [4].

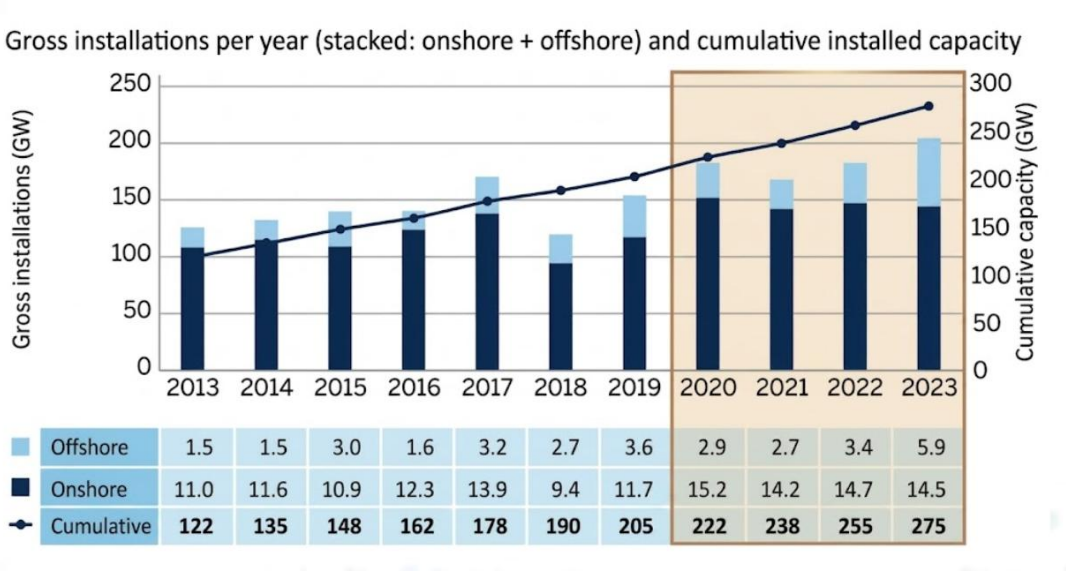


Figure 1-1 Global Wind Power Installations and Cumulative Capacity (2013–2023) adapted from [4]

This industrial expansion brings environmental benefits during the operational phase of wind turbines but it also creates a less visible problem that has received little attention: the volume of composite waste produced throughout the life cycle of Wind Turbine Blades (WTB). Within the composite waste problem, two distinct streams must be recognised. End-of-life waste comes from decommissioned components

that have completed their service life, and manufacturing waste which is produced during the production of new blades and includes scrap from trimming, milling, and finishing operations [5]. Although research on recycling composite materials has expanded considerably, manufacturing-generated powder waste from wind turbine blade production remains an emerging area of research. Recent research has highlighted the potential of reusing this powder waste as a partial replacement for conventional raw materials in cementitious mortars, demonstrating its technical feasibility and supporting its valorisation within circular economy strategies [6]. The scale of the issue is significant: global estimates indicate that around 62,000 tonnes of carbon fibre reinforced polymer waste were generated in 2020 alone . According to the European Composites Industry Association, only about 228,000 tonnes of total composite waste are currently accessible for recycling, which corresponds to roughly a quarter of the forecasted volume [6]. These numbers reveal a recycling infrastructure that is still underdeveloped relative to the volumes being produced.

The wind energy industry is one of the largest consumers of fibre-reinforced composites and therefore one of the largest producers of associated manufacturing waste. Although approximately 85–90% of decommissioned wind turbine components, including towers, foundations, generators, and gearboxes, can be recycled, the composite nature of the blades makes their separation and reprocessing significantly more challenging [3]. This complexity has made landfilling the most common disposal method, despite the associated environmental harm and, in many jurisdictions, high disposal taxation [3].

Wind turbine blades are typically manufactured from glass fibre reinforced polymer laminates bonded with epoxy or polyester resins. This combination makes them difficult to reprocess through conventional techniques [6]. Most studies on composite waste in the wind energy sector have traditionally focused on the decommissioning stage, yet the manufacturing phase is itself a substantial contributor to the overall waste burden. Between 13% and 30% of the total lifecycle waste of a wind turbine blade is generated during its manufacture, depending on the scenario considered. Cumulative global blade waste is projected to reach approximately 43 million tonnes by 2050 under the most likely scenario, with Europe expected to face the problem first due to the earlier deployment of its wind energy infrastructure [2].

The trimming and finishing stages of blade production generate a fine powder made up of fibreglass fragments and cured resin. Compositionally, this powder is close to the mineral and pozzolanic additives already used in cementitious systems. This waste stream has historically been disposed of through landfilling or incineration, yet both options are becoming increasingly restrictive under European legislation and involve rising economic costs that progressively diminish their viability [7, 8].

The regulatory context sharpens the urgency of the problem. The European Union Waste Framework Directive (Directive 2008/98/EC) [9] establishes a hierarchy of waste management strategies, with prevention and preparation for reuse at the top and disposal at the bottom as shown in Figure 1-2. Landfilling, still the dominant route for composite waste, sits at the lowest tier and is increasingly discouraged by rising taxes and stricter environmental controls. The United Kingdom (UK) landfill tax is a clear illustration: it rose from £7 per tonne in 1998 to over £80 per tonne by 2014, a steady economic signal aimed at industries that continue to rely on disposal rather than valorisation. Incineration faces similar restrictions under Directive 2000/76/EC, this time tied to its emission profile. Together, these constraints push manufacturers to find alternatives that keep composite materials inside productive systems rather than letting them become environmental liabilities [5].

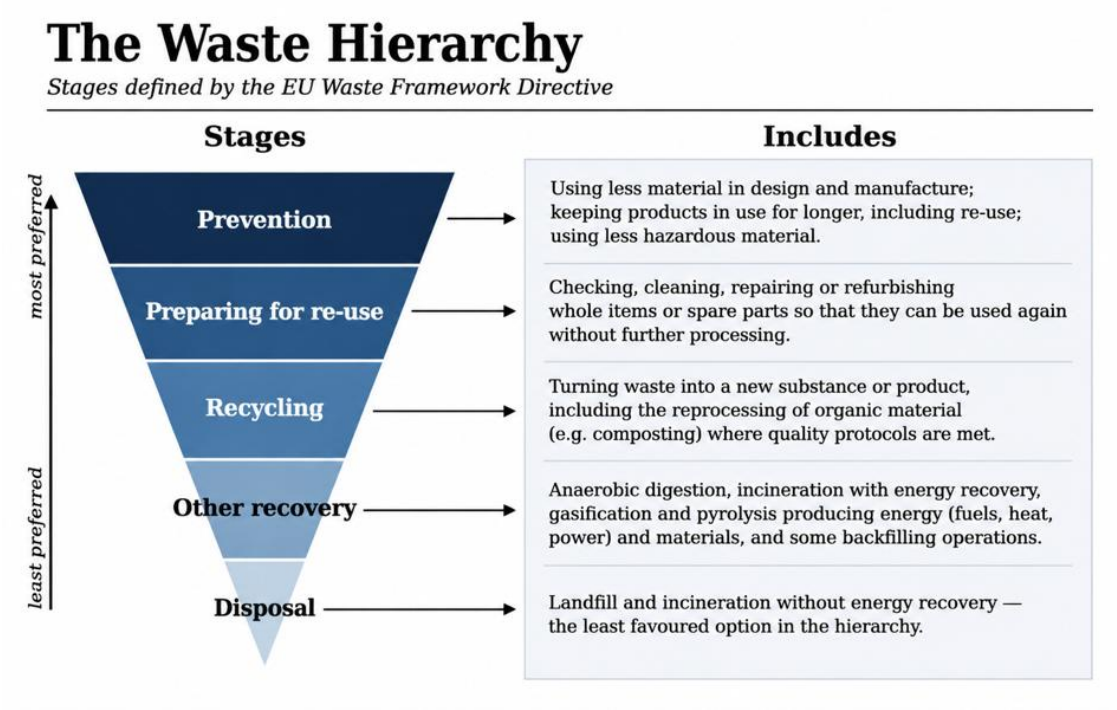


Figure 1-2 Waste hierarchy framework (adapted from [7])

Moving manufacturing powder waste up the hierarchy depends on finding reuse pathways that can absorb the material at a meaningful scale. Construction materials and cementitious systems in particular, offer a pathway. Cement and concrete sectors consume enormous volumes of raw materials and are themselves under pressure to reduce their environmental footprint. The production of one tonne of cement releases approximately 0.9 to 1 tonne of carbon dioxide, which makes cement one of the most carbon-intensive construction materials currently in use [6]. Replacing part of the cement or aggregate content with composite manufacturing powder, therefore, offers a dual benefit: it diverts an industrial by-

product from disposal while simultaneously reducing the environmental burden of cementitious material production [6].

This pathway has already drawn experimental attention. Preliminary work has shown that wind turbine blade composite powder can partially replace cement, sand, or both in mortar formulations, with replacement levels up to 20% without compromising mechanical integrity. [6]. Similar experimental studies using powder derived from retired blades have confirmed that this waste, when used as a sand replacement, can enhance mechanical performance and reduce several environmental impact categories, including acidification, climate change, land use, and water consumption [10].

This research targets the intersection of three issues. The technical case for reusing blade composite powder is already established, regulatory pressure on disposal routes is tightening, and the environmental side of the argument has not been quantified. Existing studies on blade composite powder in cementitious materials report promising mechanical and durability outcomes, but they consistently flag the lack of quantitative environmental assessment as a limitation that still needs to be addressed [6].

This dissertation picks up where Bettini et al. [6] left off. Their experimental campaign tested wind turbine blade powder waste as a partial substitute for cement, sand, and combined cement and sand in cementitious mortars, at replacement levels from 5% to 40%. The mechanical results were encouraging: substitution could be pushed beyond 20% without losing structural integrity. That missing environmental assessment matters because mechanical performance alone cannot confirm sustainability: a mortar that retains strength while significantly increasing embodied carbon or resource consumption would offer no net benefit over conventional alternatives. That is the gap this work sets out to fill, through a cradle-to-gate life cycle assessment of the same substitution strategies and replacement levels.

1.2. Objectives

The preceding discussion establishes that wind turbine blade manufacturing powder is accumulating without adequate disposal pathways, that its incorporation into cementitious mortars is technically feasible, and that its environmental performance has not been quantified. This dissertation addresses this knowledge gap by evaluating the sustainability performance of cementitious mortars incorporating wind turbine powder waste through a structured Life Cycle Assessment (LCA).

The main objective of this research is to determine the substitution levels and replacement strategies at which wind turbine blade powder waste (WTB) provide a measurable-environmental benefits compared with a conventional cementitious mortar.

Specific sub-objectives that structure the investigation:

- To quantify the environmental impacts of nineteen cement mortar formulations incorporating WTB powder at substitution levels between 5% and 40%, considering six environmental impact categories for a same functional unit.
- To compare the environmental performance of three substitution strategies (cement replacement, sand replacement, and combined replacement) with that of a conventional reference mortar providing the same function.
- To evaluate the sensitivity of the environmental results to the allocation method applied to the blade powder by analysing three scenarios representing different assumptions regarding its economic value and regulatory status.
- To identify the life cycle stages and material flows that dominate the environmental profile of the studied formulations and to assess how their relative contributions change with the introduction of wind turbine powder waste.
- To examine whether the formulations with the best environmental performance also satisfy the required mechanical and durability properties, thereby identifying the substitution strategy that provides the best balance between environmental and technical performance.

1.3. Structure of the Dissertation

The dissertation is divided into six chapters. Together they trace a single argument from the framing of the problem through to the environmental assessment of the proposed reuse strategy, and each chapter carries one or more of the objectives set out in Section 1.2.

Chapter 1 introduces the research context, defines the objectives of the study, and outlines the structure of the dissertation. It establishes the motivation for the research, clarifies its scope by focusing on waste powder generated during the manufacturing of wind turbine blades rather than end-of-life blade waste, and positions the study within the broader context of composite waste valorisation and the development of more sustainable cementitious construction materials.

Chapter 2 opens with an overview of wind turbine blade design and function, moves through the fibre reinforcements and polymer matrices that form the composite, and ends with a discussion of how waste is generated during blade production and how it is currently managed. This is the foundation for the first dissertation objective: characterising the powder waste and distinguishing it clearly from decommissioning residues.

Chapter 3 it reviews the main recycling strategies available for composite materials, with particular attention to mechanical processing since this is the route that produces powder comparable to trimming and milling scrap. Potential applications in construction materials are outlined, and the chapter closes with the challenges and limitations that continue to hold back large-scale implementation. This background prepares the ground for the environmental assessment by identifying which reuse pathways are already technically validated and therefore worth assessing.

The life cycle assessment framework is built up in Chapter 4. It begins with the fundamentals of LCA as defined by ISO 14040 [11] and ISO 14044 [12], then examines how the methodology has been applied more broadly, and sets out why LCA is the right tool for evaluating blade-waste repurposing in particular. The chapter closes with the specific approach adopted in this study: the functional unit, the cradle-to-gate system boundary, the impact categories selected under ISO 14040 [11], and the inventory data used. This chapter carries the second and third objectives of the research, the application of the LCA framework and the construction of the inventory.

Chapter 5 presents and discusses the results of the life cycle assessment across the three scenarios defined in Chapter 4. For each scenario, the characterised environmental impacts of the nineteen mortar formulations are reported, normalised using a min–max procedure, and aggregated into a single sustainability score. The results show a consistent environmental ranking across all six impact categories and all three allocation treatments. A sensitivity analysis examines the relationship between environmental performance and the measured mechanical and durability properties of the mortars. The chapter closes with a cross-scenario comparison that evaluates how sensitive the environmental conclusions are to the treatment of the wind turbine blade powder.

Chapter 6 closes the dissertation; it brings together the main findings and reflects on how far each has been achieved. The chapter also outlines directions for future research, including the lines of investigation that were kept outside the present scope, and discusses what the findings mean for industry, policy, and the continued development of circular strategies for composite manufacturing waste.

2. WIND TURBINE BLADES AND COMPOSITE MATERIALS

2.1. Overview of Wind Turbine Blades

Wind turbine blades convert kinetic energy from air flow into mechanical rotation. The rotation is then transformed into electrical power by downstream systems. Blade design combines aerodynamic shaping with structural capacity to withstand cyclic loads and fatigue across service lives of around 2 decades or more [13].

In more detail, a wind turbine consists of four principal components: a foundation, a tower, a nacelle, and a set of three blades. The blades capture aerodynamic energy from the wind and transfer it to the drivetrain housed inside the nacelle, while the tower and foundation provide structural support and stability. Among these components, the blades are the only part fabricated from polymer composite materials, and their environmental and technical management therefore differs from that of the steel and concrete elements that constitute the rest of the turbine assembly [2].

Aerodynamic and structural requirements that vary along the span of the component dictate the geometry of a wind turbine blade. The blade root features a circular or slightly elliptical cross-section that connects to the turbine nacelle through a bolted metallic joint; thereafter, the cross-section narrows and assumes an aerodynamic profile, with the side walls becoming progressively thinner toward the tip where wind-induced stresses are lower. Internal stiffeners run transversely across the blade interior to prevent lateral and local buckling under operational loads, while the greater portion of the structure is fabricated as sandwich panels in which two composite skins enclose a low-density core of balsa wood or polyurethane foam, an arrangement that increases bending stiffness without adding excessive mass [10].

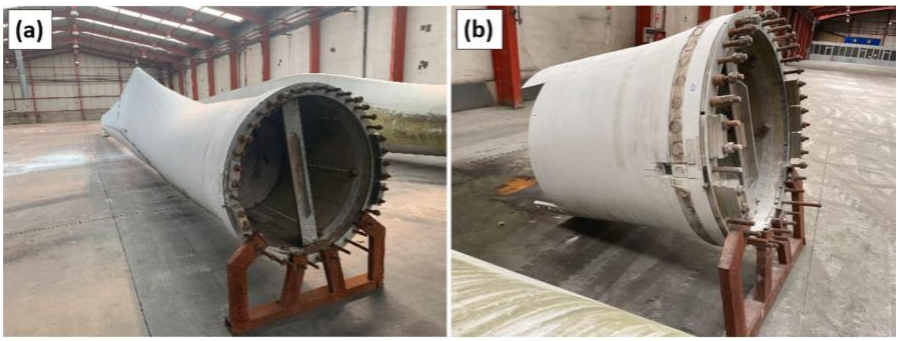


Figure 2-1 Wind Turbine Blade: a) general view- and b) root section with bolted metallic joint Adapted from [13]

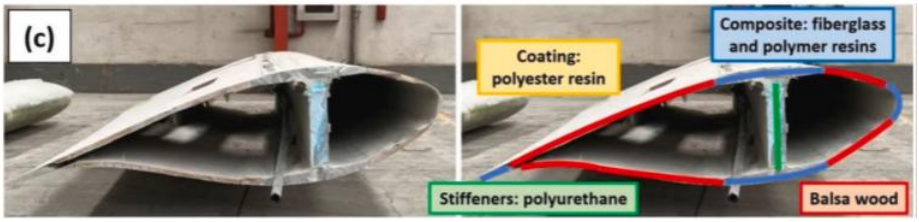


Figure 2-2 Win Turbine Blade cross section Adapted from [14]

Blade dimensions have grown substantially across successive generations of wind turbines. First-generation blades measured between twenty and thirty-five metres in length and weighed between 1.2 and 2 tonnes per unit, whereas blades produced today commonly reach fifty-five metres or more [10]. Modern commercial blades are large composite structures. The Nordex N43 blade, examined by Menna et al. [13], provides a representative example of conventional blade architecture. The blade measures 19.1 m in length and has an approximate mass of 2 tonnes. It forms part of a three-blade rotor with a diameter of 43 m and a swept area of 1,452 m^2. The associated turbine has a nominal output of 600 kW, a calculated operational lifetime of 20 years, and a rated survival wind speed of 70 m/s [13].



Figure 2-3 cross section of WTB, Explanation of numbers in picture: 1. Solid GFRP Laminated Panels; 2. Sandwich Panels adapted from[13]



Figure 2-4 Longitudinal section of WTB, Explanation of numbers in picture: 2. Sandwich Panels; 3. GFRP mesh adapted from [13]

The internal architecture of the blade is not uniform. Aerodynamic surfaces such as the leading edge, trailing edge, and shear webs use sandwich construction to deliver high stiffness at low weight. Spar caps, which carry the dominant longitudinal bending loads, are produced as monolithic laminates to maximise stiffness along the blade axis. The upper and lower halves of the blade is fabricated separately and joined using structural adhesive bonds. A polyurethane surface coating protects the assembled blade from environmental degradation and surface wear [9].

The materials used for blade construction have evolved substantially since the early stages of the wind energy industry. Metal was the dominant material in the 1940s, but it was replaced by composite materials during the 1970s due to the superior strength-to-weight properties of fibre-reinforced polymers [4]. Composites now account for more than 90% of the total weight of a wind turbine blade, making them the principal material concern from an environmental and waste-management perspective [2, 4].

The deployment of wind energy has expanded considerably over the past three decades. Global installed wind capacity rose from 7,600 MW in 1998 to 364,270 MW in 2014, reflecting a sustained pattern of

annual growth [2]. Capacity reached approximately 540 GW by 2017 and is projected to reach 5,800 GW by 2050 [13].

As showed before in Figure 1-1 European data show that cumulative installed capacity reached 275 GW by 2023, accompanied by yearly gross installations exceeding 200 GW in recent years [4].

A quick view of the composite production reflects the rate at which renewable energy infrastructure has been deployed, with the European composites market reaching approximately 3 million tonnes in 2021 and global production exceeding 12 million tonnes during the same period. Within these totals, glass fibre reinforced polymers occupy the largest share of the specialised composite segment, and their volume has tripled in recent years [6].

As an example, in the United Kingdom, wind energy accounts for 33% of national composite consumption, placing the sector immediately behind aerospace as the second-largest end-user of these materials [7]. Although the wind sector remains second to aerospace in total composite consumption, the physical size of individual blades and the volume of finishing operations they require make blade production a substantial generator of pre-consumer composite waste [7].

The volume distribution within the blade reflects this design. Approximately one-third of the blade volume consists of solid GFRP laminated panels. The remaining two-thirds is composed of sandwich panels combining GFRP skins with rigid polyurethane foam cores [4]

The internal structure of a modern blade reflects functional zoning of materials according to mechanical demands. Rotor blades exceeding 60 metres in length are typically fabricated with spar caps composed of epoxy resin reinforced with carbon fibre laminate or glass fibre laminate, while the spars and half-shell employ a sandwich construction of epoxy resin glass fibre laminate. External protection is provided by a polyurethane-based coating system designed to resist environmental exposure during the operational service of the turbine [15].

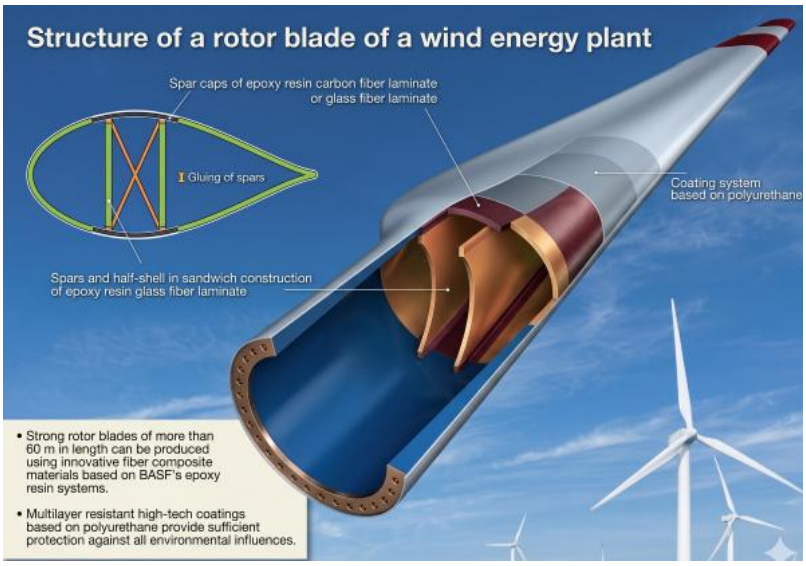


Figure 2-5 Cross-section of a wind turbine blade identifying spar caps adapted from [15]

2.2. Materials Used in Blade Manufacturing

Within the broader family of fibre-reinforced polymers, four main categories are recognised: glass fibre reinforced polymer (GFRP), carbon fibre reinforced polymer (CFRP), aramid fibre reinforced polymer (AFRP), and basalt fibre reinforced polymer (BFRP). Glass fibre sales account for approximately 65% of total FRP material profits [16].

Wind turbine blades are predominantly fabricated from glass fibre reinforced polymer composites [6]. These composites combine a fibre reinforcement that carries mechanical load with a polymer matrix that binds the fibres and transfers stress between them [16].

Quantitative analysis of blade laminates reports that reinforcing fibres account for approximately 60% to 70% of the composite mass, while the polymer matrix accounts for the remaining 30% to 40% [17].

2.2.1. Fiber Reinforcement

Polymer composites used in blade manufacturing are reinforced predominantly with glass fibre, with smaller proportions of carbon fibre and hybrid glass-carbon configurations [2]. The selection of fibre type is governed by mechanical performance requirements and material cost. The earliest generations of composite blades produced during the 1970s used E-glass fibre combined with unsaturated polyester resin, a system referred to as Glass Fibre Unsaturated Polyester composite system GF-UP [4]. Carbon fibre entered blade manufacturing in the 2000s and was primarily paired with epoxy resin, producing the

Carbon Fibre–Epoxy composite system (CF-EP) system that partially replaced GF-UP in load-bearing zones [4].

The mechanical and economic properties of these fibres differ substantially. Glass fibre has a density of 2.55–2.6 g/cm³ and a market price between 1.28 and 2.56 GBP/kg, with a tensile strength of 1,900–2,050 MPa. Carbon fibre has a density of 1.8–1.84 g/cm³, a market price between 19.7 and 26.4 GBP/kg, and a tensile strength of 4,400–4,800 MPa. When combined with epoxy resin, GF-EP composites exhibit a fatigue strength of 400 MPa, while CF-EP composites reach 1,500 MPa under equivalent testing conditions [4]. These performance advantages of carbon fibre, however, come with a substantially higher environmental burden: its embodied energy and global warming potential are approximately an order of magnitude above those of glass fibre [4]. The selection of fibre type in blade manufacturing is therefore not determined by mechanical performance alone it reflects a balance between structural demands, production cost, and embodied environmental impact. This is why glass fibre dominates the blade shell and skin, where its lower cost and environmental footprint are sufficient for the loading conditions, while carbon fibre is reserved for the spar caps, where its superior fatigue resistance justifies the additional cost and impact [18].

The cost difference between the two fibres restricts the use of carbon fibre primarily to spar caps, which carry the principal loads in the blade structure, while glass fibre dominates the remaining shell and structural regions [4].

2.2.2. Polymer Matrices

The polymer matrix in blade composites performs two functions: it transfers loads between fibres and it protects the fibre network from environmental degradation. Industrial GFRP applications typically employ either Unsaturated Polyester (UP) or epoxy resins, both of which form cross-linked thermoset networks upon cure [8].

The matrix component of blade composites consists almost exclusively of thermosetting polymeric resins [6]. High-grade epoxy and polyester are the two mainstream resin systems used in industrial blade production [2]. UP was widely used in earlier blade generations, but after 2013 epoxy (EP) became the dominant matrix for large-scale blades due to its superior mechanical performance [4].

The properties of these two resins differ in mechanical, physical, and economic terms. Epoxy resin has a density of 1.11–1.4 g/cm³, a market price of 2.32–4.31 GBP/kg, and a tensile strength of 45.0–89.6 MPa [4]. Unsaturated polyester resin has a density of 1.04–1.4 g/cm³ and a market price of 1.89–1.97 GBP/kg [4] and a tensile strength of 63 ± 2.0 MPa [19]. The lower price of polyester partly explains its

persistence in certain manufacturing applications, although epoxy continues to dominate in blades requiring higher fatigue resistance.

Epoxy resin is the most common matrix in modern blade composites. The elemental composition of epoxy resin, determined by combined thermogravimetric and infrared analysis, consists predominantly of carbon, oxygen, and hydrogen. The principal functional groups of epoxy resin include the epoxide ring, hydroxyl, amine, thiol, carbonyl, and anhydride groups [1].

Unsaturated polyester is a second thermoset matrix used in blade and broader GFRP applications. Zhou et al. [20] identified unsaturated polyester as the main resin in two of three industrial GFRP powder samples through some analyses. The third sample contained both polyester and epoxy resin signatures. This finding shows that blade manufacturing waste can contain more than one matrix type, depending on the specific components from which the powder is derived.

Polyurethane is also present in blade construction, although not as a structural matrix. The Nordex N43 blade described by Menna et al. [13] uses polyurethane as the foam core in its sandwich panels and as the surface coating applied for environmental protection. The combined presence of GFRP, polyurethane foam, and polyurethane coating produces a heterogeneous waste stream when blade material is mechanically reduced.

The thermoset character of these matrix systems determines the recycling options available for blade-derived material. Once cured, polyester and epoxy networks cannot be reshaped or remelted by thermal processing, a constraint that distinguishes them from thermoplastic polymers and forces alternative end-use strategies [8]. Thermogravimetric analysis of blade powder waste confirms the thermal stability of the cured epoxy fraction and provides quantitative data on its decomposition behaviour, illustrating the chemical permanence of the cross-linked network [6]. The cross-linked architecture of the cured matrix is the principal reason that mechanical pulverisation, rather than thermal or chemical reprocessing, remains the most viable processing route for blade composite waste, and it justifies the powder-form valorisation strategy investigated in the present work [6, 8].

The behaviour of the resin fraction can be observed in the thermogravimetric profile of milling powder. Reported in Bettini et al. [6] study, thermogravimetric analysis of wind turbine blade powder waste shows a marked mass decrease between 300 °C and 450 °C, which corresponds to the combustion of the epoxy resin component in air. The presence of this organic phase is also responsible for the chemical interaction observed when the powder is incorporated into cementitious systems. Epoxy and polyester resins react with the alkalis present in the cement mix, producing a reduction in pH and a corresponding decrease in the rate of cement hydration.

The combination of an amorphous silicate fibre with a permanently cross-linked thermoset matrix defines the material identity of the powder waste examined in this dissertation [3, 6]. Reactive oxide content within the fibre phase suggests possible cementitious activity under alkaline conditions, since silicon and aluminium present in the glass can react to produce C-(A)-S-H gel within a cement paste. The thermoset fraction, however, introduces an organic component that does not contribute to hydration and may interact with the alkaline environment in ways that reduce pH and interfere with cement setting [6].

2.3. Manufacturing Processes and Waste Generation During Production

2.3.1. Blade Fabrication Methods

Industrial production of wind turbine blades currently relies on two dominant manufacturing routes: pre-impregnated fabric (Prepreg) processing and Vacuum-Assisted Resin Transfer Moulding (VARTM) [2]. Among these two, VARTM has become the most widely used technology in commercial blade manufacturing, and most recent academic studies on blade production are based on this process. Alternative routes have either been excluded from contemporary practice or restricted to niche applications. Open-mould wet lay-up has been banned from composite manufacturing on environmental grounds, and filament winding, which was investigated during the 1970s, has not been adopted at an industrial scale [4].

Process mapping of composite manufacturing facilities provides a representative description of the operational sequence followed during vacuum infusion, the technique most closely related to blade fabrication. The full process flow includes hardener storage, resin storage, dry fibre storage, fibre cutting, preform placement into the mould, resin vacuum infusion, curing, demoulding, and final cutting and trimming of the cured component, with each of these stages producing characteristic waste outputs that differ in physical form and chemical composition [7]. Dry fibre offcuts emerge from the cutting and lay-up stages, resin waste accumulates during mixing and infusion, and cured composite trimmings are generated when the demoulded component is brought to its final geometry [7].

Wind turbine blades are produced as two separate composite half-shells. The upper and lower halves are fabricated independently and then joined using structural adhesive bonds. After assembly, the full blade undergoes surface finishing and coating before final inspection [13].

The cutting and trimming operations performed after curing are the stages that generate the powder fraction central to the present research. Once the laminate has cured into a cross-linked thermoset

network, geometric finishing is performed through mechanical processes that remove material as fine particulate. Equivalent operations on cured GFRP profiles produce a particulate waste composed of broken glass fibres, resin fragments, and filler material, with a particle size distribution that falls within the fine fraction range compatible with cement and aggregate replacement applications [8]. The blade manufacturing process produces an analogous powder, consisting of glass fibre fragments and cured epoxy resin particles in the proportions defined by the original laminate [6].

2.3.2. Waste Generation During Blade Manufacturing

The composite waste stream generated during blade manufacturing is a recognised category within the broader classification of composite residues, since composite materials produce heterogeneous waste of two principal types, namely end-of-life waste from decommissioned components and manufacturing waste from production rejects. Quantitative estimates compiled by 2015 placed end-of-life composite waste at approximately 251,000 tonnes and manufacturing waste at 53,000 tonnes, establishing pre-consumer scrap as a measurable category that warrants its own management strategies [5].

The waste generated during manufacturing falls into three primary categories: loss in resin, loss in dry fibre, and loss of cured composite and consumables. Dry fibre waste arises from fabric cutting operations performed prior to lay-up. Cured composite waste originates from curing defects and from the off-cuts produced during trimming after the curing stage. Resin waste accumulates from excess mixing operations, residues left within moulds, and resin retained in flow mesh consumables [4].

A finer breakdown of these streams shows that the four principal manufacturing waste sources, expressed as proportions of total in-process waste, are dry fibre off-cuts at 21%, cured composite off-cuts at 27%, flow mesh containing resin residue at 43%, and polishing dust at 9%. Polishing dust, which forms the central material of this dissertation, is produced specifically by the polishing operations applied to the cured blade surface. Two minor manufacturing-stage streams supplement these figures: defective blade waste accounts for 0.05% to 0.2% of production, and testing blade waste contributes a similar 0.05% to 0.2% [2].

Pre-consumer manufacturing scrap and end-of-life decommissioning waste are distinct streams that arise at different stages of the blade lifecycle and differ in volume, generation rate, and origin [2]. Manufacturing scrap is produced continuously during blade fabrication, whereas end-of-life waste accumulates only when turbines are decommissioned after their service period [2]. This distinction is relevant because each stream requires its own reuse strategy.

THIS PAGE WAS INTENTIONALLY LEFT BLANK

3. Recycling and Reuse of Composite Waste

3.1. Discussion on Current Waste Management Practices in Europe

The European Union Waste Framework Directive (2008/98/EC) establishes a hierarchical order of preference for managing all waste streams as shown in Figure 1-2 in Chapter 1, including composites. Prevention sits at the top, followed by preparation for reuse, recycling, other forms of recovery such as energy recovery, and finally disposal as the least desirable option [6, 7, 9]. Although this hierarchy is clearly defined in legislation, its practical application to composite materials remains limited. Composites are difficult to categorise and track, and the dominance of thermosetting resins in their formulation makes them particularly challenging to recover at the end of their life or after manufacturing rejection [6, 21]. Within this framework, landfilling and incineration without energy recovery occupy the bottom tier, while reuse and recycling align more closely with the principles of the circular economy. Powder waste generated during the manufacturing of wind turbine blades is currently going to landfill or incinerated, despite having a chemical composition that would suit higher-value applications [6, 7]. Reuse, although nominally the second-most preferred option in the hierarchy, is essentially infeasible for manufacturing powder waste, because the particulate has no original geometry to preserve and, more generally, the residual mechanical properties and the original fibre–matrix architecture of composite scrap are usually unknown [8].

Sending GFRP composite waste to landfill recovers neither the material nor any energy from it. Because the cured epoxy network is permanently cross-linked and resists biodegradation, the waste occupies space indefinitely and creates a long-term spatial burden [8, 21]. Incineration is similarly inefficient as a treatment route. The high inorganic glass fibre content of GFRP makes combustion poor in energy yield, the burning of the epoxy fraction releases harmful gases into the atmosphere, and a significant volume of non-combustible glass ash remains afterwards that still has to be sent to landfill [16, 21].

Several European countries have already moved against landfilling composite waste through national bans, including Germany, the Netherlands, Austria, and Finland [8, 16]. More broadly, EU waste legislation has progressively tightened the rules on landfilling composite materials, which has pushed up the cost of disposal and made alternative valorisation routes economically more attractive [8]. The trajectory of the UK landfill tax illustrates this trend clearly: the rate climbed from 7 Pounds per tonne in 1996 to 72 Pounds per tonne in 2013, a tenfold increase across seventeen years that reflects deliberate policy pressure against disposal [7].

Despite these pressures, composite manufacturing waste, including the trimming and milling powder generated during blade production, is still predominantly directed to landfill. A process-mapping survey of four UK composite manufacturing facilities found that three of them reported landfill as the default route for their production scrap [7]. An example from another sector, the aerospace sector provides an indication of the scale of the problem: it has been estimated that between 30% and 50% of the materials entering aircraft production are scrapped because of the way the parts are manufactured [7]. The reference paper for the present study confirms that powder waste from wind turbine blade manufacturing is currently handled through landfilling or incineration and explicitly notes the absence of an established environmental assessment of alternative management routes for this specific waste stream [6].
Despite the significant volumes of composite waste generated in Europe, the proportion that is realistically accessible for recycling remains far below the theoretical total. Barriers such as inadequate collection and sorting infrastructure, the export of components for reuse outside Europe, and parts permanently embedded in structures all reduce the share of waste that can practically enter a recycling route [22]. The gap between waste generation and recycling capacity points to the absence of dedicated pathways for manufacturing scrap in particular.

3.2. Recycling Methods for Composite Materials

Composite materials account for the overwhelming majority of a wind turbine blade's mass, with glass- and carbon-fibre-reinforced polymers typically constituting more than 90% of total blade weight [2]. As the global wind energy sector continues to expand, the volume of composite waste associated with blade manufacturing, in-service maintenance, and eventual decommissioning is projected to grow substantially over the coming decades. Liu and Barlow [2] note that landfilling, long the default disposal route for this waste stream, is becoming increasingly unsustainable from both environmental and economic standpoints, a conclusion that has driven growing interest in alternative recycling routes. Importantly, their lifecycle-based analysis demonstrates that composite waste does not arise solely at a blade's end of life: a meaningful proportion is generated during manufacturing itself, through operations such as trimming, grinding, and other in-process finishing steps. This observation underlines the relevance of the present study, which is concerned not with end-of-life blade recycling but with the powder waste generated during the manufacturing stage of blade production.

To divert composite waste from landfill and recover material value, several recycling technologies have been developed. These technologies are generally classified into three principal categories: mechanical, thermal, and chemical recycling, with hybrid approaches emerging more recently [16].

Mechanical recycling reduces composite waste into smaller fragments through cutting, shredding, and grinding, and is widely regarded as the most accessible recycling route because of its procedural simplicity and comparatively low capital investment [1]. Liu et al. [1] reported that the energy required for mechanical recycling, estimated between 0.1 and 4.8 MJ/kg, is considerably lower than that demanded by chemical recycling (21–91 MJ/kg) or thermal recycling (24–30 MJ/kg), positioning mechanical processing as the more energy-efficient of the three routes.

This favourable energy balance, combined with the comparatively low market value of virgin glass fibre relative to virgin carbon fibre, helps explain why mechanical recycling has become the dominant treatment specifically for GFRP, whereas chemical and thermal methods tend to be reserved for carbon fibre-reinforced polymer, whose higher-value fibres justify the additional processing cost [16]. The mechanical route is nonetheless not without drawbacks: shredded or milled fibres typically lose a substantial share of their original mechanical performance, with reductions in tensile capacity of up to 50% reported, alongside a loss of fibre integrity that limits the market competitiveness of the recovered material [16].

Thermal recycling encompasses pyrolysis and the fluidised-bed (gasification) process, both of which apply heat to decompose the polymer matrix and liberate the embedded fibres. Pyrolysis takes place within an oxygen-free environment and is capable of yielding longer and cleaner fibres than mechanical methods, with reclaimed lengths reported in the range of 6–60 mm [1]. When process parameters (like heating rate, maximum temperature, nitrogen flow rate, and isothermal dwell time) are carefully controlled, recovered fibre can retain up to 90% of the tensile strength of virgin material, which explains the preferential use of pyrolysis for the more valuable carbon-based composites [1, 16]. However, thermal exposure can damage the fibre surface and leave oxidation residues or char on the recovered fibre, while the gaseous by-products generated during the reaction, including carbon monoxide, require additional treatment before release [1, 16].

Chemical recycling, generally referred to as solvolysis, employs a chemical solvent (often combined with a catalyst) to break down the resin matrix under controlled temperature and pressure, and is typically classified according to whether it operates at Low Temperature and Pressure (LTP) or High Temperature and Pressure (HTP). LTP solvolysis, generally conducted below 200 °C using aggressive solvents such as nitric acid, tends to produce fibre of higher residual quality despite longer reaction times, whereas HTP

solvolysis under super- or sub-critical conditions has gained favour for being more environmentally benign [16].

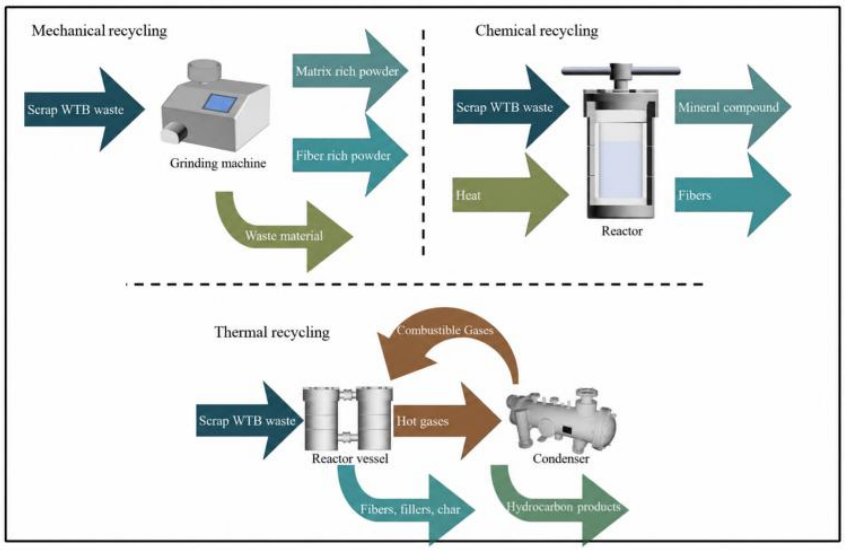


Figure 3-1 Recycling methods of WTB adapted from [16]

The selection of an appropriate recycling route ultimately depends on the characteristics of the composite waste, the intended end use of the recovered material, and the associated technical and economic constraints. As this study investigates the reuse of manufacturing-generated wind turbine blade powder, the principles and processing stages of mechanical recycling are examined in greater detail in the following section.

A further consideration is the economic logic of fibre recovery from GFRP. Life cycle assessments of these recovery pathways show that the cumulative energy demand of thermal and chemical recycling often exceeds the energy footprint of producing virgin glass fibres, which itself is around 13 to 32 MJ/kg [16, 21]. Because virgin glass fibre is itself relatively low in market value, there is little economic incentive to absorb the additional energy and chemical inputs required to liberate the fibres from a cured matrix, which weakens the case for fibre-recovery routes in this material class [16].

A further valorisation option that sits between disposal and true material recycling is cement-kiln co-processing, in which the composite waste is fed directly into a cement kiln to serve simultaneously as an alternative fuel and as a source of inorganic raw material for the clinker. The combustible polymer fraction substitutes for fossil fuel and contributes to the energy demand of the kiln, while the silica- and calcium-rich glass fraction is incorporated into the clinker mineralogy itself, replacing part of the conventional clay and limestone feed [8, 16]. Reported figures suggest that around one third of the value of the input waste

is recovered as energy and around two thirds as material, which positions co-processing as a near zero-emission treatment for composite scrap [16]. Earlier work has indicated that glass-polymer composite material can replace standard fuel in cement kilns at substitution rates of up to about 10% without significantly affecting cement performance, beyond which the boron oxide content of the glass fibres begins to interfere with the early-stage properties of the cement [8]. Although co-processing destroys the polymer fraction and therefore does not preserve the embodied value of the matrix, it currently outperforms incineration without energy recovery and remains a relevant benchmark against which alternative valorisation pathways for manufacturing powder must be compared [8, 16].

The disparity in energy footprints between recycling routes, combined with the ecological costs of conventional disposal, places mechanical processing as the most environmentally viable option, provided that a high-volume application can absorb the resulting particulate. Cementitious materials offer exactly that kind of structural sink for pre-consumer powder. The chemical composition of the glass phase in WTB waste, dominated by silicon dioxide (around 55%), calcium oxide (around 23%), and aluminium oxide (around 14%), is inherently compatible with concrete matrices and provides the reactive ingredients needed for pozzolanic activity [6, 16, 23].

3.3. Mechanical Recycling and Material Processing

The mechanical recycling of glass fibre-reinforced polymer (GFRP) composites is generally based on a sequence of physical size-reduction operations designed to transform bulky composite waste into reusable particulate materials.

According to Tao et al. [16] and Liu et al. [1], the process typically involves cutting or shredding the composite into smaller fragments, followed by crushing, grinding or milling, and finally sieving to obtain fractions with controlled particle sizes. Compared with thermal and chemical recycling, mechanical recycling requires relatively simple equipment, lower capital investment, and significantly less energy, making it the most widely adopted recycling route for GFRP composites.

A representative example of this process was reported by Menna et al. [13], who mechanically processed decommissioned wind turbine blades through successive cutting, shredding, granulation, and sieving stages. Their study showed that different blade components required different processing conditions because of differences in laminate configuration, with solid laminated sections requiring greater shredding effort than sandwich structures. This demonstrates that both the composition and structural configuration

of composite waste influence the efficiency of mechanical processing and the characteristics of the recovered material.

Mechanical recycling generally produces two principal recyclate fractions: a fine powder containing predominantly resin-rich particles and short glass fibres, and a coarser fibre-rich fraction. Tao et al. [16] and Liu et al. [1] reported that the characteristics of these fractions depend strongly on the processing conditions and the source material. Particle sizes may range from fine powders produced through intensive grinding to larger fibrous particles obtained by shredding or cutting, while bulk density, fibre content, and particle morphology vary according to the recycling process employed.

The characteristics of the recycled powder have been investigated further by Zhou et al. [20], who compared powders obtained directly through grinding with dust collected by industrial suction systems during grinding operations. Their observations showed that conventionally ground powders consisted of irregular resin particles mixed with short glass fibres, whereas the suction-collected dust contained finer and more homogeneous particles. These differences demonstrate that the method used to generate and collect the powder influences its particle morphology and composition, which may subsequently affect its behaviour when incorporated into cementitious materials.

Karuppannan Gopalraj and Kärki [24] note that mechanical recycling offers practical advantages including comparatively low energy demand and straightforward scalability to an industrial level, which has made it the most extensively studied recycling route for glass-fibre composites in particular. At the same time, the authors observe that the discontinuous nature of mechanically produced recyclate, together with its tendency to retain residual resin and surface defects, has historically confined its reuse to lower-value applications such as fillers or secondary reinforcement rather than high-performance structural composites. These limitations, together with the broader challenges associated with composite recyclate reuse, are addressed in more detail in Section 3.4. For present purposes, it is sufficient to note that the lower-value, filler-oriented applications typically associated with mechanically processed recyclate are consistent with reuse in cementitious systems; Rani et al. [21] report that mechanically recycled glass-fibre-reinforced powders and short fibres have been incorporated into cement, concrete, and mortar with mechanical properties that are improved or maintained depending on the replacement level employed.

In addition to powder characteristics, the geometry of the recovered fibres is also influenced by the mechanical processing route. Menna et al. [13] reported that fibre length, aspect ratio, and particle morphology varied according to both the blade component being processed and the sieve fraction obtained after size classification. Fibres recovered from sandwich panels generally retained higher aspect

ratios than those obtained from laminated sections, indicating that the structural configuration of the original composite influences the geometry of the recycled material.

Overall, the properties of mechanically recycled GFRP are governed not only by the recycling process itself but also by the characteristics of the original composite material and the selected processing conditions. These factors determine the particle size distribution, morphology, density, and fibre geometry of the recyclate, which ultimately influence its suitability for incorporation into cementitious materials. The application of mechanically processed GFRP powder and fibres in construction materials is discussed in the following section.

3.4. Potential Applications in Construction Materials

The incorporation of GFRP and Wind Turbine Blade Waste (WTBW) recyclate into cementitious systems has been explored along two broad conceptual lines: as a partial replacement for one of the conventional mix constituents (sand, coarse aggregate, or cement) and as a discrete reinforcing element added to the mix [1, 16]. The published studies report several common trends within each of these categories, although the magnitude and even the direction of the effect on mechanical performance varies considerably according to particle morphology, dosage, and the specific source of the recyclate.

Once mechanically processed into filler-size or fibre-size recyclate, glass-fibre-reinforced polymer (GFRP) waste becomes a candidate for incorporation into cementitious construction materials, most commonly as a partial substitute for fine aggregate [8, 21]. This application is of particular relevance to manufacturing-stage powder waste, since the filler-size fraction produced by cutting and grinding operations corresponds closely in particle morphology to the material that has been trialled as a sand replacement in concrete and mortar.

Across the available studies, partial replacement of fine aggregate with WTBW or GFRP powder produces a reduction in compressive strength in the majority of cases, generally attributed to the lower intrinsic strength of the recyclate relative to natural sand, a weaker interfacial bond arising from the irregular or cylindrical particle shape, and an increase in mixture porosity associated with the higher water demand of the waste material [1, 16]. Liu et al. [1] reported that replacing 7.5 wt% of sand with mechanically shredded WTBW powder produced an approximately 18% drop in 28-day compressive strength alongside a 4% increase in porosity, with the additional water demand attributed to the formation of a water film around the rough, irregularly shaped waste particles. Within the broader GFRP literature, Tao et al. [16] likewise reported reductions in compressive strength following fine-aggregate replacement, citing factors

such as the cylindrical particle shape of the recyclate and uneven distribution within the mix, although they also noted that some studies report increased or retained strength at low replacement levels, an outcome generally explained by a filler effect in which fine recyclate particles occupy voids between aggregates and densify the matrix.

The use of finely ground WTBW powder as a partial replacement for cement has received considerably less attention than its application as an aggregate substitute. Nevertheless, the available literature indicates that the mechanical performance of cementitious materials is governed primarily by the composition of the recycled powder, particularly its organic constituents. Liu et al. [1] reviewed experimental studies in which WTBW powder, ground to a particle size finer than cement (approximately 3 μm), replaced cement at levels between 10 and 30 wt%. The reported results showed progressive reductions in 28-day compressive strength, reaching approximately 26%, 64%, and 67% at replacement levels of 10%, 20%, and 30%, respectively. According to Liu et al. [1], these reductions were mainly associated with the presence of resin and residual wood particles, which interfere with cement hydration and increase the void content of the hardened matrix.

Similar conclusions were reported by Tao et al. [16], who noted that removing the wood fraction before incorporation significantly improved performance. At a 10 wt% replacement level, the strength reduction decreased to approximately 16%, while treated powder achieved compressive strength comparable to the reference mixture after 90 days of curing [16]. Both studies also observed that flexural strength was less affected than compressive strength, with an average reduction of approximately 6% for every 10 wt% of cement replaced. This behaviour was attributed to the presence of short fibrous fragments within the powder, which provide a limited micro-reinforcing effect and partially compensate for the reduction in compressive performance [16].

Where GFRP or WTBW recyclate is introduced as a discrete reinforcing addition rather than as a replacement for an existing constituent, the dominant effect reported across the literature is an improvement in flexural strength and toughness, generally attributed to a fibre-bridging mechanism that restrains crack propagation, often at some cost to compressive strength or workability [16]. Tao et al. [16] reported that incorporating recycled glass fibre as a supplementary reinforcing material improved compressive strength by up to 45% at higher fibre content and length, an outcome linked to the rough, resin-coated fibre surface promoting a stronger bond with the matrix and to the formation of calcium silicate hydrate gel along the fibre surface. Flexural strength improvements were still more pronounced, with gains ranging from roughly 14–58% depending on fibre dosage and replacement basis, and with longer fibres and a higher length-to-width ratio (above approximately 6) consistently associated with

greater flexural enhancement. Toughness followed the same trend, increasing progressively with both fibre content and fibre length, while workability declined as fibre dosage and length increased, owing to fibre conglomeration and the higher specific surface area of fibrous recyclate raising water demand [16]. Correia et al. [8] provide direct experimental evidence on this question, having investigated the technical feasibility of replacing fine aggregate with GFRP waste powder (GFRPW) generated during the cutting of pultruded profiles, at volumetric substitution rates of 0%, 5%, 10%, 15%, and 20%. Their results revealed a clear dependence of concrete performance on the level of substitution, which the authors characterised through three distinct behaviour zones defined by the water/cement ratio response. At low substitution (up to approximately 5%), the rounded morphology and low surface roughness of the GFRPW particles produced a modest filler effect, reducing porosity and slightly lowering the water/cement ratio relative to the unmodified reference mixture; this translated into a small improvement in water absorption by immersion. Beyond this range, the negative influence of the waste particles' high specific surface area progressively outweighed the filler benefit, so that water demand and the water/cement ratio rose sharply at substitution levels above 10% [8]. With respect to mechanical performance, even the low-substitution mixture exhibited only marginal reductions in tensile splitting strength and elastic modulus but a markedly larger loss in compressive strength, while higher substitution rates produced substantial reductions across all measured properties [8]. On this basis, Correia et al. [8] concluded that the reuse of fine GFRP cutting waste in concrete is technically feasible only at low incorporation rates and is best suited to non-structural applications, such as architectural concrete or pavement slabs, where compressive strength is not the governing design requirement.

Although many published studies have investigated mechanically recycled GFRP obtained from end-of-life composites, comparatively fewer have examined powder generated directly during the manufacturing of wind turbine blades. Nevertheless, the available evidence indicates that manufacturing-generated powder possesses similar physical characteristics and can therefore be considered a promising secondary material for incorporation into cementitious systems. This forms the basis of the experimental programme presented in the following chapters.

3.4.1. Challenges and limitations of Recycling

While the preceding sections demonstrate that mechanically recycled GFRP and WTBW material can, under favourable conditions, enhance the mechanical performance of cementitious composites, the literature also documents a consistent set of processing, chemical, and durability-related constraints that limit the reliability and scalability of this approach. These constraints span the practical and economic

limitations of mechanical recycling itself, the chemistry of the waste–cement interaction, gaps in long-term durability evidence, and an underexplored expansion mechanism specific to ultrafine recyclate.

- Mechanical Recycling Constraints and Practical Implementation

Although mechanical grinding is comparatively energy-efficient and straightforward to scale, several studies highlight a persistent gap between the technological maturity of the process and its practical, large-scale uptake. Rybicka et al. [5] note that the technology-readiness gains achieved in glass-fibre mechanical recycling have not been matched by an equivalent expansion in the supporting collection and processing infrastructure, leaving a continuing gap between what is technically demonstrable at laboratory or pilot scale and what is presently deployed commercially.

This infrastructural gap is compounded by intrinsic limitations in the quality of the resulting recyclate. Zhang et al. [25] note that residual resin remaining on the surface of mechanically recycled glass fibres can weaken the interfacial bond formed with a new matrix material, and that the resin-rich and fibre-rich powders produced by this route are generally regarded as low-value by-products rather than high-performance reinforcements. Rani et al. [21] similarly report that the mechanical recycling process tends to introduce surface defects and length reduction in the recovered fibres, degrading their mechanical properties relative to virgin material and consequently limiting their value; the authors further note that, because virgin glass fibre is itself comparatively inexpensive, the economic incentive to invest in upgrading mechanically recycled glass fibre is correspondingly weak [21]. Karuppannan Gopalraj and Kärki [24] reach a related conclusion, observing that glass-fibre recyclate produced by mechanical grinding has historically struggled to compete commercially as a filler, given the ready availability of cheaper virgin alternatives such as calcium carbonate or silica. Taken together with the absence of a universally accepted recycling standard noted by Karuppannan Gopalraj and Kärki [24], and the trade-offs Rani et al. [21] identify across mechanical, thermal, and chemical routes, where gains in resin removal efficiency or fibre-strength retention are typically achieved only at the cost of increased energy consumption, processing complexity, or capital expenditure. These findings indicate that no single recycling method simultaneously optimises for fibre quality, cost, and throughput.

The physical characteristics of mechanically processed recyclate present a further constraint specific to its incorporation in cementitious systems. As discussed in Section 3.3, Correia et al. [8] identify particle shape irregularity and the comparatively high specific surface area of GFRP cutting waste as factors that increase water demand and disrupt the cement matrix interface, while the inherent hydrophobicity of the resin-bearing particles further limits compatibility with the surrounding paste. These morphological characteristics, rather than any single chemical incompatibility, appear to be the principal mechanism by

which higher substitution rates erode mechanical performance, reinforcing the conclusion that low-level incorporation is the more technically defensible strategy for this material [8].

Taken together, these findings indicate that the principal obstacles to wider reuse of mechanically recycled glass-fibre powder are not solely a matter of chemical feasibility but also of economic value, interfacial compatibility, and supporting infrastructure, a context that reinforces the rationale for directing such powder toward low-substitution applications in cementitious mortar, where the demands placed on fibre quality are markedly lower than in structural composite reuse.

- Chemical and Physicochemical Barriers to Cement Hydration

Beyond these processing and economic constraints, a further set of limitations arises from the chemical interaction between the organic resin fraction of the recyclate and the cement hydration system itself. A mechanism distinct from the morphological water-demand effect discussed above, since it is driven by the chemistry of the resin rather than the physical shape of the particles. Liu et al. [1] identified three principal mechanisms that constrain the application of WTBW in cementitious matrices, each linked to the organic resin fraction of the waste rather than to its glass-fibre content. The first concerns water availability: although the glass fibre component of WTBW is hydrophobic and has little direct effect on water consumption, the hydroxyl groups present in epoxy resin form hydrogen bonds with pore-solution water, reducing the water available for cement particle hydration [1]. Because the resulting hydration products depend on adequate water supply, this mechanism limits the formation of portlandite and, in turn, of calcium silicate hydrate gel, with consequences for long-term strength development [1].

The second mechanism relates to a reduction in pore-solution pH: the epoxide ring, the dominant functional group in WTBW derived resin, undergoes a ring-opening reaction that consumes substantial quantities of hydroxyl ions, lowering pH and thereby slowing the dissolution of cement clinker and the precipitation of hydration products. Liu et al. [1] noted that this effect intensifies as particle size decreases, since finer WTBW fragments expose a greater proportion of epoxide groups to the pore solution, and that the resin's tendency to adsorb onto cement particle surfaces compounds the retarding effect, manifesting as extended setting time and reduced early-age strength.

The third mechanism is a broader incompatibility between the cement matrix and the organic resin phase: epoxy resin reduces the nucleation rate of cement clinker, introduces voids and pores into the hardened matrix, and weakens the interfacial transition zone between waste particle and binder, a cement-specific interfacial effect distinct from the fibre–matrix bonding issue raised by Zhang et al. [25] in the context of fibre reuse generally with the cumulative effect of these processes generally producing lower mechanical performance than an equivalent plain cement matrix [1]. The same review further observed that achieving

a uniform distribution of fibrous WTBW elements within the mix is itself a practical challenge, since although well-dispersed fibres can supply nucleation sites for hydration and help control plastic shrinkage cracking, swelling or agglomeration of fibrous material particularly at small particle sizes can introduce internal defects that reduce strength rather than improve it [1].

- Durability Limitations and Remaining Knowledge Gaps

A further category of limitation concerns the durability performance of GFRP-modified cementitious composites, an area in which the evidence base remains considerably thinner than that available for short-term mechanical strength. Tao et al. [16] reported that porosity generally increases with rising recycled GFRP content, with one cited study showing total porosity rising from 16% to 21% as fine-aggregate replacement increased from 0 to 10 wt%, and another reporting a near-linear increase in void content from 27% to 47% as GFRP content rose from 7.5% to 37.5 wt%; these increases were directly associated with the corresponding loss of compressive strength discussed in Section 3.3. The relationship is not strictly monotonic, however, since several studies cited by Tao et al. [16] found that porosity initially decreases at low recycled GFRP dosage before rising again at higher replacement levels as inter-particle voids generated by the recyclate begin to dominate.

Alkali–silica reaction (ASR) represents a related durability concern given the high reactive silica content of glass fibre, yet Tao et al. [16] reported that, in the studies reviewed, ASR expansion in recycled GFRP-containing concrete remained below recommended standard limits, an outcome attributed to the protective effect of the resin coating that encloses and shields the glass fibres from alkaline attack. The same review cautioned, however, that this finding applies primarily to small recyclate dosages of around 4% of total mass, and that the impact of larger or differently sized GFRP fractions on ASR expansion, together with the influence of testing duration, remains insufficiently investigated.

Drying shrinkage was generally found to improve with recycled GFRP incorporation, with reductions of up to 50% reported at moderate powder dosage, although results were not entirely consistent across studies and at least one case showed a slight increase in shrinkage attributable to the higher porosity and lower stiffness of the recycled fibre offering less resistance to shrinkage deformation [16].

Water absorption followed a comparable pattern, decreasing markedly at low-to-moderate replacement levels before converging toward, or in some cases exceeding, the absorption of the unmodified control at higher dosages, consistent with the porosity trends described above. Beyond these specific indicators, Tao et al. [16] explicitly identified the durability evidence base as incomplete, noting that the behaviour of recycled GFRP-containing concrete under aggressive exposure conditions (including acid attack, carbonation, and chloride ingress in marine environments) has not yet been examined, and that

mechanical properties such as modulus of elasticity, impact resistance, and abrasion resistance remain comparatively under-researched relative to compressive and flexural strength.

- Expansion Mechanisms in Ultrafine GFRP Recyclates

The particle-size sensitivity already noted before in the hydration-chemistry mechanisms extends to a more specific and, according to the reviewed literature, previously unexplained limitation: the volumetric expansion observed in mortar containing very fine, suction-collected GFRP dust. Zhou et al. [20] traced this behaviour to a gas-generating chemical reaction between the dust and the alkaline cement pore solution, rather than to the superabsorbent particle behaviour or high free-lime content that earlier studies had proposed as possible explanations. By isolating the dust in a sodium hydroxide solution and analysing the resulting gas by chromatography, the authors identified hydrogen, carbon dioxide, methane, ammonia, and ethane as reaction products, and attributed their formation to the residual amine curing agent and metallic oxide filler retained within the dust reacting with the alkaline environment; critically, the measured gas volume closely matched the observed expansion of the fresh mortar, confirming gas evolution as the direct cause.

This expansion mechanism had measurable downstream consequences: at 6 wt% dust content, compressive strength fell by close to 40% and flexural strength by up to 19.3%, while density decreased and water absorption increased, reflecting the additional porosity and microcracking introduced during the fresh-state expansion [20]. Microstructural examination supported this interpretation, showing that dust-containing pastes developed a less compact, fibrous form of calcium silicate hydrate gel together with elevated quantities of calcium hydroxide and monosulfate crystals, both indicative of a lower overall degree of hydration than was observed in mixtures containing the coarser ground powders [16, 20].

Zhou et al. [20] tested several mitigation strategies and found that only the addition of silica fume meaningfully suppressed the expansion, attributed to its pozzolanic reaction consuming the available alkaline reactants more rapidly than the dust itself could react; by contrast, adding superplasticiser increased expansion further by improving cement particle dispersion and thereby the contact area available for the dust reaction, while pre-saturating the dust in water or substituting part of the cement with fly ash produced expansion levels comparable to the unmodified dust mixture, ruling out water absorption as the underlying cause.

3.5. WTB Powder Reuse in Cementitious Materials

The findings summarised above derive largely from GFRP recyclate in general, but a smaller body of work has examined powder and fine recyclate obtained specifically from wind turbine blades, and these studies define more precisely the conditions under which powder reuse succeeds or fails. Baturkin et al. [26] incorporated WTB-derived GFRP into concrete in three forms of powder, aggregate, and short fibres, and found that the format of the recyclate governs its effect on the hardened material. The as-received powder reduced mechanical strength, a loss the authors traced to the balsa wood retained in the blade laminate rather than to the glass–resin fraction itself. Once the wood content was removed, concrete containing 10% of the treated powder as a cement substitute reached long-term strength equivalent to the reference mix, and the fibre fraction increased flexural capacity by around 16%. Two practical conclusions follow: the composition of the powder, in particular its organic impurities, matters more than the substitution level alone, and a simple pre-treatment step can shift the powder from a strength-reducing filler to a viable cement substitute.

The influence of particle size on this behaviour has since been isolated experimentally. Liu et al. [27] fractionated mechanically shredded WTB waste into size classes between 0.063 mm and above 8 mm and incorporated each into mortar. The finest fractions (0.063–2 mm) exposed a larger proportion of bare glass surface, showed measurably higher chemical reactivity in the alkaline pore solution, and improved compressive strength while reducing porosity, which supports their use as a supplementary cementitious material. The coarser fractions, on which the epoxy resin remained largely intact, behaved instead as inert or defect-introducing inclusions, increasing porosity and lowering strength. The resin coating did, however, protect the glass from alkaline attack, so the coarse fractions exhibited lower early alkali–silica expansion. This size dependence explains much of the apparent contradiction in earlier results: whether WTB recyclate acts as a reactive powder or as a weak inclusion is determined primarily by how finely it is ground and how much resin surface is broken open.

The importance of matching the recyclate fraction to the substitution target is confirmed by Rucka and Kurpinska [28], who tested two fractions of shredded end-of-life blade material in cement mortar. The coarser fraction, used as a partial aggregate replacement of up to 40% by volume, densified the mixture and improved performance substantially, reducing porosity by around 23% and raising flexural strength by close to 37% relative to the reference. The fine 0–2 mm fraction, used as a cement replacement at 10–20% by volume, produced the opposite outcome: porosity rose by roughly 28% and compressive strength fell by about 45% [28].

Evidence at the scale of full mixes points in the same direction but also shows that meaningful environmental gains are attainable. Gue et al. [10] replaced silica sand with recycled turbine blade powder

at 5%, 10%, and 15% by mass in a silica fume mortar and reported reductions of roughly 4–5% in climate change, acidification, land use, resource use, and water use relative to the reference, with mechanical performance decreasing progressively as the replacement level rose. Revilla-Cuesta et al. [29] introduced raw-crushed wind turbine blade material as an integral addition of 1.5–6% by volume in concrete and found that low contents favoured compressive strength while higher contents favoured flexural strength, with the carbon footprint of the mix decreasing as the addition displaced conventional constituents. A recent mix-design study [30] went one step further and replaced aggregate and cement simultaneously (around 10% of the aggregate and 4% of the cement by volume) using a particle packing approach, and the resulting concretes retained structural-grade 28-day compressive strengths above 45 MPa. Combined substitution of this kind remains rare in the literature, which is relevant here because the simultaneous replacement of cement and sand is one of the strategies examined in the present work.

For the manufacturing-stage powder that is the subject of this thesis, the reference experimental study of Bettini et al. [6] provides direct evidence of feasibility. Fibre–resin powder collected during blade production was used to replace cement, sand, or both at once, at levels of up to 30%. Flexural strength remained between 5.8 and 6.8 MPa across all formulations, with no significant loss relative to the reference, while compressive strength reached its maximum at a 20% replacement level, exceeding the reference value of approximately 36 MPa. The gains observed at intermediate substitution levels are attributed to densification of the microstructure through the filler effect and to slower pozzolanic reactions supported by the silicon and aluminium content of the glass phase [6, 16]. These results place the manufacturing powder at the favourable end of the behaviour range described above: it is fine, wood-free, and glass-rich, which is precisely the combination that the wider literature identifies as suitable for powder-level substitution.

Taken as a whole, this body of work establishes that WTB powder can technically replace a portion of the cement, the fine aggregate, or both, provided the powder is sufficiently fine and free of organic impurities, and that such substitution simultaneously removes an industrial waste stream from disposal and reduces the consumption of virgin constituents. What the literature has not yet delivered is a systematic environmental quantification of this pathway for manufacturing-generated powder, covering a broad range of replacement levels and both single and combined substitution strategies. That quantification is the purpose of the Life Cycle Assessment presented in the following chapters.

3.5.1. Challenges and Limitations of Reusing Powder

One limitation is the strong sensitivity of performance to particle size, which narrows the window of viable applications for any given fraction. Liu et al. [27] demonstrated that fractions of shredded blade waste behave in fundamentally different ways within the same mortar system: the finest fractions expose fresh glass surfaces and contribute reactivity, whereas coarser fractions remain coated in epoxy and act as defect-introducing inclusions that raise porosity and reduce compressive strength. The protective resin layer that limits alkali attack on the coarse material is, at the same time, the barrier that prevents it from participating in hydration. A single crushing operation inevitably produces a spectrum of sizes, so the practical consequence is that the output must be classified and each fraction directed to a different use, which again adds processing effort and means that no single substitution strategy can absorb the whole waste stream.

The evidence on fine fractions used as cement substitutes shows how severe the penalty can be when the material is not matched to the application. Rucka and Kurpiński [28] a reported that replacing 10–20% of the cement by volume with the fine fraction of shredded end-of-life blade material increased mortar porosity by more than a quarter and reduced compressive strength by around 45%, and the authors identified surface treatment and improved particle dispersion as open requirements rather than solved problems. They further noted that the durability of these mixtures under freeze–thaw exposure, chloride ingress, and carbonation has not yet been examined, which mirrors the durability knowledge gaps already identified for GFRP recyclate more generally. Even where mix design is optimised specifically to accommodate the waste, some loss of performance appears difficult to avoid: in the particle-packing study of [30], concrete replacing around 10% of the aggregate and 4% of the cement simultaneously retained structural-grade strength, but still finished below the reference mixture.

4. LIFE CYCLE ASSESSMENT (LCA) FRAMEWORK

4.1. Fundamentals of LCA

Life Cycle Assessment (LCA) is a standardised methodology for evaluating the potential environmental impacts associated with a product, process, or service throughout its life cycle. By accounting for all relevant material and energy inputs, as well as emissions and waste outputs, LCA provides a comprehensive framework for assessing environmental performance and identifying opportunities for improvement. Owing to its systematic and internationally harmonised approach, LCA has become one of the most widely applied tools for evaluating the sustainability of construction materials and waste valorisation strategies. To ensure consistency, transparency, and comparability the assessment follows the methodological framework established by ISO 14040 [11] and ISO 14044 [12]. These standards define principles, requirements and guidelines for conducting an LCA though four interconnected phases: goal and scope definition, life cycle inventory (LCI) analysis, life cycle impact assessment (LCIA), and interpretation of results [31, 32].

Although European standards such as EN 15804+A2:2019 [33] establish Product Category Rules (PCR) for the environmental assessment of construction products, and ISO 21930:2017 provides principles for Environmental Product Declarations (EPDs) of building products and services, these standards were not adopted as the methodological basis for the present study. The objective of this work is not to develop an EPD for a construction product, but to assess the environmental implications of incorporating a manufacturing waste stream into cementitious mortars. Consequently, the general LCA framework defined by ISO 14040 [11] and ISO 14044 [12] was considered the most appropriate methodological approach.

The goal and scope definition establishes the foundation of the assessment by articulating the study's purpose and the specific product system under evaluation. A key requirement of this phase is the definition of the functional unit, which serves as the quantitative reference baseline that allows direct comparison between different material formulations or production scenarios. The system boundaries must also be clearly defined to determine which lifecycle stages are included in the study. In the context of construction materials, assessments frequently adopt a cradle-to-gate boundary, encompassing raw material extraction, transportation to the production facility, and the manufacturing or mixing process, under the assumption that the subsequent use and end-of-life phases will present negligible differences between the compared alternatives [31, 32].

The Life Cycle Inventory (LCI) analysis is carried out to collect and quantify all data required to model the product's lifecycle. This includes the consumption of raw materials, energy and water, together with emissions to air, water, and soil. When secondary materials or industrial by-products are incorporated into a product, particular attention must be given to multifunctionality and the allocation of environmental burdens. ISO 14044 [12] establishes a hierarchy for addressing allocation, prioritising the avoidance of allocation through subdivision or system expansion whenever possible, followed by allocation based on physical relationships or, where appropriate, other relationships such as economic value.

The third phase, the Life Cycle Impact Assessment (LCIA), translates the raw quantitative data gathered during the inventory into comprehensible potential environmental impacts. During this stage, the LCI flows are classified and then characterised using established LCIA methodologies, which apply specific characterisation factors to evaluate the system's contribution to different environmental phenomena. Common impact categories include Global Warming Potential (GWP), Ozone Depletion Potential (ODP), Acidification Potential (AP), Photochemical Ozone Creation Potential (POCP), Abiotic Depletion Potential for Fossil Fuels (ADP-FF) and Eutrophication Potential (EP). The CML method is widely applied in environmental assessments of materials because it provides scientifically established characterisation factors and facilitates comparison between alternative material formulations.

The final phase, interpretation, synthesises the findings from the inventory and impact assessment in light of the study's original objectives. This phase is essential not only for verifying the reliability and limitations of the analytical model, but also for communicating results clearly to relevant stakeholders. Through the interpretation phase, researchers can identify the specific processes or constituent materials that contribute most significantly to the overall environmental footprint, and formulate targeted recommendations to improve the sustainability of the material under study [31, 32].

4.2. Life Cycle Assessment of mortars with WTB powder waste incorporation

4.2.1. Studied Mortars Formulations

The inventory was constructed from the mix proportions established experimentally by Bettini et al. [6] and subsequently expressed per the volumetric functional unit.

Nineteen formulations were assessed: a reference mortar (REF) and eighteen mixes incorporating WTB waste powder as a partial replacement of cement, sand, or both. The formulations are organised into the

three-substitution series, the C-series (cement replacement), the S-series (sand replacement), and the CS-series (combined replacement), with replacement levels ranging from 5% to 40%.

The mass of each constituent was calculated by first expressing the sand and powder content of each mix relative to the cement content. The cement mass was then obtained by solving the volume-balance equation for one cubic metre of mortar, after which the sand, powder, and water masses followed directly from the cement mass through their respective ratios and the water-to-binder ratio which is 0.5 in all mixes. The densities adopted were 3,120 kg/m³ for cement, 2,647 kg/m³ for sand, and 163 kg/m³ for the WTB powder [6]. The results of this calculation are presented in Table 4-1.

Table 4-1 Mix design of the nineteen mortar formulations

Mix	%C	%S	%P	Replac. ratio %	C Mass (kg)	S Mass (kg)	P Mass (kg)	Water Mass (kg)
REF	25	75	0	0	511.80	1535.41	0.00	255.90
C5P	23.75	75	1.25	0.05	423.24	1336.54	22.28	222.76
C10P	22.5	75	2.5	0.1	354.99	1183.28	39.44	197.21
C15P	21.25	75	3.75	0.15	300.77	1061.56	53.08	176.93
C20P	25	71.25	3.75	0.05	345.73	985.32	51.86	198.79
C30P	25	67.5	7.5	0.1	261.03	704.77	78.31	169.67
C40P	25	63.75	11.25	0.15	209.66	534.64	94.35	152.00
S5P	23.75	71.25	5	0.05	298.44	895.33	62.83	180.64
S10P	22.5	67.5	10	0.1	203.97	611.90	90.65	147.31
S15P	21.25	63.75	15	0.15	150.66	451.99	106.35	128.51
S20P	20	75	5	0.2	256.68	962.54	64.17	160.42
S30P	17.5	75	7.5	0.3	189.28	811.20	81.12	135.20
S40P	15	75	10	0.4	140.20	700.99	93.47	116.83
CS5P	25	60	15	0.2	175.19	420.45	105.11	140.15
CS10P	25	52.5	22.5	0.3	131.83	276.85	118.65	125.24
CS15P	25	45	30	0.4	105.68	190.22	126.82	116.25
CS20P	20	60	20	0.2	116.43	349.29	116.43	116.43
CS30P	17.5	52.5	30	0.3	75.03	225.09	128.62	101.83
CS40P	15	45	40	0.4	50.90	152.69	135.73	93.31

In addition to the mix proportions, the experimental mechanical and durability-related properties reported by Bettini et al. [6] were adopted. These properties, including flexural strength, compressive strength,

water absorption by immersion, and capillary water absorption, are summarised in Table 4-2. Missing values indicate that these formulations were not experimentally tested, as the authors discontinued further testing after a decreasing performance trend was observed.

Table 4-2 Mechanical and durability properties

Mix	Flexural Strength (MPa)	Compressive Strength (MPa)	Water Absorption Immersion	Water Absorption Capillarity
REF	6.25	35.80	19.476	0.35
C5P	6.36	34.40	18.4082	0.32
C10P	5.82	32.7	18.8445	0.37
C15P	6.46	34.7	17.23	0.32
C20P	6.83	36.4	15.9679	0.29
C30P	6.53	33.50	-	-
C40P	6.54	33	-	-
S5P	6.38	35.00	20.34	0.38
S10P	5.81	36.70	20.26	0.40
S15P	6.03	37.90	20.65	0.41
S20P	6.97	38.80	20.00	0.38
S30P	6.25	36.90	20.87	0.42
S40P	6.37	39.10	22.25	0.46
CS5P	6.02	38.80	18.51	0.30
CS10P	5.80	38.70	18.76	0.28
CS15P	6.33	37.90	18.27	0.29
CS20P	6.23	38.30	18.15	0.34
CS30P	6.48	35.60	-	-
CS40P	-	-	-	-

The life cycle inventory (LCI) quantifies the material and energy flows associated with the production of one cubic metre of each mortar formulation, within the cradle-to-gate boundary that will define further.

4.2.2. Life Cycle Assessment

- Goal of the Study

Life Cycle Assessment aims to quantify and compare the environmental impacts of partially substituting conventional raw materials in cement-based mortar with powder waste generated during wind turbine blade manufacturing.

The comparative analysis and the aggregation of environmental indicators in this study follow the multi-criteria decision support Methodology for the Relative Sustainability Assessment of Building Technologies (MARS-SC) [32]. The MARS-SC methodology is structured around three groups of sustainability categories: environmental, functional, and economic [32]. Since the present research aims at assessing the environmental performance of different mortar formulations, only the environmental category of MARS-SC was considered. The methodology is processed in five steps: (I) definition of the sustainability indicators; (II) quantification of the indicators, including the life cycle inventory; (III) normalisation of the indicators; (IV) aggregation of the indicators; and (V) sustainability score calculation and global assessment. These steps structure the assessment procedure described in the following sections.

- Functional Unit

A functional unit is defined to provide the reference basis against which all material inputs, energy flows, and environmental impact results are normalised, ensuring that every mortar formulation is compared on an equivalent technical footing. The functional unit adopted in this study is 1 m^3 of cured mortar.

4.2.3. System Boundaries

The general system boundary adopted in this study was cradle-to-gate, encompassing raw material extraction and processing, transportation of constituents to the manufacturing facility, and mortar production. Within this boundary, the following unit processes are included: extraction and processing of clinker, limestone, gypsum, and siliceous fine aggregate; upstream transport of all constituents and packaging materials to the mortar plant; mechanical treatment of the WTB powder waste prior to incorporation; and the dry-blending process through which the mortar is produced. Energy carriers, ancillary materials, and direct process emissions associated with these stages are included. The Life Cycle Assessment was conducted following the ISO 14040 [11] and ISO 14044 [12] framework. Within this methodological framework, a cradle-to-gate system boundary was adopted for the present study.

The construction stage (A4–A5), the use stage (B1–B7), the end-of-life stage (C1–C4), and the module for benefits and loads beyond the system boundary (D) are explicitly excluded. This delimitation is justified on three grounds: first, the use and end-of-life stages of cement-based mortars are governed by building-level conditions that fall outside the scope of a material-level comparison; second, primary inventory data

for these stages are not available for the experimental formulations studied; and third, the environmental differences between formulations are expected to manifest principally within modules The system boundary extends from raw material extraction and processing through transportation of constituents to the manufacturing facility and mortar production, where the substitution of clinker and quarry-derived constituents takes effect. The omission of carbonation-related CO_2 uptake during the use stage and any avoided burdens associated with end-of-life recovery is recognised as a methodological limitation and is considered during the interpretation of the results. Capital goods, infrastructure, and human labour are excluded from the system boundary because they are outside the scope of the present study and are expected to have a negligible influence on the comparative environmental performance of the investigated mortar formulations.

A central methodological question in this study concerns the environmental status of the WTB powder waste: whether it enters the system as a zero-burden co-product, as a processed secondary raw material carrying some upstream burden, or as a fully allocated co-product of the blade manufacturing process. This question is not resolved by a single correct answer, it depends on the regulatory context, the market conditions, and the allocation principles adopted. To handle this transparently and in line with the sensitivity analysis requirements of ISO 14044 [12], three distinct system boundary scenario s are defined and assessed. Each scenario represents a coherent and defensible interpretation of the powder's status, and the three are compared to evaluate how sensitive the overall environmental conclusions are to this fundamental modelling choice. The three scenarios are described in the following sections and illustrated as well.

- Scenario 1, Zero Burden, No-Processing (Cut-Off, Portuguese Waste Law)

The first system boundary scenario applies the cut-off approach in its strictest form, directly reflecting the classification of the WTB powder under Portuguese waste legislation [34] Under this framework, a waste material that carries no market price is assigned no upstream environmental burden. The wind turbine blade manufacturing process and the activity that generates the powder, therefore falls entirely outside the system boundary. The blade itself is the primary product of that process, and since the powder is classified as a waste not as a sub-product in this context, none of the environmental impacts associated powder generation are transferred to it.

In practical terms, this means the powder enters the mortar system at the factory gate with zero embodied burden. This means no extraction of raw fibres or resins and no energy consumption at the blade facility are included within the assessment boundary. Furthermore, scenario 1 assumes that the powder is used as received from the blade production facility, without any mechanical treatment such as size reduction

or sieving. The only processes attributed to the WTB stream within this boundary are the transport of the powder from the blade facility to the mortar plant, and its incorporation into the dry mix during mortar manufacturing.

This scenario represents the most favourable environmental scenario for the substituted mortars, since the powder displaces conventional materials (cement or aggregate), while contributing no upstream impact of its own. It also represents the baseline interpretation under current Portuguese regulatory practice, making it the primary reference scenario for the environmental conclusions of this study. The system boundary is illustrated in Figure 4-1.

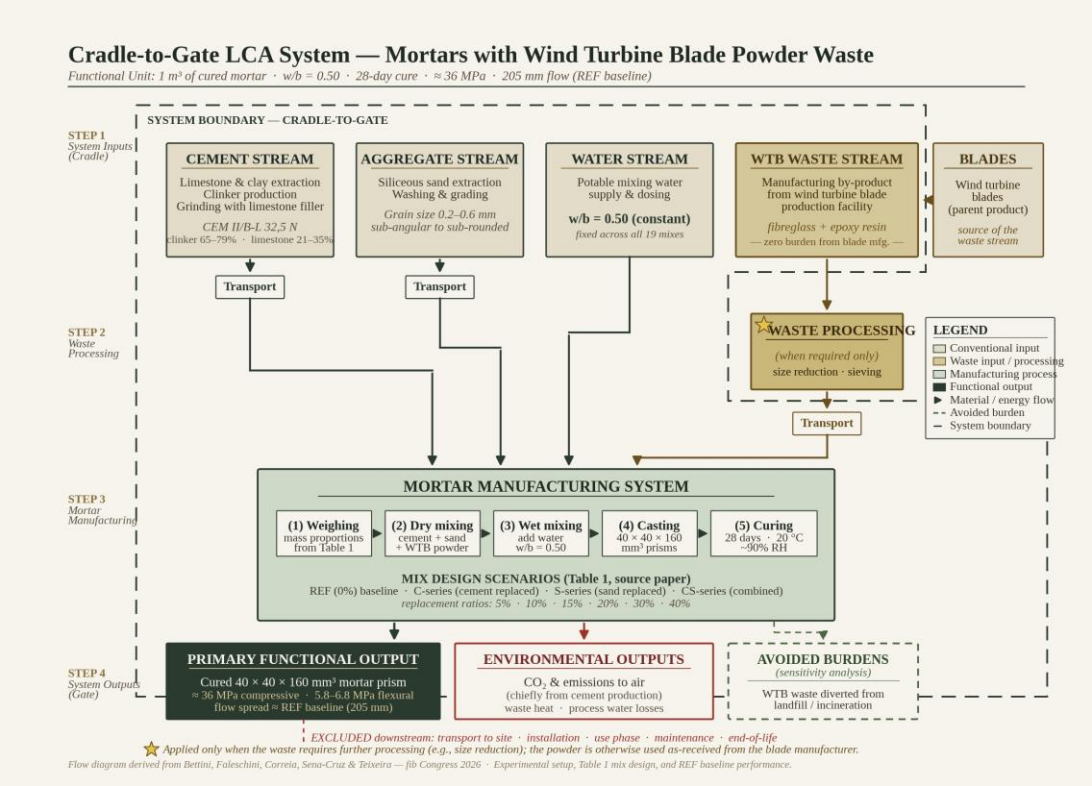


Figure 4-1 System boundary diagram for Scenario 1

- Scenario 2, Zero Burden, With Processing (Cut-Off with Processing Burden)

The second scenario retains the same legal classification as scenario 1: the powder generation impacts remain outside the system boundary, consistent with the Portuguese waste framework. However, Scenario 2 assumes that the WTB powder is subjected to a mechanical pre-treatment, including size reduction and sieving, with the aim of enhancing its functional performance in the cementitious matrix, particularly its contribution to the mechanical and durability properties of the mortar.

This processing step is not always necessary. When the powder as collected from the blade facility already falls within the particle size range compatible with mortar production, it can be used directly, as assumed in scenario 1. However, in cases where the collected material contains oversized fibrous fragments or does not meet the grading requirements for consistent mix performance, a preparation stage is required. Scenario 2 captures this situation by attributing the energy consumption, equipment uses, and any associated emissions of the size reduction and sieving operations to the WTB powder stream within the system boundary.

The environmental burden of the powder in this scenario is therefore not zero it carries the impact of its pre-treatment before mixing in mortar but it remains entirely decoupled from the upstream blade manufacturing process. The comparison between Scenario 1 and Scenario 2 isolates the specific contribution of the processing step to the overall environmental profile of the substituted mortars, providing a quantitative basis for judging whether the preparation of the powder materially changes the environmental conclusions. The system boundary is illustrated in Figure 4-2.

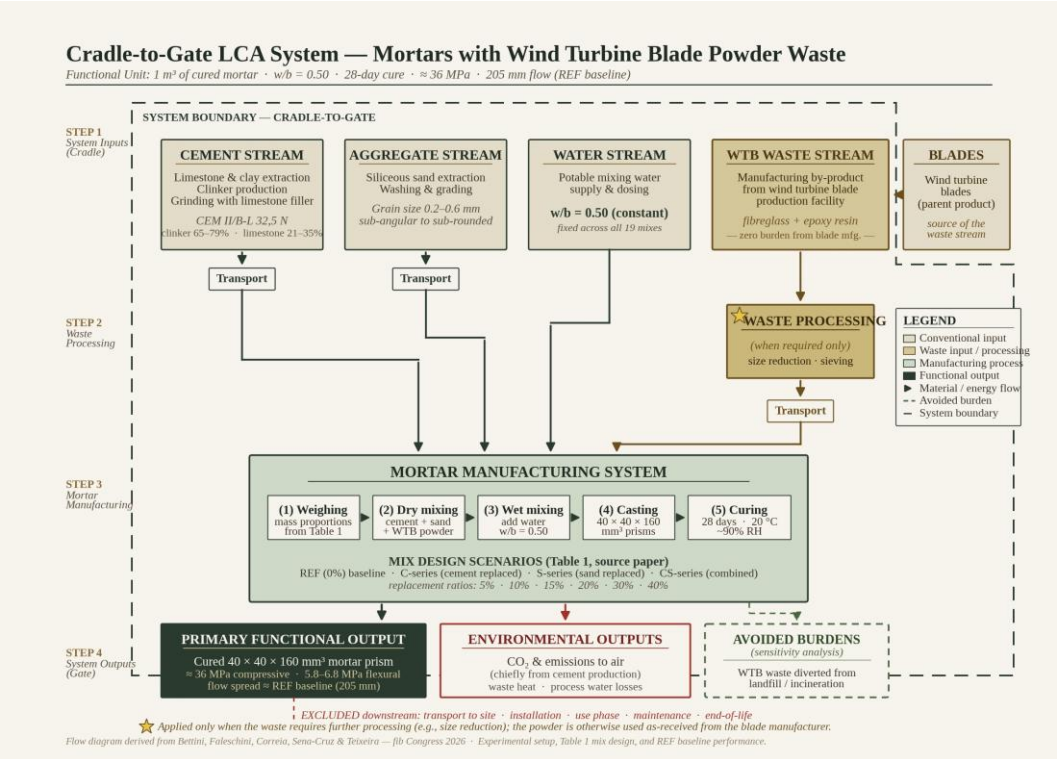


Figure 4-2 System boundary diagram for Scenario 2

- Scenario 3, Economic Allocation (Co-Product, Full Upstream Burden)

The third Scenario adopts a fundamentally different interpretation of the powder's status. Rather than treating it as a zero-burden waste residue, Scenario 3 recognises that the powder has an assignable

market value and therefore qualifies as a co-product of the wind turbine blade manufacturing process. This reclassification brings the blade manufacturing system inside the system boundary and requires that the environmental burdens of that system and requires that the environmental burdens of that system be partitioned between the blade and the powder according to a defined allocation rule. And also considers the pre-treatment of the powder.

The partitioning method applied in Scenario 3 is economic allocation, in accordance with the allocation hierarchy established by ISO 14044 [12]. Economic allocation is adopted here because the basis for treating the powder as a sub-product is precisely its market value: once the powder carries a price, it is no longer waste in the regulatory sense, and its share of the joint production burden must be determined in proportion to the relative economic values of the blade and the powder at the point of divergence. The fraction of the blade manufacturing burden assigned to the powder is therefore calculated as the ratio of the powder's market value to the combined market value of the blade and the powder produced per unit of manufacturing output.

This Scenario represents the most conservative environmental scenario for the substituted mortars. By assigning a share of the upstream blade production burden to the powder, it reduces or eliminates the environmental advantage that the powder holds over the conventional materials it displaces. The comparison between Scenario 3 and the two cut-off scenarios quantifies how much of the apparent environmental benefit of WTB powder substitution depends on the assumption that the powder is burden-free. The system boundary is illustrated in Figure 4-3.

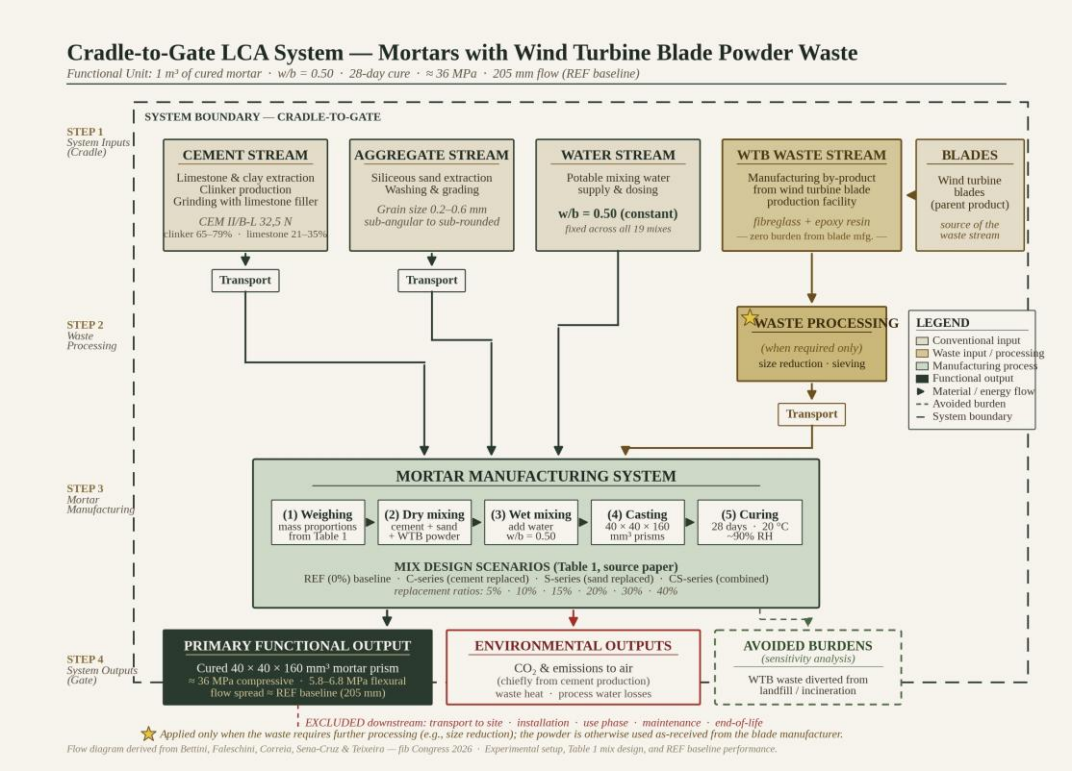


Figure 4-3 System boundary diagram for Scenario 3

The foreground inventory comprises the production of Portland cement, the production of siliceous sand, the upstream treatment of the WTB powder where applicable, the transport of each constituent to the mortar plant, and the electricity consumed during mortar manufacturing. Background inventory data were obtained using SimaPro (version 10.2.0.3) coupled with the Ecoinvent database, while manufacturer-specific Environmental Product Declarations (EPDs) were used whenever representative and methodologically compatible data were available. All the data that used are summarized in Table 4-3 and Table 4-4.

Table 4-3 Source of Cement and Sand impacts

Indicator	Cement source	Sand source
GWP-total	EPD (Secil)	SimaPro / Ecoinvent
Ozone Depletion (ODP)	EPD (Secil)	EPD (Sibelco)
Acidification (AP)	SimaPro / Ecoinvent	SimaPro / Ecoinvent
Photochemical Oxidation (POCP)	SimaPro / Ecoinvent	SimaPro / Ecoinvent
Abiotic Depletion Fossil Fuels (ADP-FF)	EPD (Secil)	SimaPro / Ecoinvent
Eutrophication (EP)	SimaPro / Ecoinvent	SimaPro / Ecoinvent

Table 4-4 Database name chosen in SimaPro

Material	Data Name
Cement	Cement production, CEM II/B Europe without Switzerland
Sand	Sand quarry operation, extraction from river bed, RoW, cut-off, U
Transportation	Transport, freight, lorry, 16-32 metric ton, diesel, EURO 6 RER
Electricity (Mechanical and Mortar Process)	Market for electricity, medium voltage PT
Powder (Blade)	Wind turbine, 2MW, onshore {GLO}| wind turbine construction, 2MW, onshore | Cut-off, U

4.2.4. Life Cycle Inventory (LCI)

The Life Cycle Inventory (LCI) was developed for the nineteen mortar formulations defined in Section 4.2.1 using a functional unit of 1 m^3. For each formulation, the inventory includes the quantities of cement, sand, WTB powder, and water, together with the transport demand associated with the raw materials incorporated into the mortar. These inventory data constitute the basis for the environmental modelling performed in SimaPro. Table 4-6 summarises the material inputs and transport requirements considered for each mortar formulation.

The environmental profile of the cement was taken from the EPD of the Portland-limestone cement CEM II/B-L 32,5 N produced by Secil [35] a company in Portugal, and that of the fine aggregate from the EPD of the dry silica sand supplied in bulk by Sibelco [36] a company in Italy.

For each impact category, the data source was selected according to methodological compatibility between the available EPDs and the SimaPro/Ecoinvent dataset. The cement and sand EPDs, do not report all six impact categories considered in this study in a directly comparable form. Therefore, EPD information was applied where methodological compatibility was ensured. The detailed data selection and integration procedure are presented for cement and sand in the Table 4-5.

Table 4-5 EPD/Ecoinvent source table

Material	Source
Cement	Secil CEM II/B-L 32,5 N (NEPD-10352-10352-2)
Sand	Sibelco Cascina Stanga, Silica Sand Dry, Bulk (EPD-IES-0030293:001)
Ecoinvent	SimaPro version 10.2.0.3 (Methodology CML-IA baseline V3.11 / EU25)

Table 4-6 Inventory of material and transport inputs per 1 m³

Mix	Cement (kg)	Sand (kg)	Powder (kg)	Water (kg)	Sand transport (tkm)	Powder transport (tkm)	Total transport (tkm)
REF	511.80	1535.41	0.00	255.90	118.84	0.00	118.84
C5P	423.24	1336.54	22.28	222.76	103.45	6.02	109.46
C10P	354.99	1183.28	39.44	197.21	91.59	10.65	102.23
C15P	300.77	1061.56	53.08	176.93	82.16	14.33	96.50
C20P	345.73	985.32	51.86	198.79	76.26	14.00	90.27
C30P	261.03	704.77	78.31	169.67	54.55	21.14	75.69
C40P	209.66	534.64	94.35	152.00	41.38	25.47	66.86
S5P	298.44	895.33	62.83	180.64	69.30	16.96	86.26
S10P	203.97	611.90	90.65	147.31	47.36	24.48	71.84
S15P	150.66	451.99	106.35	128.51	34.98	28.71	63.70
S20P	256.68	962.54	64.17	160.42	74.50	17.33	91.83
S30P	189.28	811.20	81.12	135.20	62.79	21.90	84.69
S40P	140.20	700.99	93.47	116.83	54.26	25.24	79.49
CS5P	175.19	420.45	105.11	140.15	32.54	28.38	60.92
CS10P	131.83	276.85	118.65	125.24	21.43	32.04	53.46
CS15P	105.68	190.22	126.82	116.25	14.72	34.24	48.96
CS20P	116.43	349.29	116.43	116.43	27.04	31.44	58.47
CS30P	75.03	225.09	128.62	101.83	17.42	34.73	52.15
CS40P	50.90	152.69	135.73	93.31	11.82	36.65	48.47

Transport distances were defined from the location of each supplier relative to the mortar production facility. As the cement was assumed to be produced on the same site as the mortar, it was assigned a transport distance of zero. The sand EPD used in this study was obtained from an Italian dataset. However, importing sand from Italy to Portugal would not represent a realistic supply chain for the studied mortar production. Therefore, a Portuguese company producing comparable silica sand was identified, and the distance from the supplier location to the production site (77.4 km) was considered in the LCA model using Google Maps. Similarly, for the recycled WTB powder, the actual transportation distance between the recycling source and the mortar production site (270 km) was included in the assessment. Two electricity-driven processes were included. Where applicable, the mechanical processing of the WTB waste into a usable powder was modelled using an average grinding energy demand of 0.225 MJ per kg of powder, calculated from the range of values reported by Cheng et al. [37],and the mortar

manufacturing stage using an energy demand of 0.296 MJ per kilogram of dry mix [38]. Both were linked to the Portuguese medium-voltage electricity mix from the Ecoinvent database.

Table 4-7 Environmental impact factors (all per kg, transportation per tkm)

Input	GWP	ODP	AP	POCP	ADP-FF	EP
Cement	5.75E-01	9.42E-09	1.10E-03	4.26E-05	2.51	3.81E-04
Sand	5.19E-03	2.04E-11	3.24E-05	9.15E-07	6.71E-02	8.16E-06
Transportation	1.86E-01	3.25E-09	3.22E-04	2.65E-05	2.60	8.85E-05
Powder processing electricity	1.39E-02	3.25E-10	4.86E-05	2.64E-06	0.189	9.79E-06
Mortar mixing electricity	1.82E-02	4.28E-10	6.40E-05	3.47E-06	0.249	1.29E-05
WTB powder (blade upstream)	9.62E-01	7.88E-09	4.62E-03	3.00E-04	11.9	2.46E-03

4.2.5. Life Cycle Inventory Assessment (LCIA)

The life cycle inventory data were subsequently translated into potential environmental impacts through the Life Cycle Impact Assessment (LCIA) phase using the CML-IA Baseline methodology (version 3.11), implemented in SimaPro. The CML method was selected because it is a well-established midpoint impact assessment methodology, widely applied in studies involving construction materials and the environmental valorisation of industrial by-products, thereby facilitating comparison with previous research. This midpoint-oriented method characterises the environmental burdens associated with each elementary flow by applying scientifically established characterisation factors, allowing the environmental performance of the different mortar formulations to be evaluated consistently and compared on a common basis. Based on the objectives of the present study and the characteristics of the assessed material system, the environmental performance was evaluated using the following six impact categories in Table 4-8.

Table 4-8 Environmental impact categories assessed, with their reference units

Indicator	Acronym	Unit
Global Warming Potential-total	GWP	kg CO_2-eq
Ozone Depletion Potential	ODP	kg CFC-11-eq
Acidification Potential	AP	kg SO_2-eq
Photochemical Oxidation	POCP	kg C_2H_4-eq
Abiotic Depletion Fossil Fuels	ADP-FF	MJ
Eutrophication Potential	EP	kg PO_4-eq

4.2.6. Normalization, Aggregation and Global Assessment

For all Scenarios, the characterised impact of each mortar formulation was obtained by summing the contribution of each material and process included within the system boundary: the production of cement, the transport of cement which mentioned before that is zero, the production of sand, the transport of sand, the powder itself, the transport of powder, the mechanical processing of the powder, the upstream burden of the blade, and the mortar manufacturing energy. It should be mentioned that for each mix, the mass of cement was obtained by solving the volume-balance equation for one cubic metre of mortar, after which sand, powder, and water masses followed from their respective ratios to cement.

Each component was calculated as the product of the corresponding constituent mass, obtained from the mix design, and the relevant impact factor, obtained from the EPD or SimaPro process described previously. The transport components were calculated as the product of the constituent mass, expressed in tonnes, the transport distance, and the impact factor of the road-freight process, per the procedure described above.

The mortar manufacturing and powder grinding components were calculated as the product of the corresponding constituent mass, the respective energy demand per kilogram, and the impact factor of the Portuguese medium-voltage electricity mix obtained from the Ecoinvent database, per the procedure described above.

The treatment of the powder's own upstream burden was what distinguished the three scenarios: it was excluded entirely under the cut-off approach of the first two scenarios, and partially included under the third using an economic allocation coefficient, α, In accordance with the allocation principles of ISO14044 [12] defined as:

$$\alpha = \frac{V_{Powder}}{V_{Powder} + V_{Blade}}$$ Equation 4-1

where V_{Powder} and V_{Blade} represent the economic value of the powder and of the blade, respectively, the former obtained from the assumed market price of the powder and the latter from the reported manufacturing cost of the blade. The corresponding share of the blade's upstream impact was then attributed to the powder in proportion to this coefficient and to the mass ratio between the blade and the powder it yields.

Once the total impacts were obtained, each indicator was normalised across the nineteen mixes using a linear min-max procedure, in which the normalised value of a mix for a given indicator was calculated as below by [32].

$$P_i = \frac{(Pi \; - \; P(worst))}{(P(best) \; - \; P(worst))}$$ Equation 4-2

where Pi is the total impact of the mix for that indicator, and P(worst) and P(best) are respectively, the minimum and maximum characterised values identified across the nineteen mixes for that indicator. The six normalised indicators were then combined into a single score for each mix through a weighted sum as mentioned in Table 4-9 using a weighted summation as presented in equation bellow by [32]:

$$\mathrm{ND_A} = \sum_{i=1}^{n} w_i N_i$$ Equation 4-3

where N_i represents the normalised value of the ith impact category and w_i is the corresponding weighting factor assigned to that category.

The resulting score, hereafter referred to as the NDA score, expresses the overall environmental performance of each mix on a scale from 0 to 1, where a value of 1 corresponds to the most favourable performance among the nineteen mixes and a value of 0 to the least favourable.

Table 4-9 Weighting factors applied to each impact category adapted from [32]

Indicator	Weight (%)
GWP-total	38
Ozone Depletion (ODP)	12
Acidification (AP)	12
Photochemical Oxidation (POCP)	14
Abiotic Depletion Fossil Fuels (ADP-FF)	12
Eutrophication (EP)	12
Sum	100

4.2.7. Sensitivity Analysis

A sensitivity analysis was performed to evaluate the influence of the assumptions adopted in each assessment scenario on the calculated environmental performance. The analysis was conducted independently for all three scenarios using the corresponding calculation procedures described in the previous sections.

For Scenario 1, the environmental impacts were calculated according to the zero-burden approach adopted for the wind turbine blade powder. For Scenario 2, the calculation procedure additionally incorporated the environmental burdens associated with the grinding process. For Scenario 3, the economic allocation methodology was evaluated using three powder price levels corresponding to 10%, 50%, and 100% of the reference material price.

For each case, the complete calculation sequence was repeated, including life cycle inventory calculations, life cycle impact assessment, normalisation, and NDA calculation. The resulting datasets were subsequently used in the comparative environmental and sustainability assessment presented in next chapter.

5. Results and Discussion

Chapter 5 presents and discusses the results of the life cycle assessment conducted for the nineteen mortar formulations described in Chapter 4. The assessment is organised around three scenarios, Figure 5-1 illustrates the cradle-to-gate system boundary common to all three scenarios and shows how the scope of each differs from the others with 3 different colours. Blue shows Scenario 1, yellow shows Scenario 2 and purple shows Scenario 3. With the system boundary and functional unit established, the following sections present the results for each scenario in turn, beginning with the zero-burden cut-off case.

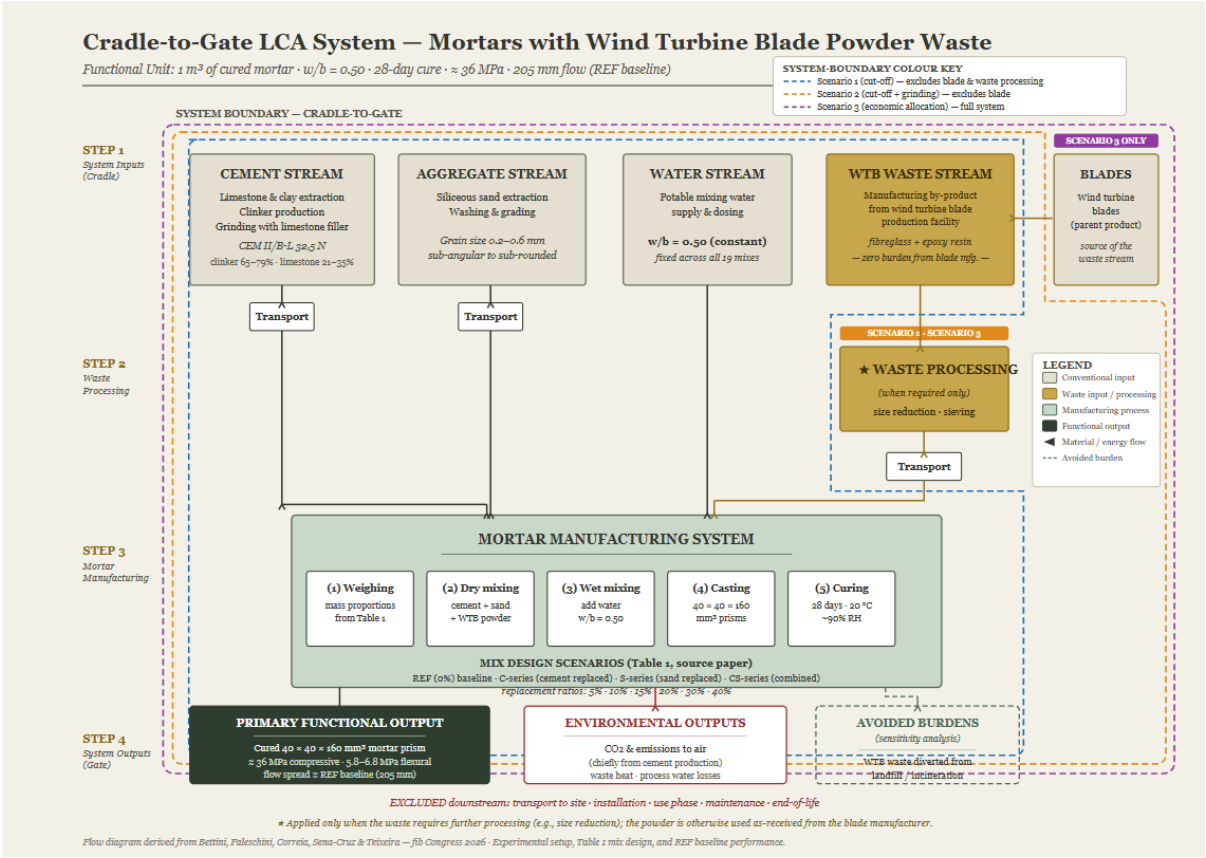


Figure 5-1 System Boundaries for all Scenarios

5.1. Results - Scenario 1

Scenario 1 implements the zero-burden, cut-off allocation approach as described before, under which the WTB powder is treated as a waste stream possessing no market value and therefore carries no share of the upstream burden associated with blade manufacturing. Within this scenario, cement is assumed to

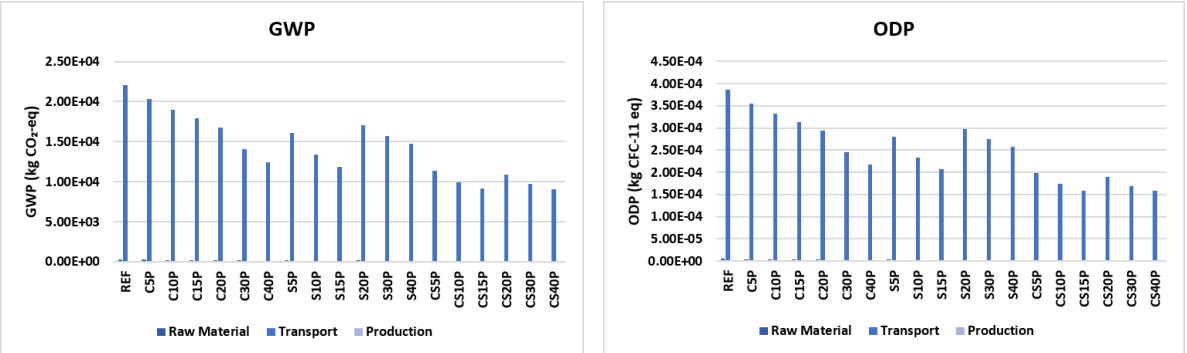
be produced at the same site as the mortar and accordingly carries no transport burden, whereas both the silica sand and the WTB powder are transported over their respective distances before being incorporated into the mix. No mechanical processing of the powder and no upstream blade burden are considered under this scenario.

To better understand the origin of the environmental impacts obtained for each mortar formulation, a stage contribution analysis was performed before comparing the total environmental results. The environmental impacts considered were GWP (kg CO_2-eq), ODP (kg CFC-11 eq.), AP (kg SO_2 eq.), EP (kg PO_4^{3-} eq.), POCP (kg C_2H_4 eq.), and ADP-FF (MJ).

The environmental impacts were grouped into three life cycle stages representing the system modelled in this study. The raw material stage includes the production of cement, sand, and WTB powder. The transportation stage comprises the transport of sand and WTB powder from the respective supplier locations to the mortar production facility, while cement transport was assumed to be zero because cement production was considered to occur at the same site as mortar manufacturing. The production stage includes the electricity consumption associated with mortar mixing and, where applicable, the mechanical grinding process applied to the WTB powder prior to its incorporation into the mortar.

In Scenario 1, no grinding process is considered because the powder is assumed to enter the system without additional treatment. Therefore, the production stage represents only the electricity required for mortar mixing. The contribution of each stage was calculated as a percentage of the total environmental impact for each mortar formulation and for each impact category, allowing the dominant environmental hotspot within the system boundary to be identified.

Table 5-1 Contribution of life cycle stages to the environmental impact categories, Scenario 1.



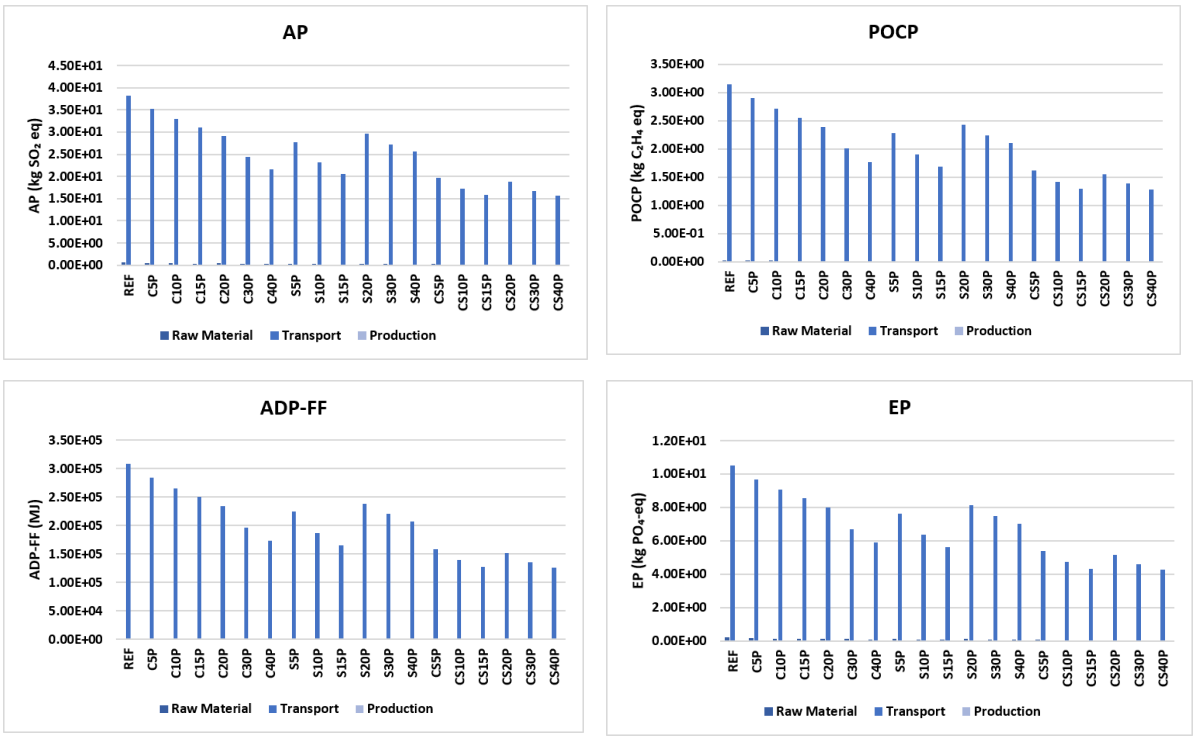


Table 5-1 presents the relative contribution of the three life cycle stages to the six environmental impact categories for the nineteen mortar formulations under Scenario 1. Across all formulations and impact categories, the transportation stage represents the largest contribution to the total environmental impacts, while the production stage contributes only a negligible proportion. The contribution of the raw material stage remains comparatively small throughout the analysis. Furthermore, the relative contribution of each stage remains highly consistent among the different mortar formulations, indicating that changing the powder substitution level does not substantially alter the overall distribution of environmental burdens among the three life cycle stages under the assumptions adopted for Scenario 1.

The characterised environmental impacts obtained for the nineteen formulations, summarised in Table 5-2, show a consistent pattern across all six indicators considered: the reference mortar (REF) records the highest impact in every category, and the introduction of WTB powder, regardless of the substitution series adopted, is associated with a reduction relative to this baseline. For GWP, the reference mix totals 2.24×10^4 kg CO_2-eq, against 9.04×10^3 kg CO_2-eq for CS40P, a reduction of approximately 60% at the highest replacement level. The same ordering is preserved across ODP, AP, POCP, ADP-FF and EP, indicating that the magnitude of the reduction differed between formulations, a consistent pattern was observed across all six impact categories. Mixes that performed well in one impact category also performed similarly in the remaining categories, and no formulation displayed a substantially different

ranking between indicators. Consequently, the characterised results indicate that the relative environmental performance of the mortar formulations is consistent across the six impact categories considered.

Table 5-2 Total characterized environmental impact of mixes, Scenario 1

Indicator	**GWP**	**ODP**	**AP**	**POCO**	**ADP-FF**	**EP**
Unit	kg CO2 eq	kg CFC-11 eq	kg SO2 eq	kg C2H4-eq	MJ	kg PO4-eq
REF	2.24E+04	3.91E-04	38.88	3.17	3.10E+05	10.72
C5P	2.06E+04	3.60E-04	35.76	2.92	2.86E+05	9.86
C10P	1.92E+04	3.36E-04	33.35	2.73	2.67E+05	9.19
C15P	1.81E+04	3.16E-04	31.44	2.57	2.52E+05	8.66
C20P	1.70E+04	2.97E-04	29.48	2.41	2.36E+05	8.13
C30P	1.42E+04	2.48E-04	24.68	2.02	1.98E+05	6.80
C40P	1.26E+04	2.19E-04	21.78	1.78	1.74E+05	6.00
S5P	1.62E+04	2.83E-04	28.13	2.30	2.25E+05	7.76
S10P	1.35E+04	2.35E-04	23.38	1.91	1.87E+05	6.44
S15P	1.19E+04	2.08E-04	20.69	1.69	1.66E+05	5.70
S20P	1.72E+04	3.01E-04	29.88	2.45	2.39E+05	8.23
S30P	1.59E+04	2.77E-04	27.50	2.25	2.21E+05	7.57
S40P	1.49E+04	2.60E-04	25.77	2.11	2.07E+05	7.09
CS5P	1.14E+04	2.00E-04	19.82	1.62	1.59E+05	5.46
CS10P	1.00E+04	1.75E-04	17.37	1.42	1.39E+05	4.78
CS15P	9.17E+03	1.60E-04	15.89	1.30	1.28E+05	4.38
CS20P	1.09E+04	1.91E-04	18.97	1.55	1.52E+05	5.22
CS30P	9.74E+03	1.70E-04	16.88	1.39	1.36E+05	4.65
CS40P	9.04E+03	1.58E-04	15.67	1.29	1.26E+05	4.31

Table 5-3 and Table 5-4 present the normalisation reference values and the corresponding normalised results for each impact category. Following min–max normalisation, the environmental profiles of the mortar mixes remain highly consistent across the six indicators. The CS40P mix achieves normalised values close to 1.00 for all impact categories, whereas the reference mix is assigned a value of 0.00. Similar trends are observed for the remaining formulations, indicating that the relative environmental ranking changes very little between impact categories. This suggests that the environmental improvements achieved through WTB powder incorporation are reflected consistently across all six impact indicators rather than being dominated by a single category.

Table 5-3 Best (minimum) and worst (maximum) characterised values identified across the mixes, for each impact category, used as the normalisation reference points.

Indicator	P*best (MIN)	P*worst (MAX)
GWP-total	9.04E+03	2.24E+04
Ozone depletion (ODP)	1.58E-04	3.91E-04
Acidification (AP)	1.57E+01	3.89E+01
Photochemical oxidation	1.29E+00	3.17E+00
Abiotic Depletion Fossil Fuels	1.26E+05	3.10E+05
Eutrophication	4.31E+00	1.07E+01

Table 5-4 Normalised Values, Scenario 1

Indicator	GWP	ODP	AP	POCO	ADP-FF	EP
REF	0.000	0.000	0.000	0.000	0.000	0.000
C5P	0.134	0.134	0.135	0.134	0.134	0.135
C10P	0.238	0.238	0.238	0.237	0.237	0.239
C15P	0.320	0.320	0.321	0.319	0.318	0.321
C20P	0.405	0.405	0.405	0.406	0.406	0.405
C30P	0.612	0.612	0.612	0.612	0.613	0.611
C40P	0.737	0.737	0.737	0.738	0.738	0.736
S5P	0.463	0.463	0.463	0.463	0.463	0.463
S10P	0.668	0.668	0.668	0.668	0.668	0.668
S15P	0.784	0.784	0.784	0.784	0.784	0.784
S20P	0.387	0.387	0.388	0.386	0.385	0.389
S30P	0.490	0.489	0.490	0.488	0.487	0.491
S40P	0.564	0.564	0.565	0.562	0.561	0.566
CS5P	0.821	0.821	0.821	0.822	0.822	0.820
CS10P	0.927	0.927	0.927	0.928	0.928	0.926
CS15P	0.991	0.991	0.990	0.992	0.992	0.990
CS20P	0.858	0.858	0.858	0.858	0.858	0.858
CS30P	0.948	0.948	0.948	0.948	0.948	0.948
CS40P	1.000	1.000	1.000	1.000	1.000	1.000

The aggregation scores (NDA) presented in Table 5-5 combines the six environmental indicators into a single environmental performance score for each mortar formulation. The resulting ranking is consistent

with the characterised and normalised results discussed previously. The reference mix records the lowest NDA value (0.00), whereas the highest scores are observed for the CS-series, with CS40P (1.00), CS15P (0.99), and CS30P (0.95) ranking as the three best-performing formulations among the nineteen mixes. The C-series and S-series occupy the intermediate range, with NDA values between approximately 0.13 and 0.78 shown in Table 5-5. Overall, the NDA results indicate that, under the zero-burden assumptions adopted in Scenario 1, the combined replacement strategy provides the best overall environmental performance, while the C-series and S-series achieve comparable intermediate improvements relative to the reference mix.

Table 5-5 NDA sustainability score of the mixes, Scenario 1

Mix	NDA score
REF	0.000
C5P	0.134
C10P	0.238
C15P	0.320
C20P	0.405
C30P	0.612
C40P	0.737
S5P	0.463
S10P	0.668
S15P	0.784
S20P	0.387
S30P	0.489
S40P	0.564
CS5P	0.821
CS10P	0.927
CS15P	0.991
CS20P	0.858
CS30P	0.948
CS40P	1.000

The radar diagrams presented in Table 5-6 and Table 5-7 display the normalised six-indicator profile of each mix alongside the reference mortar. Each axis represents one impact category, scaled from 0 (worst) to 1 (best), so a larger shaded area indicates better overall environmental performance. The diagrams

make visible what the NDA score summarises numerically: CS40P fills the hexagon almost completely across all six axes, while REF collapses to a point at the centre, confirming that it is the worst performer on every indicator simultaneously. The uniformity of each mix's profile across the six axes that is near-regular hexagonal shape, reflects the lock-step behaviour of the indicators already observed in the characterised and normalised results: no single category behaves differently from the others for any given mix.

Table 5-6 REF radar

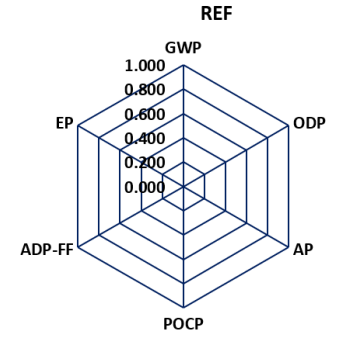
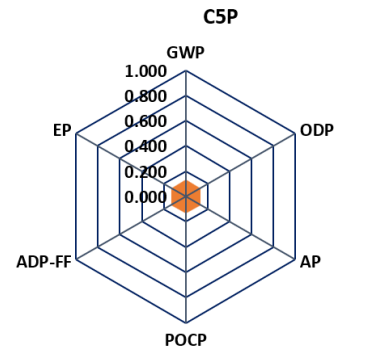
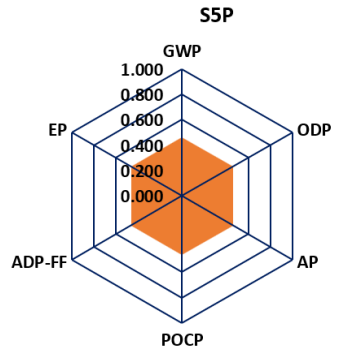
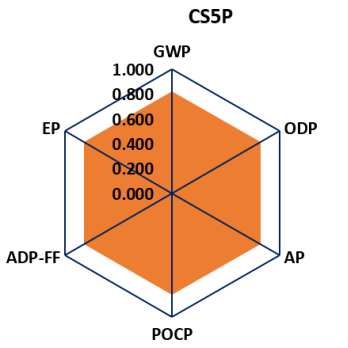
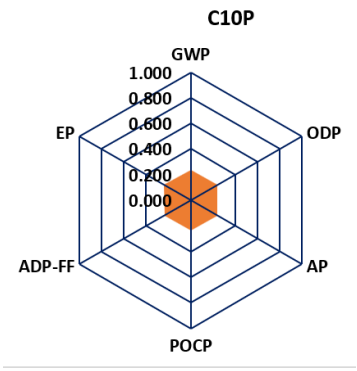
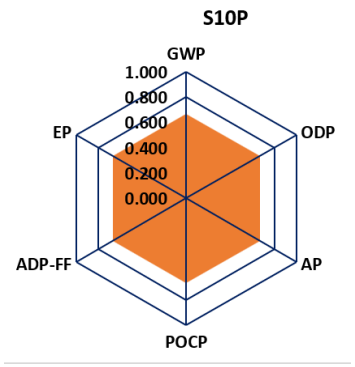
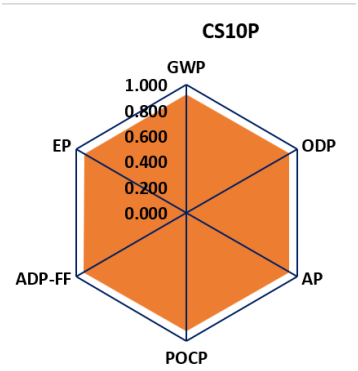
REF


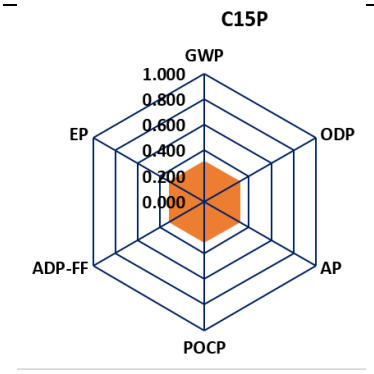
Table 5-7 Radar charts, Scenario 1

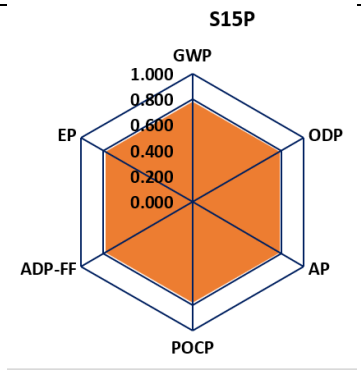
C_Series	**S_Series**	**CS_Series**
		

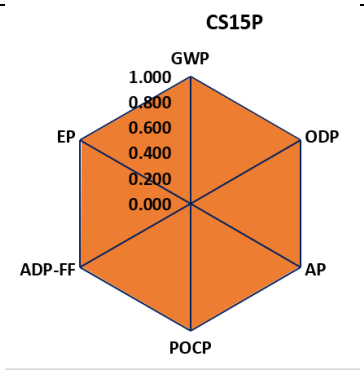

C10P
GWP
ODP
AP
POCP
ADP-FF
EP
1.000
0.800
0.600
0.400
0.200
0.000

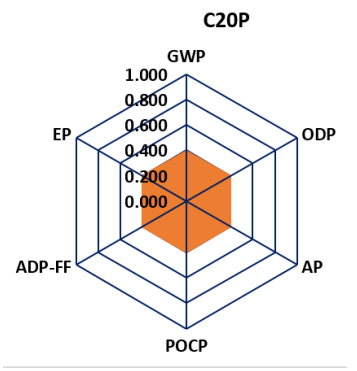

S10P
GWP
ODP
AP
POCP
ADP-FF
EP
1.000
0.800
0.600
0.400
0.200
0.000

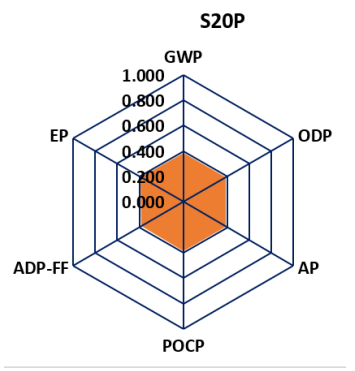

CS10P
GWP
ODP
AP
POCP
ADP-FF
EP
1.000
0.800
0.600
0.400
0.200
0.000

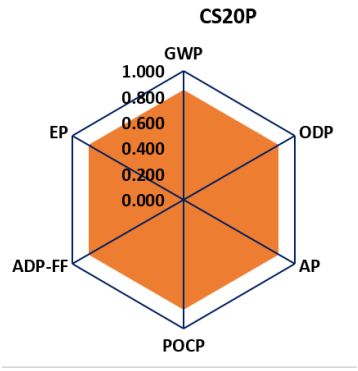

C15P
GWP
ODP
AP
POCP
ADP-FF
EP
1.000
0.800
0.600
0.400
0.200
0.000

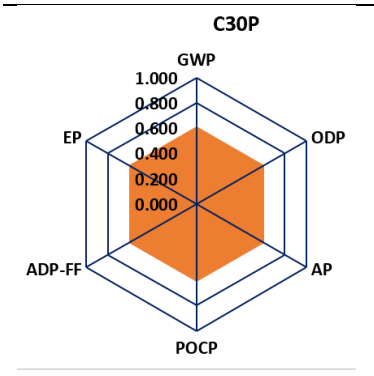

S15P
GWP
ODP
AP
POCP
ADP-FF
EP
1.000
0.800
0.600
0.400
0.200
0.000

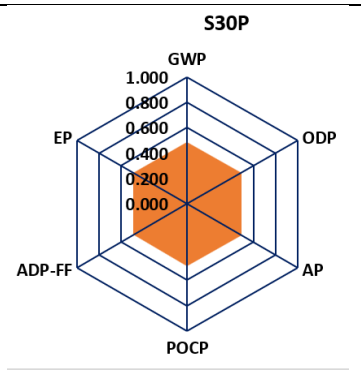

CS15P
GWP
ODP
AP
POCP
ADP-FF
EP
1.000
0.800
0.600
0.400
0.200
0.000

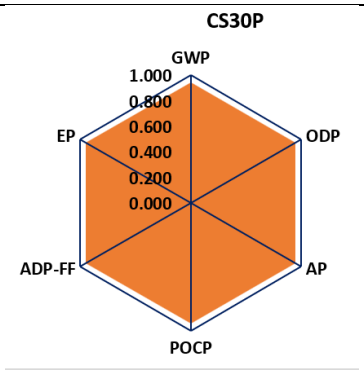

C20P
GWP
ODP
AP
POCP
ADP-FF
EP
1.000
0.800
0.600
0.400
0.200
0.000

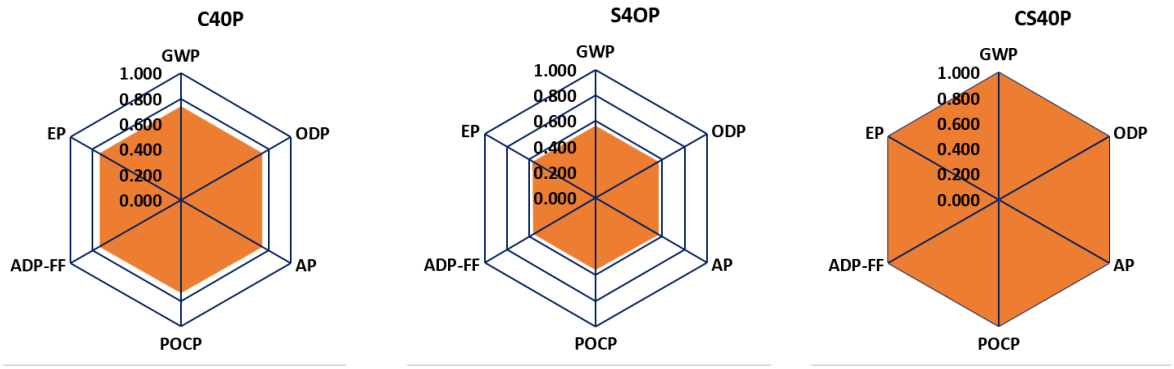

S20P
GWP
ODP
AP
POCP
ADP-FF
EP
1.000
0.800
0.600
0.400
0.200
0.000


CS20P
GWP
ODP
AP
POCP
ADP-FF
EP
1.000
0.800
0.600
0.400
0.200
0.000


C30P
GWP
ODP
AP
POCP
ADP-FF
EP
1.000
0.800
0.600
0.400
0.200
0.000


S30P
GWP
ODP
AP
POCP
ADP-FF
EP
1.000
0.800
0.600
0.400
0.200
0.000


CS30P
GWP
ODP
AP
POCP
ADP-FF
EP
1.000
0.800
0.600
0.400
0.200
0.000



The dominance of the transportation stage across all six impact categories was an unexpected outcome of the system modelled in this study, it departs from the contribution pattern most commonly reported in the literatures. In LCA studies of cementitious materials, transportation is not usually the main environmental hotspot but there are some exceptions. Pradhan et al. [39], in a cradle-to-gate assessment of natural and recycled aggregate concretes, found that cement was responsible for more than 60% of every impact category examined with transport ranking as the second-largest contributor, most visibly in ODP and the ADP categories. Kadawo et al. [40] reached the same ordering for recycled aggregate concrete in Sweden, where cement accounted for over 90% of five of the six categories assessed and transport followed in second place; the single exception was ODP, in which transport dominated the total. A similar picture emerges for mortars specifically: in the review by Santos et al. [41], the binder was consistently identified as the component with the highest impacts, contributing more than 85% of GWP in one of the reviewed studies against only 8% for natural sand, while transport appeared mainly as the driving factor behind the fossil-fuel depletion of mortars incorporating industrial wastes.

The literature supports the plausibility of this configuration-driven result. D'Orazio et al. [42], assessing mortars with fine recycled aggregates from industrial composite waste, showed that aggregate transport distances alone explained 64–94% of the variance of the LCA outcomes, and that the environmental advantage of the recycled route was lost once one-way delivery distances for the waste exceeded roughly 200 km for most impact categories. The 270 km assumed here for the WTB powder sits above that threshold, which is consistent with transport emerging as the decisive stage of the present system.

The inversion of this ranking in the present study follows directly from modelling choices described in Chapter 4. First, the WTB powder enters the system under the cut-off approach, free of any upstream manufacturing burden; its transport over 270 km from the supplier to the mortar plant is therefore the only contribution this constituent makes within the system boundary. Additionally, sand represents between 63.75% and 75% of the dry mass of all nineteen formulations, so the tonne-kilometre burden of

transporting it 77.4 km applies to the bulk of the mix mass in every single formulation. Under these conditions, the transport stage concentrates the transportation of nearly the entire material mass while the raw-material and production stages remain comparatively lean, and its dominance holds uniformly across GWP, ODP, AP, POCP, ADP-FF and EP.

In summary, Scenario 1 establishes that, under the cut-off allocation prescribed by Portuguese waste legislation, the substitution of conventional constituents by WTB powder produces a consistent reduction in characterised impact across all six categories considered, driven principally by the avoided transport burden of the displaced sand rather than by differences in material production. The CS-series achieves the most favourable environmental profile of the three substitution strategies, and the magnitude of the benefit is not associated with any corresponding change, favourable or adverse, in the mechanical and durability properties examined.

Accordingly, CS40P exhibits the lowest environmental impacts among the nineteen formulations, as it incorporates the highest proportion of WTB powder while requiring the lowest quantities of conventional materials. Conversely, the reference mortar shows the highest impacts because it relies entirely on conventional constituents. The consistent dominance of the transportation stage also explains the similar ranking obtained for all six impact categories, resulting in comparable normalised profiles and an identical overall sustainability ranking. These findings are specific to the system boundaries and transport assumptions adopted in the present study.

5.2. Results - Scenario 2

Scenario 2 extends the cut-off model of Scenario 1 by accounting for the electricity consumed in mechanically grinding the manufacturing-generated blade powder into a usable fineness. Its purpose is not to re-establish the environmental hierarchy of the mortars but to test whether that hierarchy survives the inclusion of the energy needed to prepare the powder. If a recovered material appears environmentally attractive only because the cost of processing it has been omitted, that attractiveness is not defensible. Scenario 2 is the step that examines this directly.

Grinding energy is the only inventory component that changes between Scenario 1 and Scenario 2; cement, sand, powder, the associated transport stages, and the mortar mixing energy are all identical between the two scenarios. Its contribution is confined to the powder-containing mixes and ranges from approximately 0.31 kg CO_2-eq/m^3 at the lowest replacement level to 1.82 kg CO_2-eq/m^3 for CS40P as

shown in Table 5-8. Comparing to mortar totals on the order of 9,000–22,000 kg CO_2-eq/m^3, these impacts are so less and not effective.

Table 5-8 Additional grinding energy data, Scenario 2

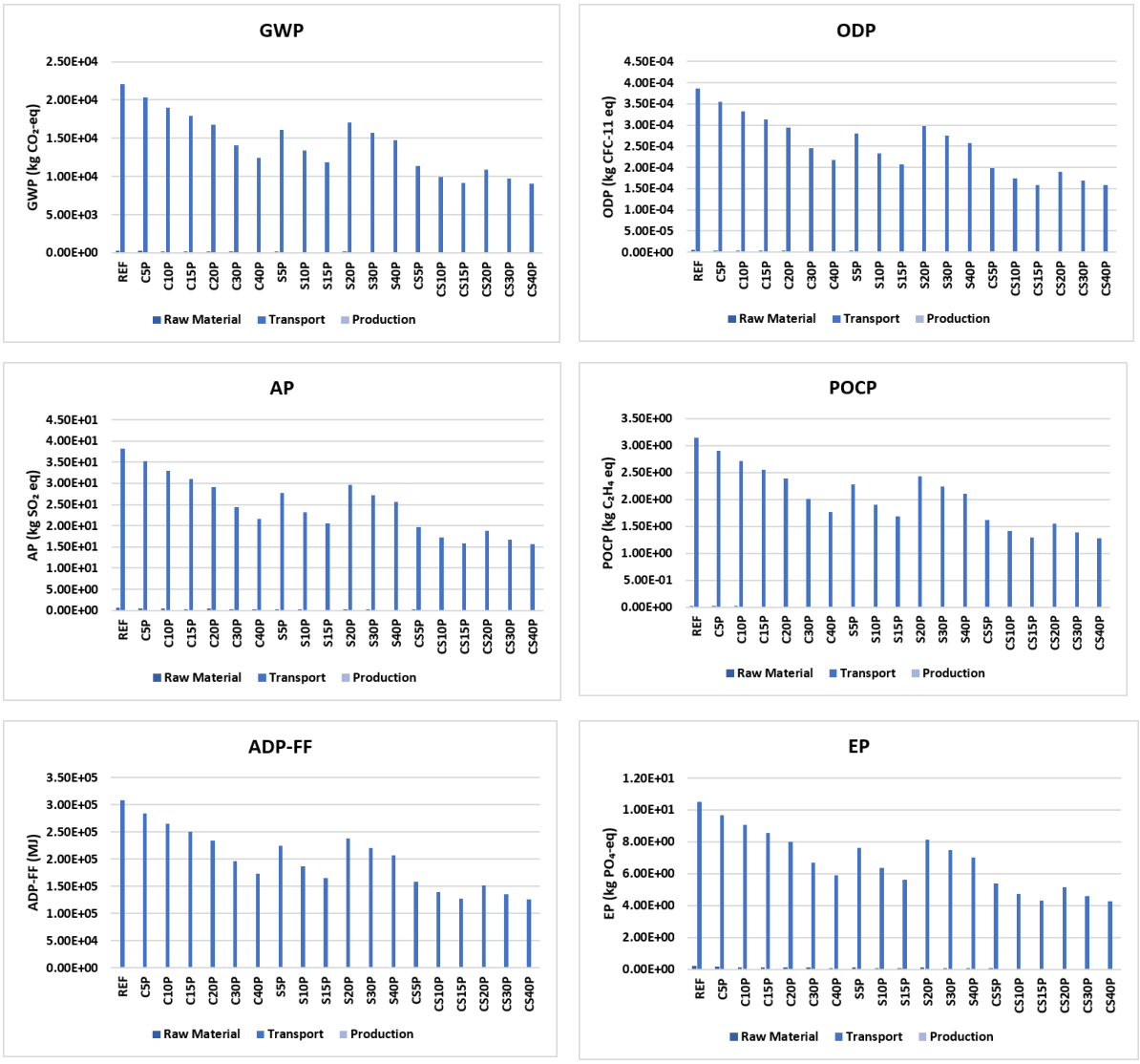
Indicator	GWP	ODP	AP	POCO	ADP-FF	EP
REF	0.00E+00	0.00E+00	0.00E+00	0.00E+00	0.00E+00	0.00E+00
C5P	3.10E-01	7.24E-09	1.08E-03	5.88E-05	4.21E+00	2.18E-04
C10P	5.48E-01	1.28E-08	1.92E-03	1.04E-04	7.45E+00	3.86E-04
C15P	7.38E-01	1.73E-08	2.58E-03	1.40E-04	1.00E+01	5.20E-04
C20P	7.21E-01	1.69E-08	2.52E-03	1.37E-04	9.80E+00	5.08E-04
C30P	1.09E+00	2.55E-08	3.81E-03	2.07E-04	1.48E+01	7.67E-04
C40P	1.31E+00	3.07E-08	4.59E-03	2.49E-04	1.78E+01	9.24E-04
S5P	8.73E-01	2.04E-08	3.05E-03	1.66E-04	1.19E+01	6.15E-04
S10P	1.26E+00	2.95E-08	4.41E-03	2.39E-04	1.71E+01	8.87E-04
S15P	1.48E+00	3.46E-08	5.17E-03	2.81E-04	2.01E+01	1.04E-03
S20P	8.92E-01	2.09E-08	3.12E-03	1.69E-04	1.21E+01	6.28E-04
S30P	1.13E+00	2.64E-08	3.94E-03	2.14E-04	1.53E+01	7.94E-04
S40P	1.30E+00	3.04E-08	4.54E-03	2.47E-04	1.77E+01	9.15E-04
CS5P	1.46E+00	3.42E-08	5.11E-03	2.77E-04	1.99E+01	1.03E-03
CS10P	1.65E+00	3.86E-08	5.77E-03	3.13E-04	2.24E+01	1.16E-03
CS15P	1.76E+00	4.12E-08	6.16E-03	3.35E-04	2.40E+01	1.24E-03
CS20P	1.62E+00	3.78E-08	5.66E-03	3.07E-04	2.20E+01	1.14E-03
CS30P	1.79E+00	4.18E-08	6.25E-03	3.40E-04	2.43E+01	1.26E-03
CS40P	1.89E+00	4.41E-08	6.60E-03	3.58E-04	2.57E+01	1.33E-03

The significance of this result lies in its size. The grinding step required to convert the waste powder into a usable constituent adds an environmentally negligible burden, which demonstrates that the favourable impacts recorded in Scenario 1 are not an artefact of excluding powder preparation. The environmental case for the powder does not depend on ignoring the energy needed to process it.

In this scenario, the stage contribution analysis was repeated to evaluate the influence of including the mechanical grinding process applied to the WTB powder prior to its incorporation into the mortar. Unlike Scenario 1, the production stage includes both the electricity required for mortar mixing and the electricity consumed during the grinding process. The environmental impacts associated with the additional mechanical processing are presented in Table 5-9 with same impacts and units of Scenario 1.

The addition of the mechanical grinding process for the WTB powder introduces a contribution to the production stage that was absent in Scenario 1, however, as can be seen from the figures, this addition has no perceptible effect on the overall stage distribution. Transportation remains overwhelmingly dominant across all impact categories, and the visual pattern of the charts is effectively identical to that of Scenario 1, while the production stage increases only slightly due to the inclusion of grinding electricity and overall results remained unchanged compared to previous scenario.

Table 5-9 Contribution of life cycle stages to the environmental impact categories, Scenario 2.



The total characterised environmental impacts of the nineteen mortar formulations, obtained after incorporating the grinding process into the Scenario 1 inventory, are presented in table below. Compared with Scenario 1, only minor differences are observed in the powder-containing formulations, affecting only

the last significant figures, while the ranking of the formulations remains unchanged across all impact categories.

Table 5-10 Total characterized environmental impact of mixes, Scenario 2

Indicator	**GWP**	**ODP**	**AP**	**POCO**	**ADP-FF**	**EP**
Unit	kg CO2 eq	kg CFC-11 eq	kg SO2 eq	kg C2H4-eq	MJ	kg PO4-eq
REF	2.24E+04	3.91E-04	38.88	3.17	3.10E+05	10.72
C5P	2.06E+04	3.60E-04	35.76	2.92	2.86E+05	9.86
C10P	1.92E+04	3.36E-04	33.35	2.73	2.67E+05	9.19
C15P	1.81E+04	3.16E-04	31.44	2.57	2.52E+05	8.66
C20P	1.70E+04	2.97E-04	29.48	2.41	2.36E+05	8.13
C30P	1.42E+04	2.48E-04	24.69	2.02	1.98E+05	6.80
C40P	1.26E+04	2.19E-04	21.78	1.78	1.74E+05	6.00
S5P	1.62E+04	2.83E-04	28.14	2.30	2.25E+05	7.76
S10P	1.35E+04	2.35E-04	23.38	1.91	1.87E+05	6.44
S15P	1.19E+04	2.08E-04	20.70	1.70	1.66E+05	5.70
S20P	1.72E+04	3.01E-04	29.88	2.45	2.39E+05	8.23
S30P	1.59E+04	2.77E-04	27.51	2.25	2.21E+05	7.57
S40P	1.49E+04	2.60E-04	25.78	2.11	2.07E+05	7.10
CS5P	1.14E+04	2.00E-04	19.83	1.62	1.59E+05	5.46
CS10P	1.00E+04	1.75E-04	17.38	1.42	1.39E+05	4.79
CS15P	9.17E+03	1.60E-04	15.89	1.30	1.28E+05	4.38
CS20P	1.09E+04	1.91E-04	18.97	1.56	1.52E+05	5.22
CS30P	9.75E+03	1.70E-04	16.89	1.39	1.36E+05	4.65
CS40P	9.05E+03	1.58E-04	15.67	1.29	1.26E+05	4.31

The normalisation reference points for Scenario 2 were extracted from the recalculated totals following the same min–max procedure applied in the first scenario. CS40P and REF again define the best and worst bounds of every impact category, so the normalisation scale is effectively identical to that of Scenario 1.

Table 5-11 Best (minimum) and worst (maximum) characterised values identified across the mixes, for each impact category, used as the normalisation reference points, Scenario 2.

Indicator	P*best (MIN)	P*worst (MAX)
GWP-total	9.05E+03	2.24E+04
Ozone depletion (ODP)	1.58E-04	3.91E-04
Acidification (AP)	1.57E+01	3.89E+01
Photochemical oxidation	1.29E+00	3.17E+00
Abiotic Depletion Fossil Fuels	1.26E+05	3.10E+05
Eutrophication	4.31E+00	1.07E+01

Because the grinding energy increases with powder content, mixes containing more powder receive a slightly larger additional environmental burden. However, this increase is negligible and does not affect the relative ranking of the mixes after normalisation. The normalised results therefore follow the same pattern as in Scenario 1, with no impact category responding differently to the inclusion of grinding energy. This indicates that grinding energy has no meaningful influence on the environmental profile of the mortars.

As the NDA ranking obtained in Scenario 2 is identical to that presented in Scenario 1, the corresponding table and figure are not repeated to avoid unnecessary duplication.

Table 5-12 Normalised Values, Scenario 2

Indicator	GWP	ODP	AP	POCO	ADP-FF	EP
REF	0.000	0.000	0.000	0.000	0.000	0.000
C5P	0.134	0.134	0.135	0.134	0.134	0.135
C10P	0.238	0.238	0.238	0.237	0.237	0.239
C15P	0.320	0.320	0.321	0.319	0.318	0.321
C20P	0.405	0.405	0.405	0.406	0.406	0.405
C30P	0.612	0.612	0.612	0.612	0.613	0.611
C40P	0.737	0.737	0.737	0.738	0.738	0.736
S5P	0.463	0.463	0.463	0.463	0.463	0.463
S10P	0.668	0.668	0.668	0.668	0.668	0.668
S15P	0.784	0.784	0.784	0.784	0.784	0.784
S20P	0.387	0.387	0.388	0.386	0.385	0.389
S30P	0.490	0.489	0.490	0.488	0.487	0.491
S40P	0.564	0.564	0.565	0.562	0.561	0.566
CS5P	0.821	0.821	0.821	0.822	0.822	0.820
CS10P	0.927	0.927	0.927	0.928	0.928	0.926
CS15P	0.991	0.991	0.990	0.992	0.992	0.990
CS20P	0.858	0.858	0.858	0.858	0.858	0.858
CS30P	0.948	0.948	0.948	0.948	0.948	0.948
CS40P	1.000	1.000	1.000	1.000	1.000	1.000

Table 5-13 NDA sustainability score of the mixes, Scenario 2

Mix	NDA score
REF	0.000
C5P	0.134
C10P	0.238
C15P	0.320
C20P	0.405
C30P	0.612
C40P	0.737
S5P	0.463
S10P	0.668
S15P	0.784
S20P	0.387
S30P	0.489
S40P	0.564
CS5P	0.821
CS10P	0.927
CS15P	0.991
CS20P	0.858
CS30P	0.948
CS40P	1.000

The radar profiles for Scenario 2 are visually indistinguishable from those of Scenario 1, confirming that the addition of grinding energy does not alter the normalised six-indicator shape of any mix as shown in Table 5-14 and Table 5-15.

Table 5-14 Ref radar chart, Scenario 2

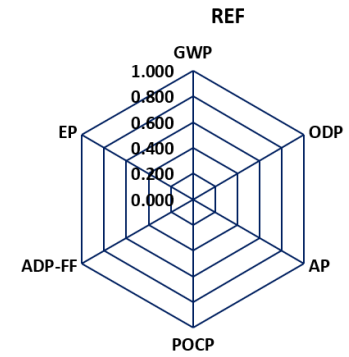
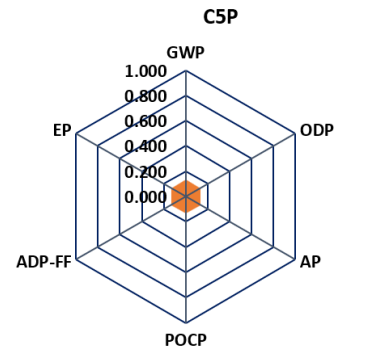
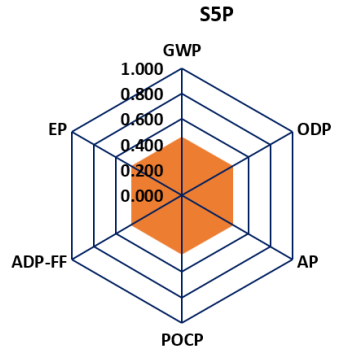
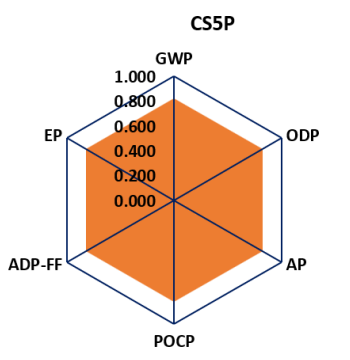
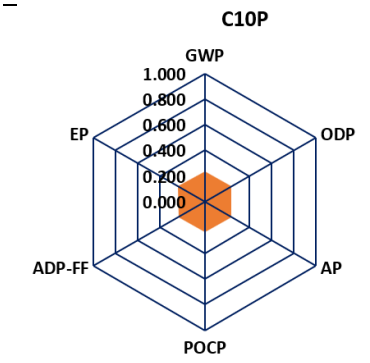
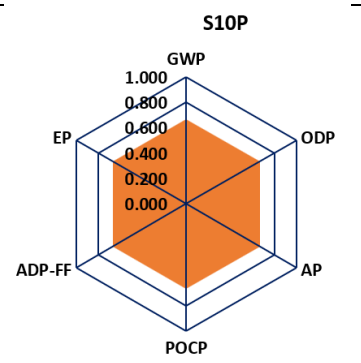
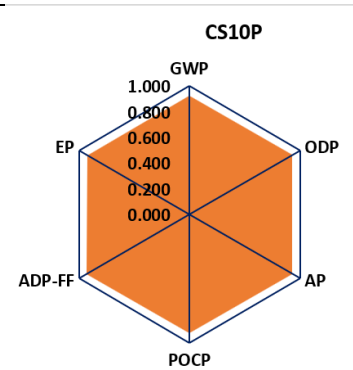
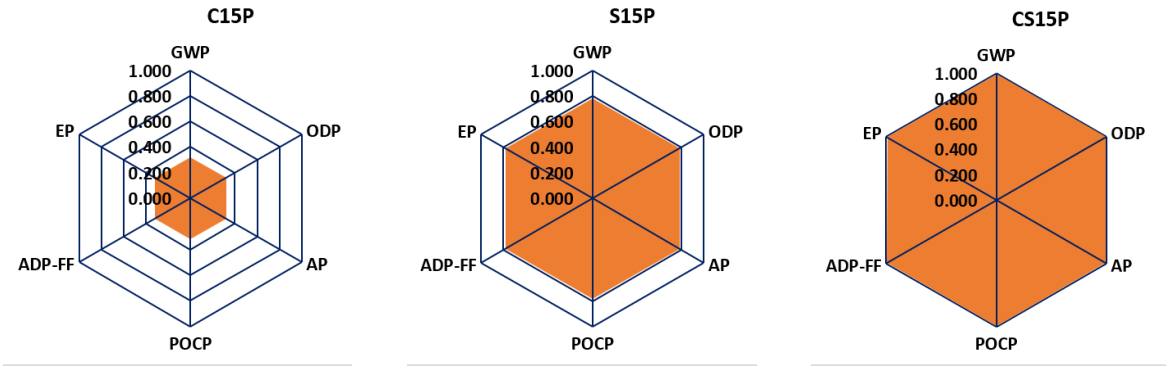
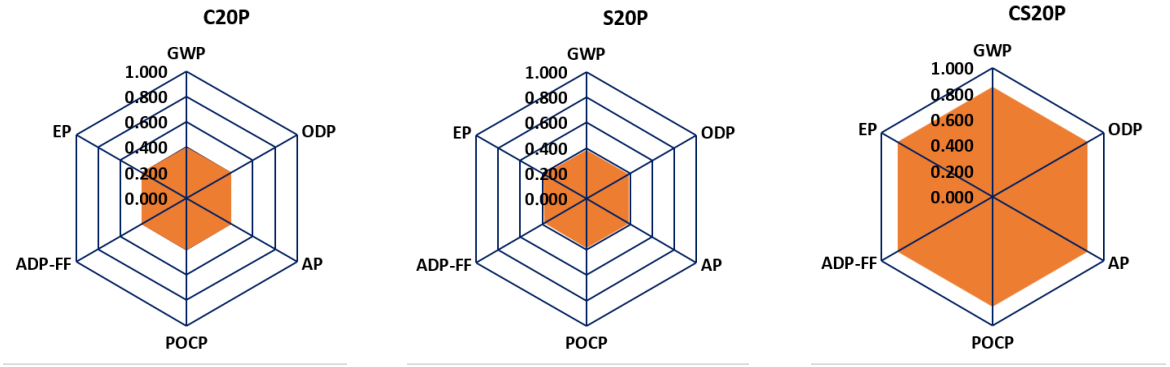
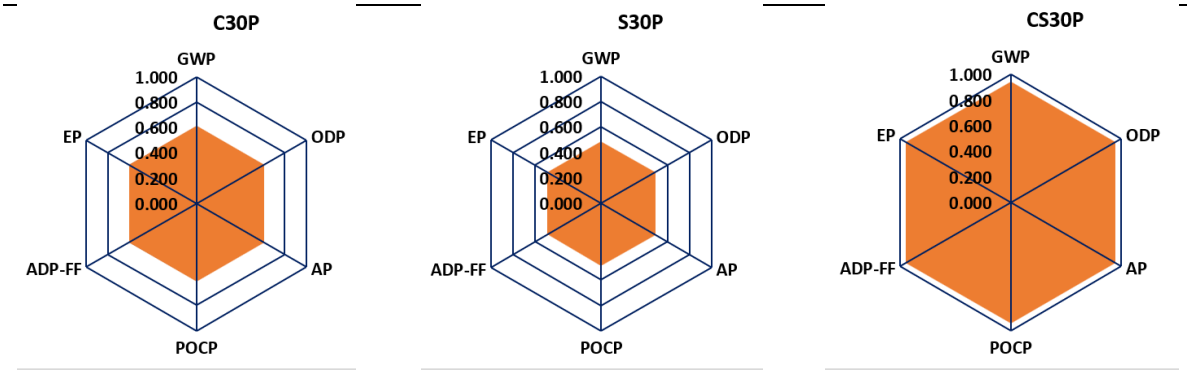
REF


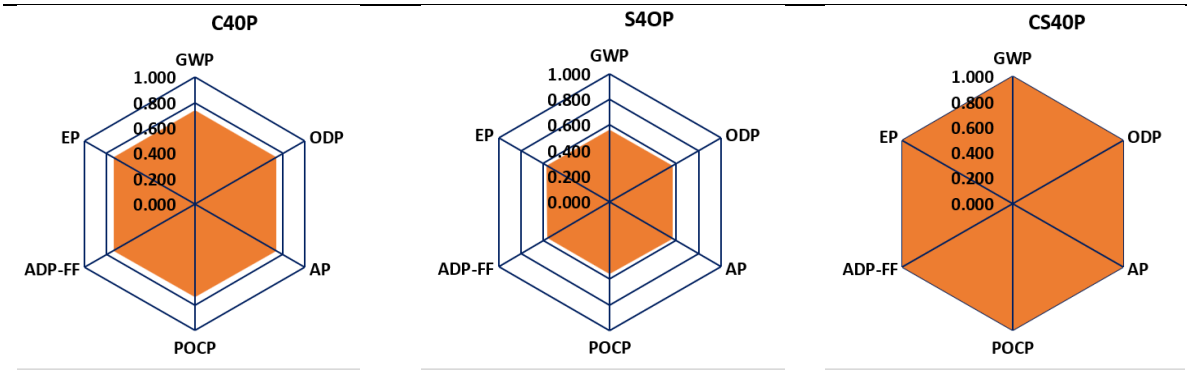
Table 5-15 Radar charts, Scenario 2

C_Series	**S_Series**	**CS_Series**
		
		









Although the contribution of the grinding process is negligible, the normalisation results provide an additional observation. The worst reference value in each impact category remains unchanged from

Scenario 1 because the reference mortar contains no WTB powder and therefore incurs no grinding burden. In contrast, the best reference value increases slightly (approximately 0.02–0.04%) because CS40P, which defines the minimum environmental impact, receives the largest grinding contribution among all formulations. Consequently, the additional burden is applied primarily to the powder-rich formulations. Despite this, the resulting changes are extremely small, with the maximum variation in the normalised indicators reaching only 3.5×10^{-5} and the largest change in the NDA score only 2.2×10^{-5}. The ranking of the mortar formulations therefore remains unchanged across all environmental impact categories. These results demonstrate that including the energy required for mechanical grinding does not alter the environmental conclusions obtained in Scenario 1, indicating that the environmental advantage of incorporating WTB powder is not dependent on neglecting its preparation energy.

As discussed for Scenario 1, transport remains the dominant contributor because of the modelling assumptions adopted in this study: the WTB powder enters the system under the cut-off approach, cement transport is excluded due to co-location of production and mortar manufacturing, and sand, which represents 63.75–75% of the dry mix mass, is transported over 77.4 km. Since Scenario 2 changes none of these conditions and only adds a small processing burden, the overall contribution pattern remains unchanged. These results suggest that reducing the environmental impact of the mortars is unlikely to be achieved through optimisation of the grinding process. Instead, the greatest opportunity for improvement lies in reducing the transport distance of the WTB powder and aggregates.

5.3. Results - Scenario 3

The two preceding scenarios treated the manufacturing-generated blade powder as a burden-free residue, carrying at most the energy required to grind it. That treatment is defensible only while the powder has no economic value. Scenario 3 relaxes this assumption and assigns the powder a share of the upstream blade-manufacturing burden in proportion to its economic value, following the economic allocation principle. This makes Scenario 3 the most representative of a real manufacturing system, in which a residue that acquires market value can no longer be considered environmentally free. The question it addresses is therefore specific: once the powder is charged with an economic share of the blade-manufacturing burden, does the environmental performance of the mortars, and the ranking established under the cut-off scenarios, change, and how sensitive is that answer to the price assigned to the powder?

5.3.1. Allocation basis: production data, prices and the allocation coefficient

The economic allocation was built from the production data of the blade-manufacturing facility. The reference blade is the SNL-100-03 design [43],100 meters blade with a mass of 49 977 kg and a reported manufacturing cost of 471 529.55 Euros (converted from 547 723.35 United States Dollar (USD) at 0.8607 USD to EUR). Since detailed industrial cost data for wind turbine blade constituents are not generally publicly available, the cost data used in this study were adopted from the NREL blade cost model developed by the National Renewable Energy Laboratory (NREL) [43], which provides a comprehensive bill of materials and corresponding unit prices for modern composite wind turbine blades. I was assumed that companied produced 1 blade per day (Estimated 30 blades per month) and 29 tonnes of manufacturing powder over the same period, which corresponds to a powder yield of 1.93% of the blade mass, or 966.7 kg of powder per blade. These figures fix the physical quantities that enter the allocation: the mass of powder recovered from each blade and the economic value of the system from which it originates.

Because the WTB powder has no established market price, its value was expressed as a fraction of the price of the constituent it replaces. For the C-series the powder was priced against cement (207.6 Euros per tonne) adapted from [44] and for the S-series against silica sand (314 Euros per tonne) adapted from [45] . Three price levels were examined for each of the reference material price percentage (10%, 50% and 100%) giving powder prices of 20.76, 103.8 and 207.6 Euros per tonne for the C-series and 31.4, 157 and 314 Euros per tonne for the S-series as shown totally in Table 5-16. The allocation coefficient α, defined as the ratio of the powder value to the combined value of the blade and the powder, follows directly from these prices.

Table 5-16 Powder prices

Series	Reference material	10% price (€/t)	50% price (€/t)	100% price (€/t)
C-series	Cement (207.6 €/t)	20.76	103.8	207.6
S-series	Sand (314 €/t)	31.4	157	314

The resulting allocation coefficients are reported in Table 5-17 For the C-series, α rises from 4.26×10^{-5} at the 10% price to 4.25×10^{-4} at the 100% price; for the S-series, which is valued against the more expensive sand, α is slightly higher at each level, from 6.44×10^{-5} to 6.43×10^{-4}. The CS-series is a distinct case: because the powder simultaneously displaces cement and sand, its price was computed as a mass-weighted combination of the cement and sand prices according to each mix's cement-to-sand ratio, so the CS-series carries its own set of coefficients.

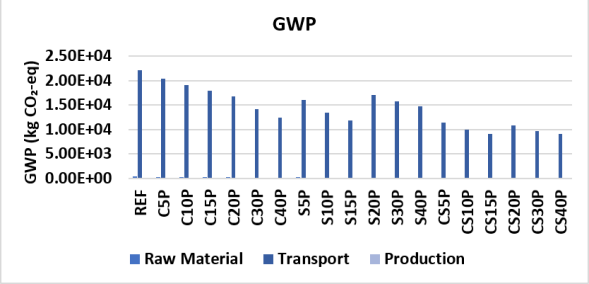
Table 5-17 Economic allocation coefficient for all mixes, Scenario 3

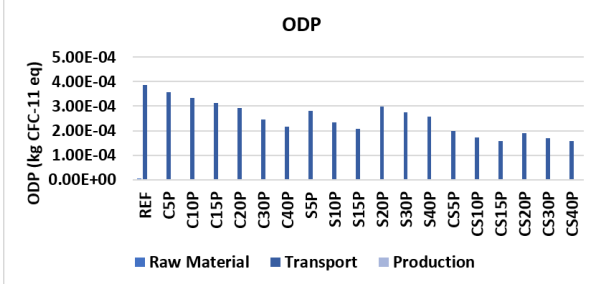
Series / Mix	$\alpha - 10\%$	$\alpha - 50\%$	$\alpha - 100\%$
C-series (all C mixes)	4.26×10^{-5}	2.13×10^{-4}	4.25×10^{-4}
S-series (all S mixes)	6.44×10^{-5}	3.22×10^{-4}	6.43×10^{-4}
CS5P	5.80×10^{-5}	2.90×10^{-4}	5.79×10^{-4}
CS10P	5.73×10^{-5}	2.87×10^{-4}	5.73×10^{-4}
CS15P	5.66×10^{-5}	2.83×10^{-4}	5.65×10^{-4}
CS20P	5.89×10^{-5}	2.95×10^{-4}	5.89×10^{-4}
CS30P	5.89×10^{-5}	2.95×10^{-4}	5.89×10^{-4}
CS40P	5.89×10^{-5}	2.95×10^{-4}	5.89×10^{-4}

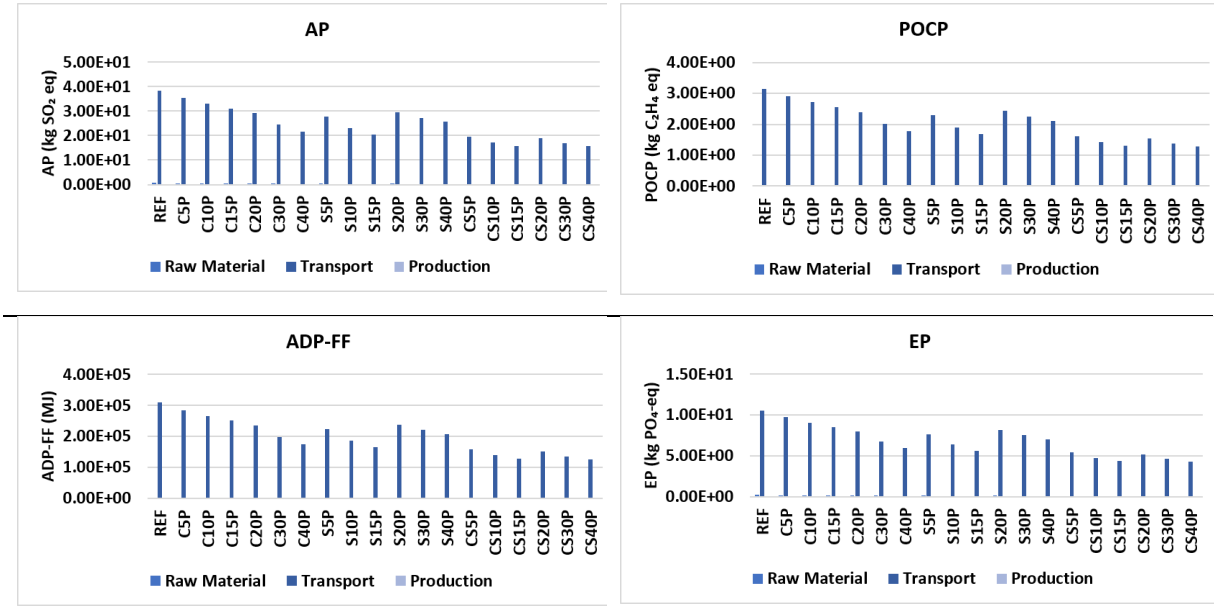
Introducing economic allocation assigns, for the first time, a burden to the powder-containing mixes; REF contains no powder and is unchanged from the earlier scenarios. Table 5-19 reports the characterised impacts at the 10% price level. The reference mortar again records the highest GWP, 2.24×10^{4} kg CO_2-eq, and CS40P the lowest, 9.05×10^{3} kg CO_2-eq, with the same ordering preserved across all six indicators. The best and worst performing formulations are identical to those of the cut-off scenarios, the CS-series at the favourable end and REF at the unfavourable end.

The stage contribution analysis was repeated under the economic allocation with same impacts and units to verify where the newly allocated burden appears in the system. Unlike the two previous scenarios, the raw material stage now includes a share of the blade manufacturing burden carried by the powder, in addition to the production of cement and sand. The charts below in Table 5-18 show the resulting distribution at the 50% price level. The allocated share is too small to be visible, transportation remains the dominant stage in every impact category and for every formulation, and the distribution of burdens among the three stages is unchanged from the cut-off scenarios at the resolution of the charts.

Table 5-18 Contribution of life cycle stages to the environmental impact categories, Scenario 3 (50%)







The characterised results are reported in full for the 50% price level, which serves as the central estimate of the analysis, the 10% and 100% levels behave in the same way.

Table 5-19 Total characterised environmental impact of mixes, Scenario 3 (50% price)

Indicator	GWP	ODP	AP	POCO	ADP-FF	EP
Unit	kg CO2 eq	kg CFC-11 eq	kg SO2 eq	kg C2H4-eq	MJ	kg PO4-eq
REF	2.24E+04	3.91E-04	3.89E+01	3.17	3.10E+05	10.72
C5P	2.06E+04	3.60E-04	3.58E+01	2.92	2.86E+05	9.86
C10P	1.92E+04	3.36E-04	3.34E+01	2.73	2.67E+05	9.19
C15P	1.81E+04	3.16E-04	3.14E+01	2.57	2.52E+05	8.67
C20P	1.70E+04	2.97E-04	2.95E+01	2.41	2.36E+05	8.13
C30P	1.42E+04	2.49E-04	2.47E+01	2.02	1.98E+05	6.81
C40P	1.26E+04	2.19E-04	2.18E+01	1.78	1.74E+05	6.00
S5P	1.62E+04	2.83E-04	2.81E+01	2.30	2.25E+05	7.76
S10P	1.35E+04	2.35E-04	2.34E+01	1.91	1.87E+05	6.44
S15P	1.19E+04	2.08E-04	2.07E+01	1.70	1.66E+05	5.70
S20P	1.72E+04	3.01E-04	2.99E+01	2.45	2.39E+05	8.24
S30P	1.59E+04	2.77E-04	2.75E+01	2.25	2.21E+05	7.58
S40P	1.49E+04	2.60E-04	2.58E+01	2.11	2.07E+05	7.10
CS5P	1.14E+04	2.00E-04	1.98E+01	1.62	1.59E+05	5.47
CS10P	1.00E+04	1.75E-04	1.74E+01	1.42	1.39E+05	4.79
CS15P	9.17E+03	1.60E-04	1.59E+01	1.30	1.28E+05	4.38
CS20P	1.09E+04	1.91E-04	1.90E+01	1.56	1.52E+05	5.23
CS30P	9.75E+03	1.70E-04	1.69E+01	1.39	1.36E+05	4.65
CS40P	9.05E+03	1.58E-04	1.57E+01	1.29	1.26E+05	4.32

Introducing economic allocation adds a burden to the powder-containing mixes for the first time, since REF carries no powder and is identical to its value in the earlier scenarios. The size of this addition is small. Even under the most demanding price assumption, the allocated burden raises the characterised impacts of all mixes reported in Table 5-19. The allocated burden per kilogram of powder is small in absolute terms, for GWP it amounts to 0.021 kg CO_2-eq/kg for the C-series and 0.032 kg CO_2-eq/kg for the S-series at the 100% price, so that the impact of each mortar remains governed by its cement and sand content. Under this scenario the reference mix again records the highest GWP at 2.24×10^4 kg CO_2-eq, while CS40P records the lowest at 9.05×10^3 kg CO_2-eq, and the same ordering holds across the remaining five indicators.

The best- and worst-performing formulations are the same as those identified in the earlier scenarios, with the CS-series at the favourable end and REF at the unfavourable end.

Table 5-20 Best (minimum) and worst (maximum) characterised values identified across the mixes, for each impact category, used as the normalisation reference points.

Indicator	P*best (MIN)	P*worst (MAX)
GWP-total	9.05E+03	2.24E+04
Ozone depletion (ODP)	1.58E-04	3.91E-04
Acidification (AP)	1.57E+01	3.89E+01
Photochemical oxidation	1.29E+00	3.17E+00
Abiotic Depletion Fossil Fuels	1.26E+05	3.10E+05
Eutrophication	4.32E+00	1.07E+01

Raising the powder price to 50% and then to 100% of the reference-material price multiplies α roughly fivefold and tenfold in turn, yet the characterised impacts barely respond. For CS40P, the mix carrying the most powder and therefore the largest allocated burden, GWP moves from 9,045 kg CO_2-eq at the 10% price to 9,047 at the 50% price and 9,049 at the 100% price. The largest change anywhere in the dataset, again for CS40P, amounts to less than 0.04% of the mix's total impact. For the reference mix the value does not move at all across the three levels, as expected for a mortar that contains no powder. The allocated burden is not distributed evenly across the indicators (relative to the powder it weighs most on fossil-fuel depletion and least on ozone depletion) but these differences are far too small, set against the total for each category, to shift any mix relative to another.

Because the allocated burden moves every powder-containing mix in the same direction and by a comparable, very small amount, the normalisation step returns essentially the same picture at each price level. CS40P holds the maximum normalised value of 1.00 in every impact category and at every price, while REF holds 0.00 throughout. The normalised profiles of the intermediate mixes are, to three decimal places, indistinguishable between the 10%, 50% and 100% cases: C40P sits at 0.737 in each, S15P at 0.784 in each, and CS15P at 0.991 in each. As in the earlier scenarios, the six indicators normalise to nearly identical values for any given mix, so the environmental profiles remain close to regular hexagons and no single category governs the outcome.

The normalisation reference points show the same asymmetry already observed in Scenario 2. The worst (maximum) value of every category is identical to the earlier scenarios, since the reference mix contains no powder and receives no allocated burden, while the best (minimum) value is marginally higher, because CS40P, which defines it, carries the largest allocated burden of the study. The interval over which the mixes are normalised is therefore essentially unchanged.

Table 5-21 Normalised Values, Scenario 3 (50% price)

Indicator	GWP	ODP	AP	POCO	ADP-FF	EP
REF	0.000	0.000	0.000	0.000	0.000	0.000
C5P	0.134	0.134	0.135	0.134	0.134	0.135
C10P	0.238	0.238	0.238	0.237	0.237	0.239
C15P	0.320	0.320	0.321	0.319	0.318	0.321
C20P	0.405	0.405	0.405	0.406	0.406	0.405
C30P	0.612	0.612	0.612	0.612	0.613	0.611
C40P	0.737	0.737	0.737	0.738	0.738	0.737
S5P	0.463	0.463	0.463	0.463	0.463	0.463
S10P	0.668	0.668	0.668	0.668	0.668	0.668
S15P	0.784	0.784	0.784	0.784	0.784	0.783
S20P	0.387	0.387	0.388	0.386	0.385	0.388
S30P	0.490	0.489	0.490	0.487	0.487	0.491
S40P	0.564	0.564	0.564	0.562	0.561	0.566
CS5P	0.821	0.821	0.821	0.822	0.822	0.820
CS10P	0.927	0.927	0.927	0.928	0.928	0.926
CS15P	0.991	0.991	0.990	0.992	0.992	0.990
CS20P	0.858	0.858	0.858	0.858	0.858	0.858
CS30P	0.948	0.948	0.948	0.948	0.948	0.948
CS40P	1.000	1.000	1.000	1.000	1.000	1.000

The aggregated NDA scores confirm that the economic allocation, across the full range of prices tested, leaves the environmental ranking intact as shown in Figure 5-2. CS40P is the best-performing formulation at every price level with a score of 1.00, followed by CS15P (0.99) and CS30P (0.95); REF remains the lowest at 0.00. The C-series and S-series occupy the intermediate range, between roughly 0.13 and 0.78. Moving from the 10% to the 100% price changes, the complete ordering of the nineteen formulations is identical at all three levels. Within the S-series the same non-monotonic pattern noted earlier persists: S15P (0.78) is the strongest of the series, while S20P falls to 0.39 before the scores recover at S30P and S40P.

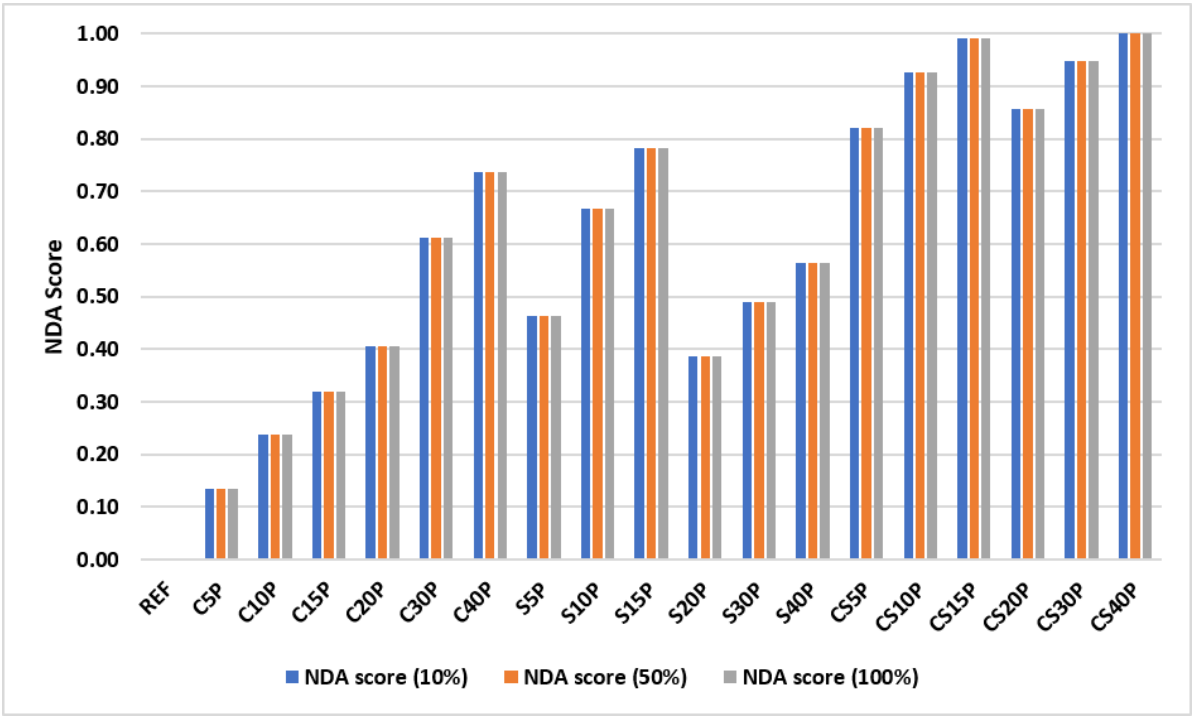


Figure 5-2 NDA sustainability score of the mixes, Scenario 3 (all prices)

The radar profiles shown in Table 5-22 and Table 5-23 are indistinguishable from those of the cut-off scenarios. The largest difference in any normalised value between Scenario 1 and Scenario 3 at the 50% price level is 2×10^{-4}, below the resolution of any graphical representation, so the six-indicator shape of every mix is preserved.

Table 5-22 Reference radar chart, Scenario 3

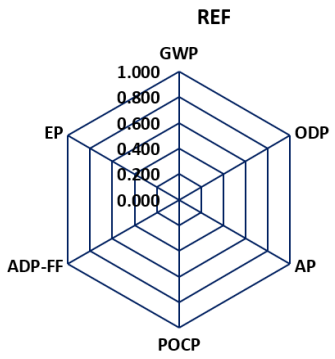
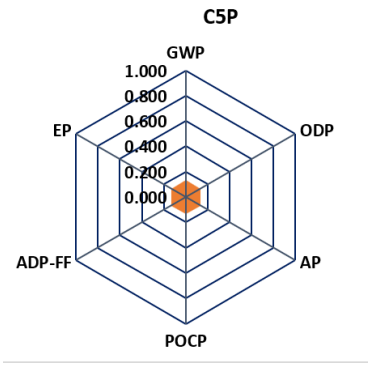
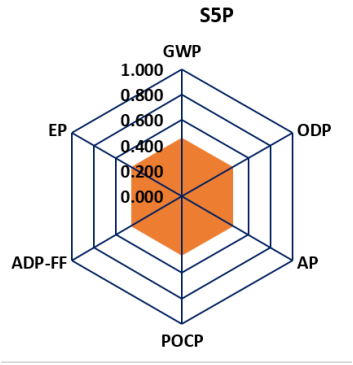
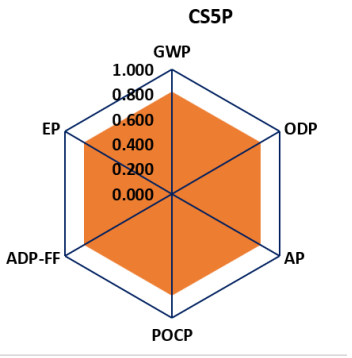
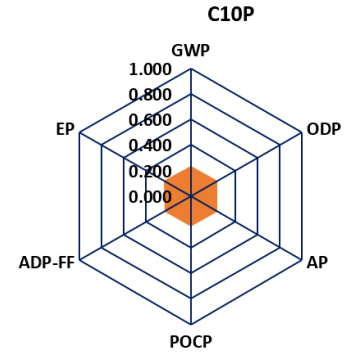
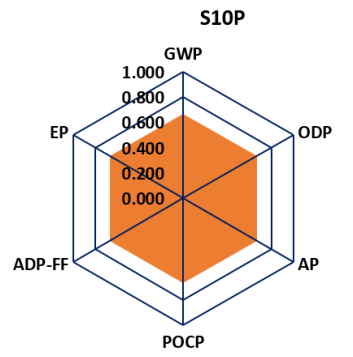
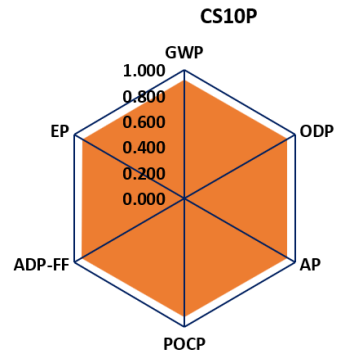
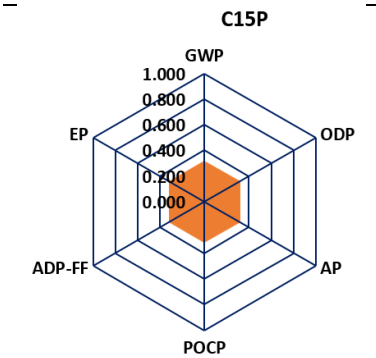
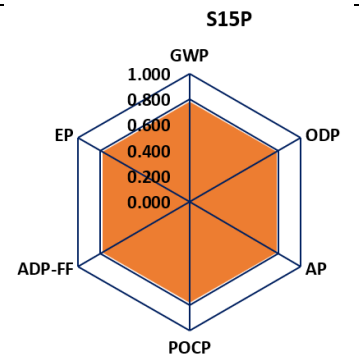
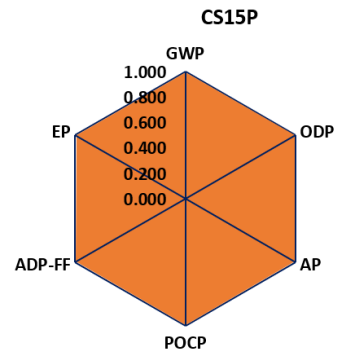
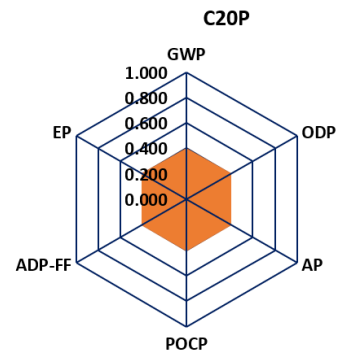
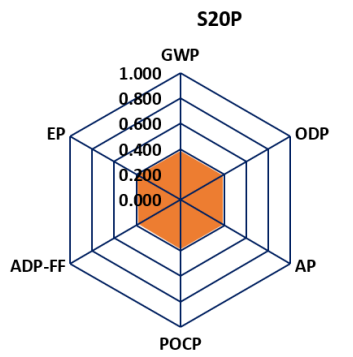
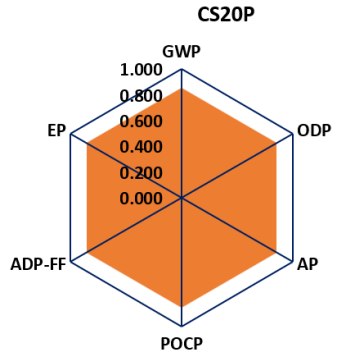
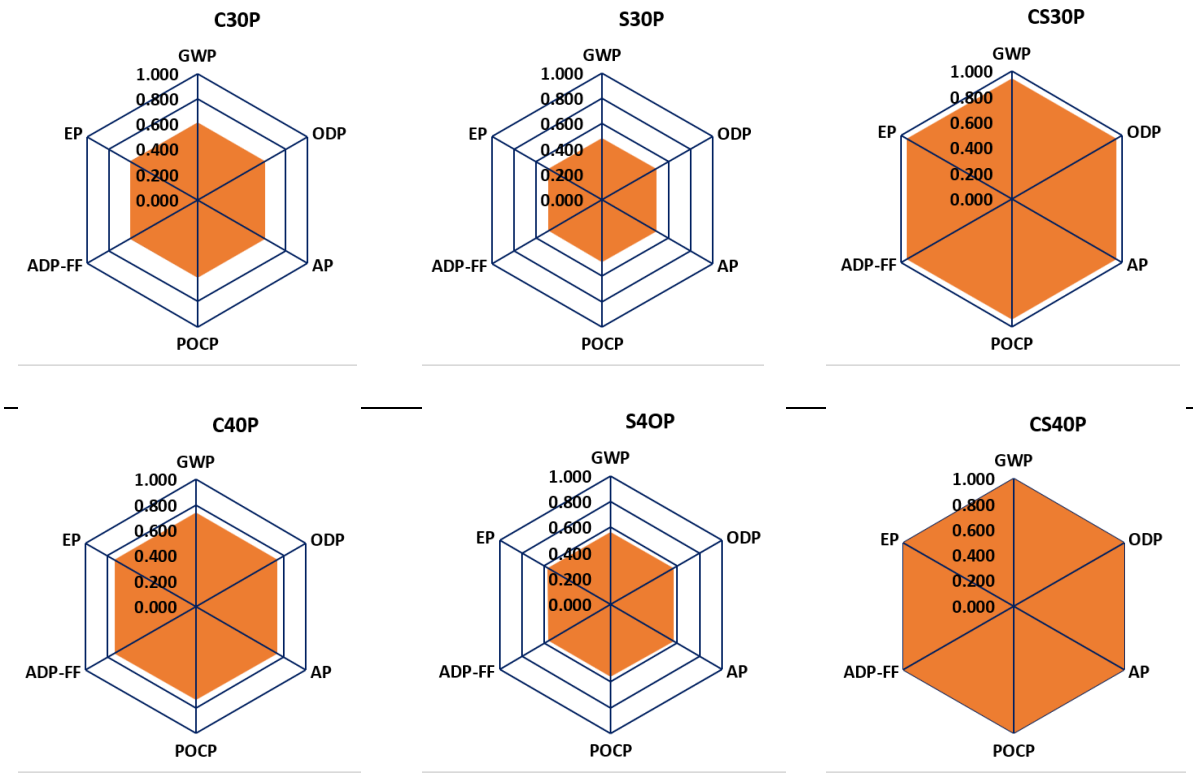
REF


Table 5-23 Radar charts Scenario 3 (50%)

C_Series	S_Series	CS_Series
		
		
		
		



5.3.2. Sensitivity

The characterisation step produced total environmental impacts in absolute units for each mortar formulation across the three scenarios. The purpose of the sensitivity analysis is twofold: first, to test whether those absolute impact values are stable when the assumptions underlying the economic allocation are varied across scenarios and price levels; and second, to confront the characterised environmental results with the measured mechanical and durability behaviour of the mortars, so that the formulations can be judged not only on their environmental impact but on their overall engineering suitability. The analysis was carried out for all three scenarios and, within Scenario 3, at the three powder-price levels, using the two most representative impact indicators, GWP and ADP-FF, against four measured properties reported Bettini et al. [6].

Table 5-24 Sensitivity Data

Mix	ADP-FF	GWP	Flexural Strength	Compressive Strength	Water Absorption Immersion	Water Absorption Capillarity
REF	3.10E+05	2.24E+04	6.25	35.80	19.476	0.35
C5P	2.86E+05	2.06E+04	6.36	34.40	18.4082	0.32
C10P	2.67E+05	1.92E+04	5.82	32.7	18.8445	0.37
C15P	2.52E+05	1.81E+04	6.46	34.7	17.23	0.32
C20P	2.36E+05	1.70E+04	6.83	36.4	15.9679	0.29
C30P	1.98E+05	1.42E+04	6.53	33.50	-	-
C40P	1.74E+05	1.26E+04	6.54	33	-	-
S5P	2.25E+05	1.62E+04	6.38	35.00	20.34	0.38
S10P	1.87E+05	1.35E+04	5.81	36.70	20.26	0.40
S15P	1.66E+05	1.19E+04	6.03	37.90	20.65	0.41
S20P	2.39E+05	1.72E+04	6.97	38.80	20.00	0.38
S30P	2.21E+05	1.59E+04	6.25	36.90	20.87	0.42
S40P	2.07E+05	1.49E+04	6.37	39.10	22.25	0.46
CS5P	1.59E+05	1.14E+04	6.02	38.80	18.51	0.30
CS10P	1.39E+05	1.00E+04	5.80	38.70	18.76	0.28
CS15P	1.28E+05	9.17E+03	6.33	37.90	18.27	0.29
CS20P	1.52E+05	1.09E+04	6.23	38.30	18.15	0.34
CS30P	1.36E+05	9.75E+03	6.48	35.60	-	-
CS40P	1.26E+05	9.05E+03	-	-	-	-

Before relating the impacts to the engineering properties, the stability of the impact values themselves was examined. The reference mortar, which contains no powder, returns an identical GWP of 2.24×10^4 kg CO_2-eq under all five cases (Scenario 1, Scenario 2, and Scenario 3 at 10%, 50% and 100% powder price), confirming that neither the grinding energy nor the allocation affects a mix without powder. For the powder-containing mixes the values move only marginally: taking CS40P, the mix with the highest powder content and therefore the largest allocated burden, GWP shifts from 9,045 kg CO_2-eq under the cut-off treatment to 9,049 kg CO_2-eq under Scenario 3 at the full powder price. Across every mix the spread between the 10% and 100% price levels stays below 0.04%. The impact values are therefore effectively invariant to the allocation method and to the powder price, which establishes that any relationship observed between impact and engineering performance will hold equally in all scenarios.

For each scenario, GWP and ADP-FF were regressed linearly against the four engineering properties. Because the two impact indicators are strongly collinear across the mixes, they produce almost identical regressions, and because the impact values are stable across scenarios, the coefficients of determination are unchanged from one scenario to the next — the GWP-versus-compressive-strength relationship, for example, returns R^2 = 0.183 under Scenario 1 and R^2 = 0.183 under Scenario 3 at the full price. The regression results are summarised in Table 5-27 and shown sensitivity of Scenario 3 (50% price) as example in Table 5-25 and Table 5-26.

Table 5-25 Sensitivity graphs (GWP)

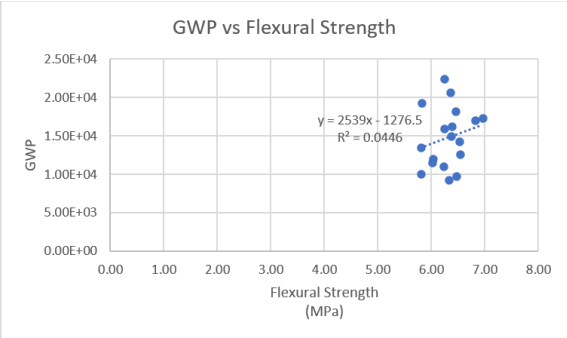
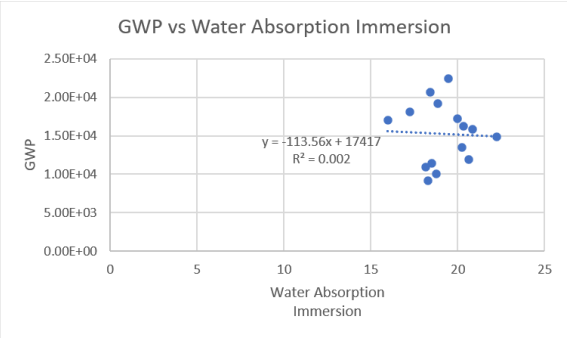
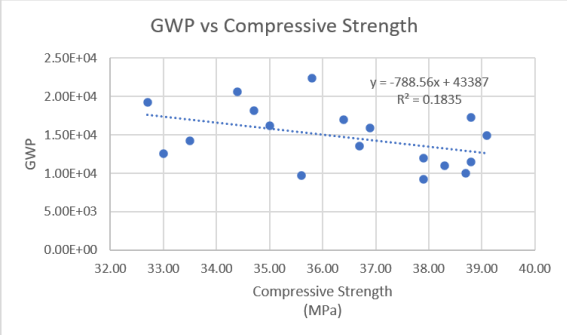
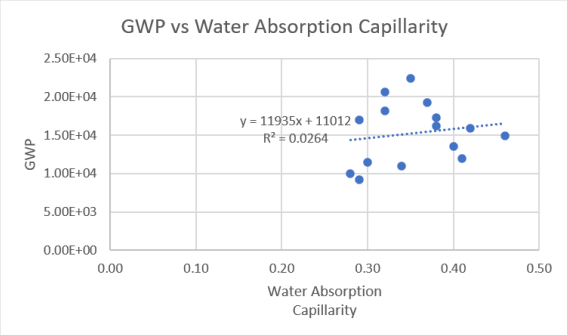
GWP vs Mechanical Properties	**GWP vs Durability**
	
	

Table 5-26 Sensitivity graphs (ADP-FF)

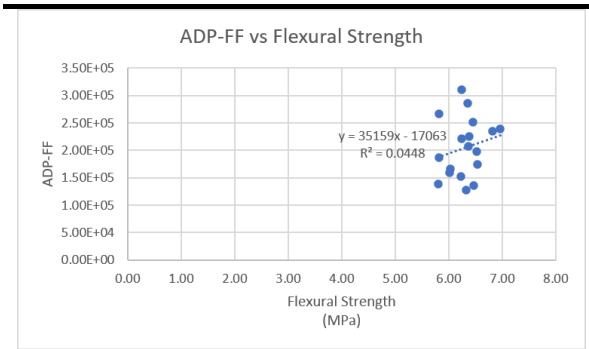
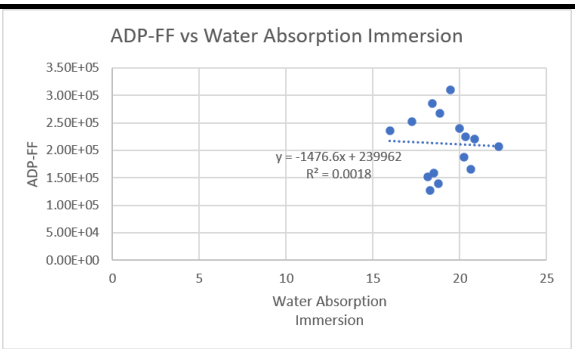
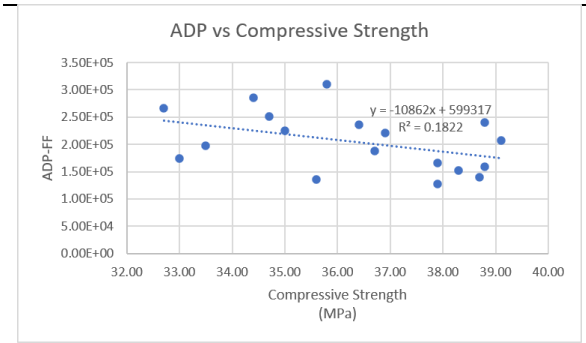
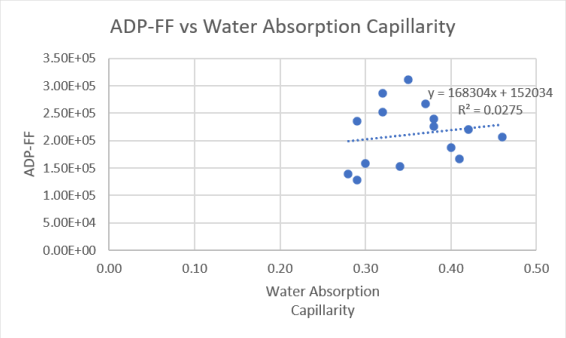
ADP-FF vs Mechanical Properties	ADP-FF vs Durability
	
	

Table 5-27 Linear regression of environmental impact against engineering properties

Impact vs Property	R^2	Slope (sign)	Interpretation
GWP vs Compressive strength	0.18	negative	weak
GWP vs Flexural strength	0.04	positive	none
GWP vs Water absorption (immersion)	0.00	negative	none
GWP vs Water absorption (capillarity)	0.03	positive	none
ADP-FF vs Compressive strength	0.18	negative	weak
ADP-FF vs Flexural strength	0.04	positive	none
ADP-FF vs Water absorption (immersion)	0.00	negative	none
ADP-FF vs Water absorption (capillarity)	0.03	positive	none

The regressions show that environmental performance and engineering performance are, for the most part, statistically unrelated across the set of mortars. Compressive strength shows the only relationship of any strength, a weak negative correlation with both impact indicators ($R^2 \approx 0.18$): mortars with lower environmental impact tend, slightly, to exhibit higher compressive strength rather than lower. This is a favourable indication, since it means that the environmental gains achieved through powder incorporation are not obtained at the expense of compressive capacity; but with only 18% of the variance explained, the

relationship is too weak to support prediction. Flexural strength ($R^2 \approx 0.04$) and both water-absorption measures ($R^2 \approx 0.00$ and 0.03) show no meaningful relationship with impact at all. Environmental performance and durability therefore vary independently: reducing the impact of a mortar neither improves nor degrades its water absorption within the range tested.

The practical consequence is important. Because the environmental ranking and the engineering properties are largely decoupled, a mix that performs well environmentally is not guaranteed to perform well mechanically or in terms of durability. This is precisely why the environmental ranking alone is insufficient to identify the most suitable formulation, and why the two sets of results must be considered together.

5.3.3. Sensitivity analysis: strength–environment trade-off and weighting of criteria

The correlation analysis presented above showed that no strong linear relationship links the environmental indicators to the engineering properties of the mortars. The trade-off between the two was therefore examined directly, in two steps. The first step follows the environmental and mechanical response of each series across the full substitution range, to check whether a threshold exists beyond which the material becomes unviable. The second step combines the two criteria into a single score under three different weighting schemes, to test whether the preferred formulation depends on the priority given to each criterion. Both steps were carried out for Scenario 3 at the 50% price level, the most representative configuration of the study. CS40P is included in the environmental comparison but excluded from the combined scoring, since no strength data are available for this mix.

Scale convention. Throughout this section, all normalised values follow a higher-is-better scale from 0 to 1, in which 1 represents the best performance and 0 the worst. The environmental score is derived from the Scenario 3 normalisation of the GWP: CS40P, the mix with the lowest global warming potential, receives a score of 1, and REF, the mix with the highest, receives a score of 0. A higher environmental score therefore means a lower environmental impact. The compressive strength is normalised on the same convention in the multi-criteria step, where 1 corresponds to the highest strength of the dataset (S40P, 39.1 MPa) and 0 to the lowest (C10P, 32.7 MPa).

For each series, the compressive strength and the environmental score were plotted together against the substitution level, with the strength on the primary axis and the environmental score on the secondary axis. The data are listed in the table below and the three series are shown in the figure that follows.

Table 5-28 Compressive strength and environmental score by substitution level, Scenario 3, (50%), (best=1)

Substitution (%)	C: Strength	C: Env. score	S: Strength	S: Env. score	CS: Strength	CS: Env. score
0 (REF)	35.8	0.000	35.8	0.000	35.8	0.000
5	34.4	0.134	35.0	0.463	38.8	0.821
10	32.7	0.238	36.7	0.668	38.7	0.927
15	34.7	0.320	37.9	0.784	37.9	0.991
20	36.4	0.405	38.8	0.387	38.3	0.858
30	33.5	0.612	36.9	0.490	35.6	0.948
40	33.0	0.737	39.1	0.564	–	1.000

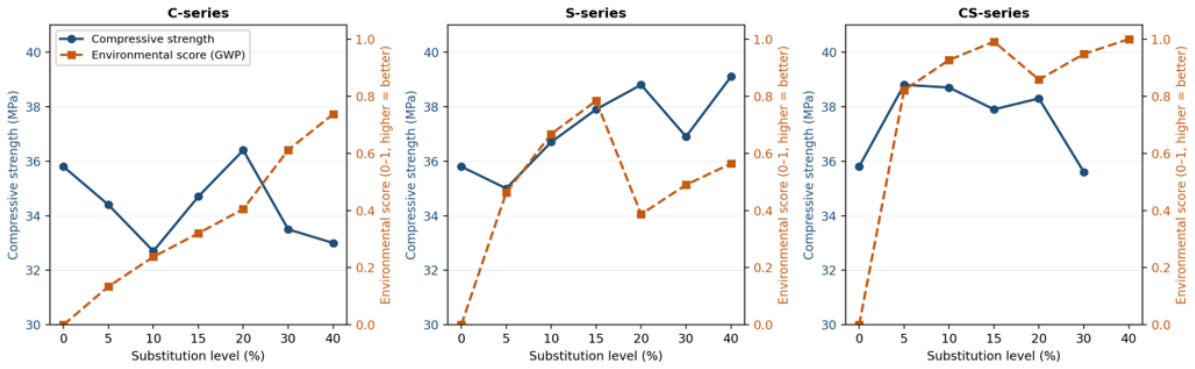


Figure 5-3 Compressive strength and environmental score against the substitution level, per series

The charts do not show the threshold behaviour that a strength–environment trade-off would produce. Across the full 0–40% range the compressive strength remains inside a narrow band, from 32.7 MPa (C10P) to 39.1 MPa (S40P), between −8.7% and +9.2% of the reference value of 35.8 MPa, while the environmental score rises from 0 to 0.99. In the S-series and the CS-series the strength increases with substitution rather than decreasing: S40P records the highest strength of the dataset, and CS5P to CS20P all remain at or above 37.9 MPa. Only the C-series shows small dips, and its weakest mix still retains 91% of the reference strength. The two curves never converge towards a crossing point in any series. The sensitivity conclusion is therefore the opposite of the usual trade-off: the strength is insensitive to the substitution level over the tested range, the environmental gain is obtained without a mechanical penalty, and no viability threshold exists between 0 and 40%. On the environmental axis alone, the most favourable region is the CS-series between 10% and 20%, where the environmental score already lies between 0.86 and 0.99 while the strength stays above the reference.

5.3.4. Multi-criteria comparison with weight sensitivity

The compressive strength was normalised to the same higher-is-better 0–1 scale as the environmental score, using the form (value − minimum)/ (maximum − minimum), computed over the eighteen mixes with strength data (minimum 32.7 MPa, maximum 39.1 MPa). Each mix then received a single score, defined as the normalised strength multiplied by the mechanical weight plus the environmental score multiplied by the environmental weight, under three weighting schemes: a balanced scheme (0.50/0.50), a structural scheme that favours the strength (0.80/0.20), and an ecological scheme that favours the carbon footprint (0.20/0.80). The scores and rankings are reported in the table below and compared in the figure that follows, it should be mentioned that CS40P is excluded as strength data was unavailable.

Table 5-29 MCDM scores and rankings under the three weighting schemes, Scenario 3 (50%)

Mix	Strength (MPa)	Env. score	Norm. strength	Score A (0.5/0.5)	Score B (0.8/0.2)	Score C (0.2/0.8)	Rank A	Rank B	Rank C
REF	35.8	0.000	0.484	0.242	0.387	0.097	16	12	18
C5P	34.4	0.134	0.266	0.200	0.239	0.161	17	15	17
C10P	32.7	0.238	0.000	0.119	0.048	0.190	18	18	16
C15P	34.7	0.320	0.313	0.316	0.314	0.319	15	14	15
C20P	36.4	0.405	0.578	0.492	0.544	0.440	11	11	14
C30P	33.5	0.612	0.125	0.368	0.222	0.514	14	16	11
C40P	33.0	0.737	0.047	0.392	0.185	0.599	13	17	9
S5P	35.0	0.463	0.359	0.411	0.380	0.442	12	13	13
S10P	36.7	0.668	0.625	0.646	0.634	0.659	9	8	7
S15P	37.9	0.784	0.812	0.798	0.807	0.789	5	7	6
S20P	38.8	0.387	0.953	0.670	0.840	0.500	8	6	12
S30P	36.9	0.490	0.656	0.573	0.623	0.523	10	9	10
S40P	39.1	0.564	1.000	0.782	0.913	0.651	6	3	8
CS5P	38.8	0.821	0.953	0.887	0.927	0.848	3	2	5
CS10P	38.7	0.927	0.938	0.932	0.935	0.929	1	1	2
CS15P	37.9	0.991	0.812	0.902	0.848	0.955	2	5	1
CS20P	38.3	0.858	0.875	0.866	0.872	0.861	4	4	3
CS30P	35.6	0.948	0.453	0.700	0.552	0.849	7	10	4

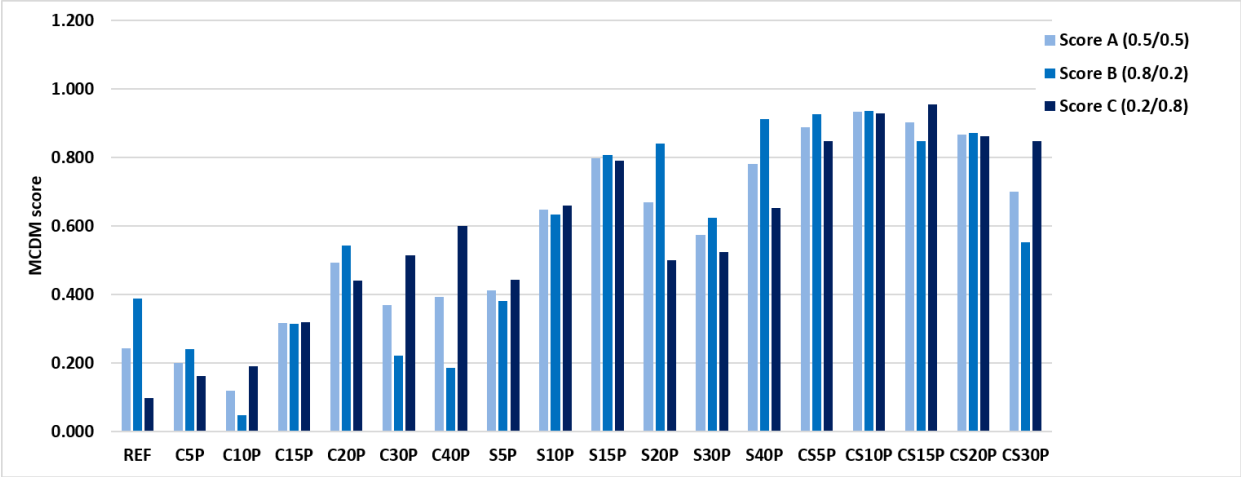


Figure 5-4 MCDM score of each mix under the three weighting schemes.

The weighting sensitivity analysis shows that the choice of optimal formulation is not strongly sensitive to how mechanical and environmental performance are prioritised. CS10P achieved the highest combined score under both the balanced (50/50) and the structurally oriented (80/20) weighting schemes. Only when environmental performance was weighted most heavily (20/80) did CS15P move ahead, with CS10P falling to second place.

The reason is straightforward. CS15P records a compressive strength of 37.9 MPa against 38.7 MPa for CS10P, and an environmental score of 0.991 against 0.927. Under equal or mechanical-oriented weights, the strength advantage of CS10P is sufficient to keep it in first place. Under the ecological weighting, the 0.064-point environmental advantage of CS15P outweighs the 0.8 MPa strength difference, and the ranking reverses. The gap between the two scores in that scenario is 0.026, which illustrates how narrow the margin is.

Despite this, the broader picture does not change across the three schemes. The top of the ranking is occupied by the CS series throughout, and REF finishes 16th, 12th and 18th out of 18 mixes depending on the scheme, confirming that WTB powder incorporation improves overall performance under any weighting. The main practical conclusion is that the combined cement-and-sand substitution strategy at 10–15% powder represents a robust design choice: the weighting determines which of the two formulations is nominally preferred, but both deliver very similar results and both outperform all single-constituent substitution strategies.

It should be mentioned that extending the system to economic allocation changes the stage pattern far less than might be expected. The transport stage of Scenario 3 is identical to that of the previous scenarios, since the powder travels the same 270 km regardless of how its upstream burden is treated,

and the production stage carries the same grinding electricity as Scenario 2. The only additional thing is the economically allocated share of the blade-manufacturing burden assigned to the powder in the raw-material stage. At the 50% price level this share remains very small (in absolute terms of the order of 1 kg CO_2-eq per cubic metre even at the highest incorporation ratios) because the low market value of the powder relative to the finished blade keeps the allocation factor low. As a result, the contribution profile of Scenario 3 shows transportation as the dominant stage in all six categories again.

This insensitivity to the allocation choice is itself a meaningful finding. It indicates that the environmental profile of these mortars is governed by logistics rather than by the accounting convention applied to the waste stream, which is consistent with the observation of D'Orazio et al. [42] that transport distances, not the treatment of the secondary material, control the outcome of such assessments. It also reinforces the practical recommendation, already advanced for mortars with industrial wastes in the review of Santos et al. [41], that sourcing the secondary material locally is the most direct way to reduce the shipping burden.

5.4. Comparison of Scenarios

The differences between the scenarios are too small to change the ranking, and too small to register at the precision at which the results are reported. The largest characterised change in the dataset occurs for CS40P, the mix with the most powder and therefore the largest allocated burden. Its GWP moves from 9,045 kg CO_2-eq under the cut-off treatment of Scenario 1 to 9,047 kg CO_2-eq at the 50% powder price and 9,049 kg CO_2-eq at the 100% price an increase of approximately 4 kg CO_2-eq, or about 0.04% of the total impact of the mix. For every mix, the spread between the 10% and 100% price levels stays below 0.04%. The reference mortar, which contains no powder, returns an identical GWP of 2.24×10^4 kg CO_2-eq under all five cases. After normalisation and aggregation, the picture is the same: the maximum variation in any normalised indicator caused by the grinding energy of Scenario 2 is 3.5×10^{-5}, the largest change in any NDA score is 2.2×10^{-5}, and the largest difference in any normalised value between Scenario 1 and Scenario 3 at the 50% price is 2×10^{-4} below the resolution of any graphical representation, and smaller than the rounding applied to the reported results.

The weak response of the results to the scenario assumptions has a structural explanation. Under Scenario 1, the transportation stage contributes between 98% and 99.6% of the characterised impact across all six impact categories and all nineteen formulations, while the production stage is negligible and the raw material stage comparatively small. The three scenarios differ only in the treatment of the powder

stream, so every scenario modification acts on a quantity that is already small before the modification is applied.

The mass of the powder reinforces this. It ranges from 22.28 kg/m³ in C5P to 135.73 kg/m³ in CS40P, which is small in absolute terms against the cement content of the mixes, up to 511.80 kg/m³ in the reference mortar. A per-kilogram burden assigned to the powder is therefore applied to a minor constituent. The grinding energy added in Scenario 2 behaves the same way: at 0.225 MJ per kilogram of powder, it adds between approximately 0.31 kg CO_2-eq/m³ at the lowest replacement level and 1.89 kg CO_2-eq/m³ for CS40P, against mortar totals of 9.04×10^3 to 2.24×10^4 kg CO_2-eq/m³, at least three orders of magnitude below the totals it is added to.

The economic allocation of Scenario 3 is limited by the allocation coefficient. At its maximum, reached by the S-series at the 100% price level where the powder is valued against sand at 314 Euros/t, α is 6.43×10^{-4}; the C-series peaks at 4.25×10^{-4} and the CS-series at 5.89×10^{-4}. The coefficient is the ratio of the economic value of the powder to the combined value of the blade and the powder, and these two quantities are of entirely different orders: one SNL-100-03 blade carries a reported manufacturing cost of 471,529.55 Euros and yields 966.7 kg of powder, worth approximately 304 Euros even at the full sand price. The powder can therefore never attract more than a small fraction of one tenth of one percent of the blade burden, and the resulting allocated GWP per kilogram of powder amounts to only 0.021 kg CO_2-eq for the C-series and 0.032 kg CO_2-eq for the S-series at the 100% price. Increasing the powder price from 10% to 100% of the reference value multiplies a quantity that is negligible to begin with, and the characterised impacts barely respond. In every scenario, the dominant terms of the impact calculation remain identical, and the convergence of the rankings, the impact magnitudes, the regressions and the multi-criteria selection follow from that.

The trade-off analysis was carried out under Scenario 3 at the 50% price level as the central configuration of the study, and its conclusions transfer unchanged to the other four cases because the impact values that define the environmental score differ between the cases by less than 0.04%. Across the full 0–40% substitution range, the compressive strength of the tested mixes stays inside a narrow band, from 32.7 MPa (C10P) to 39.1 MPa (S40P), between 8.7% and +9.2% of the reference value of 35.8 MPa, while the environmental score rises from 0 to 0.99. The threshold behaviour that a genuine trade-off would produce does not appear in any series: the strength and environmental curves never converge towards a crossing point. In the S-series and the CS-series, strength increases with substitution rather than decreasing S40P records the highest strength of the dataset, and CS5P to CS20P all remain at or above 37.9 MPa. Only the C-series shows small dips, and its weakest mix still retains 91% of the reference strength. The

substitution therefore delivers its environmental gain without a mechanical penalty in every scenario, no viability threshold exists between 0 and 40% replacement, and the most favourable region on the environmental axis is the CS-series between 10% and 20%, where the environmental score already lies between 0.86 and 0.99 while the strength stays above the reference.

The last comparison concerns the formulation that would actually be selected once mechanical and environmental performance are considered together. The multi-criteria assessment normalised the compressive strength to the same higher-is-better 0–1 scale as the environmental score, over the eighteen mixes with strength data (CS40P is excluded, as no strength data are available for this mix), and computed a single weighted score under three schemes: balanced (0.50/0.50), structural (0.80/0.20) and ecological (0.20/0.80). The outcome is stable in two ways. It is stable across scenarios, because the environmental scores entering the weighted sum are invariant to the allocation treatment, so the rankings computed under Scenario 3 at the 50% price hold for all five cases. It is also stable across weightings: CS10P achieves the highest combined score under both the balanced scheme (0.932) and the structural scheme (0.935), and only under the ecological weighting does CS15P move ahead, with 0.955 against 0.929 for CS10P. The reversal rests on a narrow margin in both criteria (a compressive strength of 38.7 MPa for CS10P against 37.9 MPa for CS15P, and an environmental score of 0.927 against 0.991) and the gap between the two scores under the ecological scheme is only 0.026. The top of the ranking belongs to the CS-series under all three schemes, while the reference mortar finishes 16th, 12th and 18th out of the eighteen mixes depending on the scheme. The combined cement-and-sand substitution at 10–15% powder is therefore the preferred design choice under every scenario, every powder price, and every weighting tested; the weighting decides only which of two very similar formulations is nominally first.

The convergence of results across all three scenarios is ultimately a consequence of the transport dominance identified in Section 5.1. When a single life cycle stage accounts for 98–99.6% of the characterized impact across all categories and all nineteen formulations, the scope available for the remaining stages to influence the outcome is structurally constrained from the outset. Scenarios 1, 2 and 3 differ only in how the powder stream is accounted for, yet in each case they are modifying a constituent that represents a minor fraction of the total mix mass against a backdrop in which freight dominates. The allocation method is therefore not the decisive variable in this system; the transport distances are. This structural property of the model is not a limitation of the sensitivity analysis but an outcome that carries practical relevance: any future modification to the powder supply chain, whether a change in price, processing route, or allocation convention, is unlikely to alter the environmental ranking of the mortars as long as the transport distances remain unchanged.

6. Conclusions and Future Work

6.1. Conclusions

This dissertation evaluated the environmental performance of cementitious mortars incorporating pre-consumer WTB powder through a cradle-to-gate LCA. While previous studies had demonstrated that this manufacturing residue could be successfully incorporated into cement-based mortars from a mechanical perspective, its environmental implications had not been systematically assessed. This work addressed that gap by quantifying the environmental impacts of nineteen mortar formulations, comparing three substitution strategies, and evaluating the influence of alternative allocation approaches for the WTB powder.

The results demonstrate that incorporating WTB powder consistently improves the environmental performance of cementitious mortars compared with the conventional reference mortar. This conclusion remained unchanged regardless of the allocation approach adopted. Treating the powder as a burden-free waste, including the energy required for mechanical grinding, or assigning an economically allocated share of the blade-manufacturing burden all produced the same environmental rankings: the largest change in any NDA score across the five cases was 2.2×10^{-5}, and the largest change in any characterised impact was 0.04%, observed for CS40P at the highest powder price. The sensitivity analysis therefore confirmed that the conclusions of this study are not dependent on the modelling assumptions associated with the recovered material.

Among the substitution strategies investigated, the combined replacement of cement and sand consistently delivered the best overall environmental performance. Although increasing the powder content generally reduced the environmental impacts, the combined substitution strategy achieved the greatest reductions while maintaining satisfactory mechanical and durability performance throughout the investigated substitution range. The CS-series also maintained water absorption by immersion and by capillarity at or below the reference values, whereas the S-series showed a progressive increase in both durability indicators with substitution level, which explains its lower position in the combined ranking despite carrying comparable or higher compressive strength. When environmental, mechanical and durability performance were considered together, formulations containing approximately 10–15% WTB powder, particularly CS10P and CS15P, provide the most balanced solution. CS10P is the preferred formulation under balanced and mechanically oriented decision criteria, with a combined score of 0.932 and 0.935 respectively, whereas CS15P becomes preferable only when environmental performance is

given substantially greater weight, reaching 0.955 against 0.929 for CS10P. The difference between the two is 0.026 at most, and both constitute robust design alternatives for practical implementation.

An important outcome of this study is that the environmental improvements were achieved without compromising the engineering suitability of the mortars. The incorporation of WTB powder did not introduce a significant trade-off between environmental and mechanical performance within the investigated substitution range. In the S-series and CS-series, compressive strength increased with substitution level while the environmental score improved simultaneously, so several formulations are at once stronger and environmentally better than the reference. This confirms that the environmental benefits obtained through the valorisation of pre-consumer composite waste can be realised without sacrificing structural performance.

From a broader perspective, this dissertation demonstrates that pre-consumer wind turbine blade manufacturing waste is a viable secondary raw material for cementitious construction products. Critically, this conclusion holds even under the most conservative accounting of the powder's origin: assigning it an economically allocated share of the blade manufacturing burden under ISO 14044 [12] produced no meaningful change to the results.

6.2. Limitations

The conclusions above must be read within the boundaries of the study that produced them. The assessment is cradle-to-gate: it ends at the factory gate of the mortar and says nothing about the use phase, service life, or end-of-life behaviour of the formulations. A mortar that carbonates faster or requires earlier replacement could lose part of its production-stage advantage over a full life cycle, and this study cannot rule that out.

The inventory rests on EPDs and background database processes rather than primary data collected from industry. This is standard practice for a study of this scope, but it means the results inherit the assumptions, geographies, and reference years of those sources. The economic allocation, in particular, was built from a single blade design and the production figures of a single manufacturing facility, and different blade geometries or plant efficiencies would shift the allocated quantities.

Finally, the assessment covers six impact categories; effects outside them, such as toxicity or water use, remain unexamined.

6.3. Future Work

Several directions follow naturally from these limitations. The most immediate is the extension of the system boundary from cradle-to-gate to cradle-to-grave, incorporating the use phase and demolition of the mortars. The carbonation behaviour observed experimentally makes this extension more than a formality: it is the point where the environmental case could genuinely change, and it should be tested.
A second direction is the replacement of database and declaration-based inventory data with primary data from blade manufacturers and mortar producers. The allocation model in particular would benefit from production data covering multiple facilities and blade designs, which would allow the single-facility assumption of this study to be tested rather than assumed.
Finally, the scope could be widened in two directions: toward other waste streams, since blade powder varies in composition between manufacturers and processing routes, and toward other applications, since mortar is only one of several cementitious products into which the powder could be incorporated. Concrete, blocks, and non-structural elements each present different performance requirements and different volumes of potential uptake, and each deserves the same assessment this dissertation has given to mortar.

REFERENCES

[1] T. Liu *et al.*, 'Mechanisms and applications of wind turbine blade waste in cementitious composites: A review', Mar. 01, 2025, *Elsevier Ltd*. doi: 10.1016/j.matdes.2025.113732.

[2] P. Liu and C. Y. Barlow, 'Wind turbine blade waste in 2050', *Waste Management*, vol. 62, pp. 229–240, Apr. 2017, doi: 10.1016/j.wasman.2017.02.007.

[3] T. Liu, H. Reascos, U. A. Mughal, G. M. Kirkelund, and A. T. Lima, 'Improving mortar properties with waste wind turbine blade fibers and superplasticizer', *Constr. Build. Mater.*, vol. 472, Apr. 2025, doi: 10.1016/j.conbuildmat.2025.140864.

[4] J. Liu, C. Zhao, S. Zhong, and L. Johanning, 'The Recyclability of Wind Turbine Blade Material, Manufacturing Process, and Recycling Technology', *Marine Energy Research*, vol. 2, no. 3, pp. 10014–10014, 2025, doi: 10.70322/mer.2025.10014.

[5] J. Rybicka, A. Tiwari, and G. A. Leeke, 'Technology readiness level assessment of composites recycling technologies', *J. Clean. Prod.*, vol. 112, pp. 1001–1012, Jan. 2016, doi: 10.1016/j.jclepro.2015.08.104.

[6] A. Bettini, F. Faleschini, L. Correia, J. Sena-Cruz, and E. Teixeira, 'The effect on mechanical and durability performance indicators of incorporating powder waste from wind turbine blades into cement-based mortars'.

[7] J. Rybicka, A. Tiwari, P. Alvarez Del Campo, and J. Howarth, 'Capturing composites manufacturing waste flows through process mapping', *J. Clean. Prod.*, vol. 91, pp. 251–261, Mar. 2015, doi: 10.1016/j.jclepro.2014.12.033.

[8] J. R. Correia, N. M. Almeida, and J. R. Figueira, 'Recycling of FRP composites: Reusing fine GFRP waste in concrete mixtures', *J. Clean. Prod.*, vol. 19, no. 15, pp. 1745–1753, Oct. 2011, doi: 10.1016/j.jclepro.2011.05.018.

[9] European Union, *Directive 2008/98/EC of the European Parliament and of the Council of 19 November 2008 on waste and repealing certain Directives*. 2008, pp. 3–30.

[10] Y. Guo, S. Chen, M. T. Lakhiar, Q. Chen, and B. Li, 'Effect of recycled turbine blade powder and fibres on mechanical and life cycle properties of mortar', *Case Studies in Construction Materials*, vol. 23, Dec. 2025, doi: 10.1016/j.cscm.2025.e05041.

[11] 'ISO 14040', 2006.

[12] *ISO 14044*. 2018.

[13] C. Menna, L. De Simone, and V. Capozzi, 'Mechanical recycling of GFRP wind turbine blades: Evaluating the sustainability and economic potential of recycled fibers', *Developments in the Built Environment*, vol. 23, Oct. 2025, doi: 10.1016/j.dibe.2025.100710.

[14] V. Revilla-Cuesta, M. Skaf, V. Ortega-López, and J. M. Manso, 'Raw-crushed wind-turbine blade: Waste characterization and suitability for use in concrete production', *Resour. Conserv. Recycl.*, vol. 198, Nov. 2023, doi: 10.1016/j.resconrec.2023.107160.

[15] K. Piotrowska and I. Piasecka, 'Specification of environmental consequences of the life cycle of selected post-production waste of wind power plants blades', *Materials*, vol. 14, no. 17, Sep. 2021, doi: 10.3390/ma14174975.

[16] Y. Tao, S. A. Hadigheh, and Y. Wei, 'Recycling of glass fibre reinforced polymer (GFRP) composite wastes in concrete: A critical review and cost benefit analysis', *Structures*, vol. 53, pp. 1540–1556, Jul. 2023, doi: 10.1016/j.istruc.2023.05.018.

[17] M. Rucka and M. Kurpińska, 'Sustainable cement-based mortar with shredded material recycled from end-of-life wind turbine blades', *Sci. Rep.*, vol. 15, no. 1, Dec. 2025, doi: 10.1038/s41598-025-15364-3.

[18] R. J. Tapper, M. L. Longana, A. Norton, K. D. Potter, and I. Hamerton, 'An evaluation of life cycle assessment and its application to the closed-loop recycling of carbon fibre reinforced polymers', Mar. 01, 2020, *Elsevier Ltd*. doi: 10.1016/j.compositesb.2019.107665.

[19] M. Davallo, H. Pasdar, and M. Mohseni, 'Mechanical Properties of Unsaturated Polyester Resin'.

[20] B. Zhou, M. Zhang, and G. Ma, 'Multi-scale experimental study on the effect of crushed GFRP powder and dust on physical-mechanical properties of cement mortar', *Journal of Building Engineering*, vol. 57, Oct. 2022, doi: 10.1016/j.jobe.2022.104853.

[21] M. Rani, P. Choudhary, V. Krishnan, and S. Zafar, 'A review on recycling and reuse methods for carbon fiber/glass fiber composites waste from wind turbine blades', Jun. 15, 2021, *Elsevier Ltd*. doi: 10.1016/j.compositesb.2021.108768.

[22] 'Reimagining end-of-use composites as a new resource'. [Online]. Available: www.eucia.eu

[23] D. Baturkin, O. A. Hisseine, R. Masmoudi, A. Tagnit-Hamou, S. Metiche, and L. Massicotte, 'Compressive behavior of FRP-tube-confined concrete short columns using recycled FRP materials from wind turbine blades: Experimental investigation and analytical modelling', *Clean Technologies and Recycling*, vol. 2, no. 3, pp. 136–164, 2022, doi: 10.3934/ctr.2022008.

[24] S. Karuppannan Gopalraj and T. Kärki, 'A review on the recycling of waste carbon fibre/glass fibre-reinforced composites: fibre recovery, properties and life-cycle analysis', Mar. 01, 2020, *Springer Nature*. doi: 10.1007/s42452-020-2195-4.

[25] W. Zhang, H. Yu, B. Yin, A. Akbar, and K. M. Liew, 'Sustainable transformation of end-of-life wind turbine blades: Advancing clean energy solutions in civil engineering through recycling and upcycling', *J. Clean. Prod.*, vol. 426, Nov. 2023, doi: 10.1016/j.jclepro.2023.139184.

[26] D. Baturkin, O. A. Hisseine, R. Masmoudi, A. Tagnit-Hamou, and L. Massicotte, 'Valorization of recycled FRP materials from wind turbine blades in concrete', *Resour. Conserv. Recycl.*, vol. 174, Nov. 2021, doi: 10.1016/j.resconrec.2021.105807.

[27] T. Liu, C. Paraskevoulakos, D. J. De Souza, W. Kunther, and A. T. Lima, 'Impact of wind turbine blade waste fiber size on the properties of mortar: From material characteristics to performance', *Constr. Build. Mater.*, vol. 525, May 2026, doi: 10.1016/j.conbuildmat.2026.146416.

[28] M. Rucka and M. Kurpińska, 'Sustainable cement-based mortar with shredded material recycled from end-of-life wind turbine blades', *Sci. Rep.*, vol. 15, no. 1, Dec. 2025, doi: 10.1038/s41598-025-15364-3.

[29] V. Revilla-Cuesta, J. Manso-Morato, N. Hurtado-Alonso, M. Skaf, and V. Ortega-López, 'Mechanical and environmental advantages of the revaluation of raw-crushed wind-turbine blades as a concrete component', *Journal of Building Engineering*, vol. 82, Apr. 2024, doi: 10.1016/j.jobe.2023.108383.

[30] C. Duyal, M. Chevalier, N. Lushnikova, F. Gauvin, and H. J. H. Brouwers, 'Optimized incorporation of shredded wind turbine blade waste in concrete using a particle packing approach', *Constr. Build. Mater.*, vol. 521, Apr. 2026, doi: 10.1016/j.conbuildmat.2026.146102.

[31] A. C. Paula Junior, C. Jacinto, C. Turco, J. Fernandes, E. Teixeira, and R. Mateus, 'Analysis of the effect of incorporating construction and demolition waste on the environmental and

mechanical performance of earth-based mixtures', May 02, 2022, *Elsevier Ltd*. doi: 10.1016/j.conbuildmat.2022.127244.

[32] E. R. Teixeira, R. Mateus, A. F. Camões, L. Bragança, and F. G. Branco, 'Comparative environmental life-cycle analysis of concretes using biomass and coal fly ashes as partial cement replacement material', *J. Clean. Prod.*, vol. 112, pp. 2221–2230, 2016, doi: 10.1016/j.jclepro.2015.09.124.

[33] European Committee for Standardization, 'EN 15804:2012+A2:2019 Sustainability of construction works — Environmental product declarations — Core rules for the product category of construction products', Brussels, 2019.

[34] Portuguese Republic Government, 'Decree-Law No. 102-D/2020 of 10 December 2020 – General Waste Management Regime', Lisbon, 2020.

[35] P. Operator, 'General Information Product CEM II/B-L 32,5 N PORTLAND LIMESTONE CEMENT'.

[36] 'Environmental Product Declaration'. [Online]. Available: www.environdec.com.

[37] S. Cheng, K. H. Wong, C. P. Shen, X. L. Liu, and C. Rudd, 'Shredding energy consumption of GFRP composite waste', in *Journal of Physics: Conference Series*, IOP Publishing Ltd, Jan. 2021. doi: 10.1088/1742-6596/1765/1/012015.

[38] 'Secil company - mortar manufacturing'.

[39] S. Pradhan, B. R. Tiwari, S. Kumar, and S. V. Barai, 'Comparative LCA of recycled and natural aggregate concrete using Particle Packing Method and conventional method of design mix', *J. Clean. Prod.*, vol. 228, pp. 679–691, Aug. 2019, doi: 10.1016/j.jclepro.2019.04.328.

[40] A. Kadawo, M. Sadagopan, O. During, K. Bolton, and A. Nagy, 'Combination of LCA and circularity index for assessment of environmental impact of recycled aggregate concrete', *J. Sustain. Cem. Based. Mater.*, vol. 12, no. 1, pp. 1–12, 2023, doi: 10.1080/21650373.2021.2004562.

[41] T. Santos, J. Almeida, J. D. Silvestre, and P. Faria, 'Life cycle assessment of mortars: A review on technical potential and drawbacks', Jun. 21, 2021, *Elsevier Ltd*. doi: 10.1016/j.conbuildmat.2021.123069.

[42] M. D'Orazio, E. Di Giuseppe, and M. Carosi, 'Life Cycle Assessment of Mortars with Fine Recycled Aggregates from Industrial Waste: Evaluation of Transports Impact in the Italian Context', *Sustainability (Switzerland)*, vol. 15, no. 4, Feb. 2023, doi: 10.3390/su15043221.

[43] P. Bortolotti *et al.*, 'A Detailed Wind Turbine Blade Cost Model', 2019. [Online]. Available: www.nrel.gov/publications.

[44] 'Cement Price from Leroy Merlin'.

[45] 'Sand Price from Atila'.